

AN ABSTRACT OF THE THESIS OF

LAWRENCE ALAN HANSEN for the degree MASTER OF SCIENCE
(Name of student) (Degree)

in Civil Engineering presented on May 8, 1975
(Major Department) (Date)

Title: PENETRATION RESISTANCE PREDICTIONS FOR
DRIVEN PILING

Abstract approved: Redacted for privacy
W. L. Schroeder

This paper presents a method of predicting penetration resistance for driven piles, using known driving records for driving the same type piling in similar subsurface conditions. As known driving records are not always available to the analyst, a method was also investigated using soil data only. The analytical tools employed included the Hiley pile driving formula and the wave equation, as programmed for computer solution by T. C. Edwards.

Predictions were made for five projects where driving records were available for two different hammers. Predictions were made for one hammer using a statistically determined mean driving record of the second hammer, and vice-versa. Predictions were also made using only soil data for both hammers.

In comparing the predicted values with the actual mean field values, it was found that reliable penetration resistance versus depth

relationships could be predicted using a known driving record with either the Hiley formula or the wave equation. Predictions made using only soil data were found to be reasonable, though significantly more inaccurate than those using a known driving record. Where only soil data was used, it was found that the wave equation is a better predictive tool than the Hiley formula.

Penetration Resistance Predictions for Driven Piling

by

Lawrence Alan Hansen

A THESIS

submitted to

Oregon State University

in partial fulfillment of
the requirements for the
degree of

Master of Science

June 1975

APPROVED:

Redacted for privacy

Professor of Civil Engineering
in charge of major

Redacted for privacy

~~Head of~~ Department of Civil Engineering

Redacted for privacy

Dean of Graduate School

Date thesis is presented May 8, 1975

Typed by Ilene Anderton for Lawrence Alan Hansen

ACKNOWLEDGEMENTS

I wish to thank my major professor, Dr. W. L. Schroeder, for his valuable assistance and advice during the preparation of this thesis, as well as during the course of my graduate studies.

I am indebted to Dr. J. R. Bell for his advice and interest, and as a continuing source of inspiration.

I am ever grateful to my wife, Judy, for her patience and understanding.

I wish to thank Don Bills for the many excellent figures he prepared for this thesis, and Ilene Anderton for the typing of the final manuscript.

TABLE OF CONTENTS

<u>Chapter</u>	<u>Page</u>
I. INTRODUCTION	1
II. PURPOSE AND SCOPE	4
III. OUTLINE OF ANALYTICAL METHOD	6
Estimating Driving Resistance	7
Penetration Resistance Predictions	8
Driving Time and Driven Pile Length Estimates	13
IV. ANALYTICAL TOOLS	15
The Hiley Pile Driving Formula	16
Wave Equation Analysis	18
Simulation of Hammer-pile-soil System	26
Critical Time Interval	28
Hammer	29
Capblocks and Cushions	30
Soil Properties	33
Soil Resistance	36
V. ANALYTICAL STUDIES	38
Project Selection	38
Project A	41
Project B	48
Project C	55
Project D	62
Project E	69
VI. RESULTS AND DISCUSSION	78
Predictions Using the Wave Equation and a Field Driving Record	79
Predictions Using the Hiley Formula and a Field Driving Record	83
Comparison of Wave Equation and Hiley Formula Predictions	86
Predictions Using the Wave Equation and Soil Data Only	89
Predictions Using the Hiley Formula and Soil Data Only	93

<u>Chapter</u>	<u>Page</u>
Comparison of Wave Equation and Hiley Formula	
Predictions	96
Summary	99
VII. CONCLUSIONS AND RECOMMENDATIONS	101
BIBLIOGRAPHY	104
APPENDIX	106

LIST OF TABLES

<u>Table</u>	<u>Page</u>
1. Typical secant moduli of elasticity, E, and coefficients of restitution, e, of various pile cushioning material.	33
2. Projects selected for analysis.	40
A1. Piling and hammer data, Project A.	46
A2. Computer model of hammer, piling and soil, Project A.	47
B1. Piling and hammer data, Project B.	53
B2. Computer model of hammer, piling and soil, Project B.	54
C1. Piling and hammer data, Project C.	60
C2. Computer model of hammer, piling and soil, Project C.	61
D1. Piling and hammer data, Project D.	67
D2. Computer model of hammer, piling and soil, Project D.	68
E1. Piling and hammer data, Project E.	76
E2. Computer model of hammer, piling and soil, Project E.	77
3. Statistics, by project, for ratio of predicted to mean field penetration resistance (driving record available).	87
4. Statistics, by project, for ratio of predicted to mean field penetration resistance (driving record unavailable).	97
5. Summary of statistics by method.	100

LIST OF FIGURES

<u>Figure</u>	<u>Page</u>
1. Penetration resistance versus depth (schematic).	9
2. Capacities computed from penetration resistance using pile driving formulas.	10
3. Stress wave propagation in a hammer-pile-soil system.	20
4. Mathematical model for pile driving analysis.	23
A1. Penetration resistance vs. depth for Vulcan 65C, Project A.	43
A2. Penetration resistance vs. depth for Vulcan 50C, Project A.	44
A3. Pile and boring locations, Project A.	45
B1. Penetration resistance vs. depth for Vulcan 06, Project B.	50
B2. Penetration resistance vs. depth for Vulcan 50C, Project B.	51
B3. Pile and boring locations, Project B.	52
C1. Penetration resistance vs. depth for Vulcan 014, Project C.	57
C2. Penetration resistance vs. depth for Vulcan 140C, Project C.	58
C3. Pile locations, Project C.	59
D1. Penetration resistance vs. depth for Delmag D-30, Project D.	65

<u>Figure</u>		<u>Page</u>
D2.	Penetration resistance vs. depth for Delmag D-36, Project D.	66
E1.	Penetration resistance vs. depth for Delmag D-44, 14" piles, Project E.	71
E2.	Penetration resistance vs. depth for Delmag D-44, 12" piles, Project E.	72
E3.	Penetration resistance vs. depth for Kobe K-42, 14" piles, Project E.	73
E4.	Penetration resistance vs. depth for Kobe K-42, 12" piles, Project E.	74
E5.	Pile and boring locations, Project E.	75
5.	Predicted vs. mean field penetration resistance for Projects A, C, D, E,, using field driving records and wave equation analysis.	80
6.	Statistical frequency plot for predictions made using field driving records and wave equation analysis.	82
7.	Predicted vs. mean field penetration resistance for Projects A, C, D, E, using field driving records and the Hiley formula.	84
8.	Statistical frequency plot for predictions made using field driving records and the Hiley formula.	85
9.	Predicted vs. mean field penetration resistance for Projects A, C, D, E, using wave equation analysis and soil data only.	91
10.	Statistical frequency plot for predictions made using wave equation analysis and soil data only.	92
11.	Predicted vs. mean field penetration resistance for Projects A, C, D, E, using the Hiley formula and soil data alone.	94

<u>Figure</u>		<u>Page</u>
12.	Statistical frequency plot for predictions made using the Hiley formula and soil data alone.	95

LIST OF APPENDIX FIGURES

<u>Figure</u>		<u>Page</u>
13.	Predicted vs. field penetration resistance for Vulcan 65C, Project A.	106
14.	Predicted vs. field penetration resistance for Vulcan 50C, Project A.	107
15.	Predicted vs. field penetration resistance for Vulcan 06, Project B.	108
16.	Predicted vs. field penetration resistance for Vulcan 50C, Project B.	109
17.	Predicted vs. field penetration resistance for Vulcan 014, Project C.	110
18.	Predicted vs. field penetration resistance for Vulcan 140C, Project C.	111
19.	Predicted vs. field penetration resistance for Delmag D-30, Project D.	112
20.	Predicted vs. field penetration resistance for Delmag D-36, Project D.	113
21.	Predicted vs. field penetration resistance for Kobe K-42, 14" piles, Project E.	114
22.	Predicted vs. field penetration resistance for Delmag D-44, 12" piles, Project E.	115

Figure

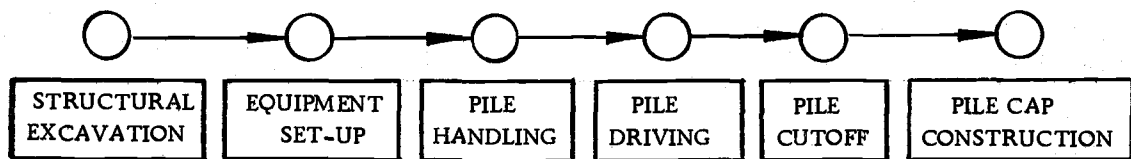
Page

- | | | |
|-----|--|-----|
| 23. | Predicted vs. field penetration resistance for
Delmag D-44, 14" piles, Project E. | 116 |
| 24. | Predicted vs. field penetration resistance for
Kobe K-42, 12" piles, Project E. | 117 |

PENETRATION RESISTANCE PREDICTIONS FOR DRIVEN PILING

I. INTRODUCTION

The elements of a typical pile driving operation are diagrammed below:



To prepare a bid, a time estimate for each of these operations is required. On most jobs reasonable estimates of all operations except pile driving can be reliably and easily made. In making an estimate of driving time, the construction contractor is faced with two principal items of uncertainty:

1. The penetration rate which can be achieved with varying types of equipment in varying types of subsurface conditions.
2. The driven length of piling required when length is not specified.

The uncertainty is lessened when the design engineer specifies either the final driven length or a pile order list. The penetration rate remains an uncertainty, and is not usually estimated in a rational manner. Often it is guessed at. If personal experience is the only

guide, the contractor may be faced with the task of extrapolating his experience to conditions other than those under which it was obtained in order to make these guesses. Experience with driving in any conditions has not been well-documented and made available to the construction industry at large. At least one attempt has been made to do so, but it has met with only limited success.

The Oregon State Highway Department (7) over a period of years has attempted to correlate Standard Penetration Test blow counts and blow counts for a miniature pile sounding device to pile driving resistance. Its intent is to devise a method of predetermining pile penetration based on actual driving records and in situ foundation soils and conditions. The limited success achieved to date is partially due to the use of the Engineering News formula for calculating driving resistance from driving records. The Engineering News formula is recognized as being inaccurate for this purpose (14).

The contractor must also consider the possibility that the driven length estimated based on requirements for capacity, and shown in contract documents, will not always correspond to the length which will be reached in the field. If piles are to be tip bearing piles driven to bedrock, where the bedrock surface is well defined, the uncertainty is reduced and the estimating task faced by the contractor involves only driving time. If the piles are

friction piles and the driven length is to be determined in the field on the basis of estimated capacity of piles from pile driving formulas, the uncertainty is compounded. The contractor, in preparing his estimate, must determine the pile length and the driving time required during construction. In essence, he is asked to determine penetration resistance of the driven pile anywhere in the soil profile. To accomplish this reliably, he must relate the pile-soil system to the driving equipment by means of some quantitative method.

II. PURPOSE AND SCOPE

The purpose of this study was to investigate the feasibility of estimating penetration resistance in blows per foot for a specific set of subsurface conditions, piling and driving equipment. A penetration resistance estimate would allow an estimate of required pile length, and subsequently an estimate of driving time.

To accomplish this a rational method of estimating penetration resistance was proposed. The method presumes the contractor having certain information available during his bid preparation. It was assumed the information available would include a complete set of soil boring records, the types of pile driving equipment available, and a reasonably complete set of driving records for the construction of pile foundations in similar subsurface conditions. Since a set of driving records is not as readily available as the other information, another method was investigated assuming this information was unavailable.

During an information gathering phase of the study, pile driving records were obtained from four projects where soil conditions were reasonably uniform and where more than one pile hammer had been used to drive the same type piling. The records included a complete physical description of the piling and the driving equipment and a record of the penetration resistance for each foot of

each pile driven. Soil conditions for each project were documented in an engineering report. A fifth project, where soil conditions were not reasonably uniform and different piling were driven by the different hammers, was included to illustrate the importance of these assumptions in the proposed method.

For each project, an analytical mechanical model of each soil-pile-hammer system was developed. Predictions of the behavior of each system model were made based on the other model on the same project using wave equation analysis. The investigation of the feasibility of estimating penetration resistance was accomplished by comparing the predicted driving record for each hammer-pile-soil system with the actual field record. Statistical parameters were determined for the comparisons to quantify the feasibility. The proposed method was investigated further by comparing the results of the method with those of a similar analysis utilizing the Hiley pile driving equation.

III. OUTLINE OF ANALYTICAL METHOD

The initial step of the proposed method is to model the soil-pile-hammer system. Initially, the driving records for a number of the same type piles driven in similar soil conditions with a given hammer are collected. The varying penetration resistance versus depth relationships are statistically reduced to a single "typical" driving record, and may be presented graphically as a plot of mean penetration resistance in blows per foot as a function of depth. A normal distribution of blow count values at any depth is assumed; hence, it is preferable to have twenty or more complete driving records.

The "typical" driven piling is also characterized. Mean values of driven length, total length, butt diameter and tip diameter are calculated for any given type of piling.

Subsurface conditions determined by borings and laboratory test results are represented. Drilling logs with identifications of soil strata are plotted. Available test data for the soil strata, such as water content, Atterberg limits, density and unconfined compressive strength, are plotted as a function of depth. Standard Penetration Resistance test N-values are plotted for the sand strata. Engineering judgement is then used in reviewing these data and formulating a model profile. The various strata are assigned

representative values of cohesion, density, and internal friction angle, based on test data or correlations with test data. In areas where subsurface conditions are reasonably uniform, developing a model profile is a relatively simple task. If, however, the subsurface conditions vary extensively, developing a model profile is a painstaking and difficult task. The method of analysis is as weak as its weakest link, hence a representative model is important.

For a given pile-soil system, the capacity of the pile at a given depth must be the same regardless of the hammer used to drive it to that depth. This basic concept allows the use of the proposed method of analysis. It should be emphasized that if uniform or at least similar subsurface conditions do not exist, the proposed method based on driving resistance computed from penetration resistance is invalid.

Estimating Driving Resistance

Driving resistance can be estimated from penetration resistance using wave equation analysis or one of many available pile driving formulas. Standard pile driving equations attempt to relate the inverse of penetration resistance, or set, to the resistance offered by the soil during driving, incorporating factors of the hammer-pile-soil system. By assuming sequential values of set, the relationship between penetration resistance and driving

resistance for any given depth and any one hammer can be determined. The one dimensional wave equation analysis calculates a similar relationship for each depth of penetration considered.

Figure 1 is a schematic representation of typical penetration resistance versus depth curves recorded during pile driving. For the purpose of this study, they are representative of the same type piling being driven in adjacent sites, or the same site, with different hammers. They are generally representative of similar ground conditions irrespective of areal location. Using plots such as either of the two shown in Figure 1 in conjunction with the driving resistance versus penetration resistance curve, the driving resistance at any depth can be determined.

Penetration Resistance Predictions

Figure 2 shows how knowledge of the penetration resistance for one hammer might be used to predict that expected for a second hammer. Having computed the two driving resistance versus penetration resistance curves, either by use of the wave equation or a conventional pile driving formula, one first determines the driving resistance corresponding to an observed penetration resistance with one hammer. Since the static resistance or capacity, which is assumed related to the driving resistance, is independent of the hammer used, the predicted penetration resistance for the

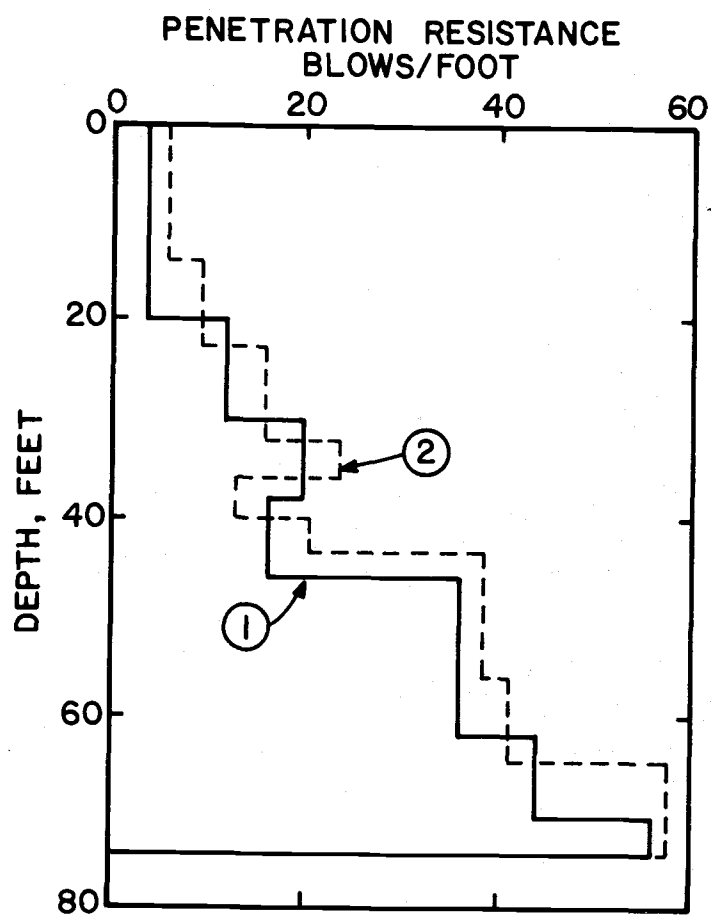


Figure 1. Penetration resistance versus depth (schematic).

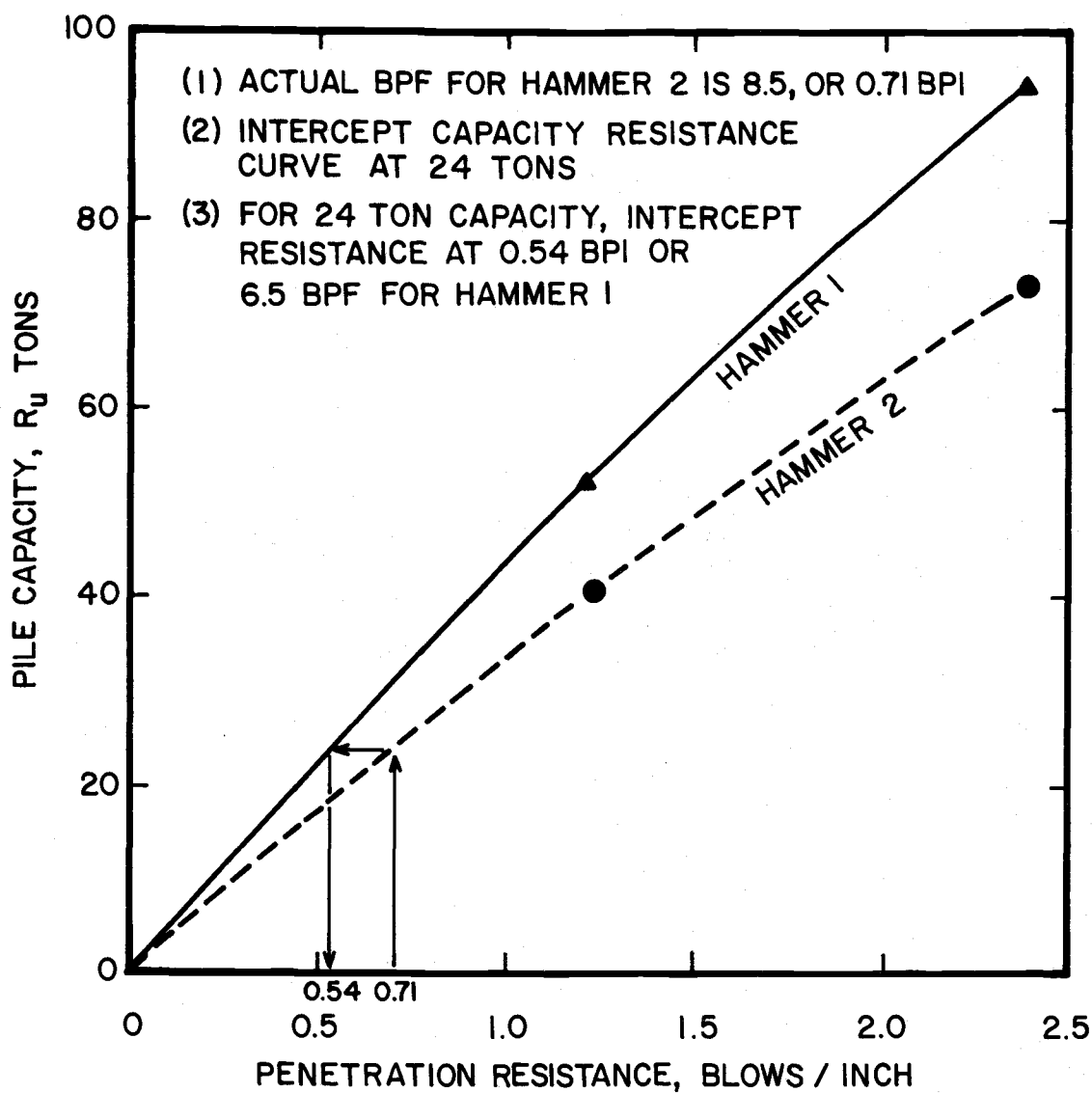


Figure 2. Capacities computed from penetration resistance using pile driving formulas.

second hammer may be determined as illustrated in Figure 2. By repeating the procedure for a sequence of penetration depths, a known penetration resistance versus depth plot such as that shown in Figure 1 may be used to predict a similar plot for another hammer.

If a known driving record is not available, the static capacity is estimated by standard methods for a desired depth of penetration. This estimate is assumed equal to the driving resistance, and is used directly with the driving resistance versus penetration resistance relationship computed by the wave equation or with a conventional pile driving formula to predict the penetration resistance.

In either case, a relationship between static capacity and driving resistance is assumed. Where a known driving record is used, the assumption is of secondary importance because a measurable parameter indicative of the dynamic behavior of the hammer-pile-soil system, penetration per blow, is used in the predictive method. Where only soil parameters are used, the validity of the dynamic analysis is more dependent on the assumption that the dynamic resistance to penetration is related to the static capacity of the pile after driving. Depending on the type of soil penetrated, a correlation may or may not be expected. For cohesive soils or fine grained loose saturated soils, pore pressure buildup is expected during driving. This generally decreases the resistance to penetration, whereas under a static load of long duration the pore pressures

dissipate and the effective stresses in the soil correspondingly change. Similarly, if the cohesive soil is sensitive, penetration changes the structure of the soil, reducing its strength and making driving easier. After a period of time, the pore pressures will dissipate and there can be a significant thixotropic regain in strength. These processes are variously termed soil freeze or set-up, and are evidenced by higher resistance to penetration on redriving a pile a few days or weeks after it was initially driven. For fine-grained saturated soils or cohesive soils, a correlation between dynamic resistance during initial driving and static resistance is not expected. In free draining soils such as medium to dense sands, however, dynamic and static resistances are more closely related, and may be equal.

In this study, sites where two hammers were used were investigated. Thus, the penetration resistance versus depth relationship for the first hammer was used to predict a similar relationship for the second hammer, and a known relationship for the second hammer was used to predict a relationship for the first hammer. Assuming the driving records were not available, estimated static capacities were used to predict penetration resistance versus depth relationships for both hammers. Because the relationship between static capacity and driving resistance is less critical to the proposed

predictive method employing a known driving record, it was expected that better predictions could be made with that method.

Driving Time and Driven Pile Length Estimates

Pile length, for piles which are tip bearing on a firm bearing stratum may be estimated reliably from soil boring records. Where friction piles are used it is common practice to specify they will be driven to some minimum depth and some minimum penetration resistance. In those cases where the final determination of pile length is made in the field, based on penetration resistance, the predicted relationship corresponding to that shown in Figure 1 is first developed using the wave equation and a known driving record. If such records are unavailable, the alternative of using an estimate of static capacity based on soil properties is used. It is necessary then only to note the depth corresponding to the penetration resistance required. The required penetration resistance may be specified for a given project based on a conventional pile driving formula. If this is the case, it is necessary to determine the required penetration resistance for the required capacity using the formula specified. This penetration resistance would then be used with the predicted penetration resistance versus depth relationship to determine the required driven length.

The driving time estimate may be made, after total required

driven length is determined, by the following procedure. Predicted penetration resistance in blows per foot for each pile segment is determined as described previously. Representative values of predicted penetration resistance are then selected for each depth over which the records are reasonably constant. The total number of predicted blows to drive to that depth is calculated. The time required is then determined from the operating rate of the hammer. These values for each pile are summed to give a total driving time estimate for the project.

IV. ANALYTICAL TOOLS

The origin of dynamic pile driving formulas is probably indicated by the apparent truism that the greater the resistance of a pile to driving, the greater should be the pile's capacity to support load. From this it is simple, if erroneous, to conclude that it is possible to calculate the capacity of a pile from a knowledge of the energy imparted by the hammer and the penetration of the pile under a hammer blow. All common pile driving formulas based on this conclusion equate the energy delivered by the hammer to the work done by the pile as its tip penetrates a distance, s , against a resistance, R , with allowances for energy losses associated with the pile driving procedure.

The method of accounting for the energy losses can be very simplistic, sometimes empirical, or complex. The Engineering News formula, for example, assumes all the energy losses occurring during each hammer blow of a single-acting steam hammer are equivalent to the work that would have been done by a penetration of 0.1 inch against the resistance R . The total of the work accomplished during the penetration, s , and the assumed lost penetration, is

$$W_h = R(s + 0.1) \quad (1)$$

where W_h is the hammer weight in the same units as R , h is the height the hammer falls in inches, and s is in inches.

The Hiley Pile Driving Formula

The Hiley formula, often called the complete driving formula, attempts to account for the energy losses in a more rational manner. It attempts to account for the temporary elastic compression of the capblock, cushion, pile and soil using the physical properties of the materials involved. It also attempts to account for the energy loss that occurs because the capblock and cushion have coefficients of restitution less than unity.

As given in Chellis (3) the Hiley formula is:

$$R_u = \frac{12e_f E_n}{s + 1/2(C_1 + C_2 + C_3)} \times \frac{W_r + e^2 W_p}{W_r + W_p} \quad (2)$$

where

R_u = ultimate resistance of pile (lbs)

W_r = ram weight (lbs)

E_n = rated energy of hammer (ft-lbs)

e_f = efficiency of hammer in delivering energy

W_p = pile weight including weights of capblock and anvil
if used (lbs)

e = coefficient of restitution

- s = final set of pile (using average of last 20 blows for all hammers other than drop hammers) (in)
- C_1 = temporary compression allowance for pile head and cap (in)
- C_2 = temporary compression of pile (in)
- C_3 = temporary compression allowance for ground (quake) (in)

Because the Hiley formula is generally recognized as being one of the better pile driving formulas, and is applicable to all hammer types, it was used in this study to provide an alternative to wave equation analysis. In order that comparisons between the methods might be made, input common to both the wave equation analysis and the Hiley formula analysis are given the same values. The quake, C_3 , has a constant value of 0.1 in, independent of soil type or difficulty of driving. Values of C_2 and C_3 are computed using the same estimates of R_u calculated for use in the wave equation analysis. Manufacturers' rated energy is used for all hammers, although Chellis (3) specifies a somewhat different relationship for double acting and differential acting steam hammers than that of Equation (2). Chellis' values of coefficient of restitution are used. These may differ from those used in the wave equation, since the wave equation requires separate values for capblock, anvil, cushion and pile.

Wave Equation Analysis

All pile driving formulas neglect the fundamental time-dependent aspects of the phenomena of stress transmission. Pile driving mechanics are not governed by the relatively simple theory of Newtonian impact.

Instead, pile driving is a problem of impact and longitudinal wave transmission that is well-represented by the wave equation (13). Application of the wave equation method of analysis requires a knowledge of static and dynamic soil properties, dimensions and material properties of the pile, and the physical properties of the pile driver and associated equipment.

Smith (15) has fully examined the wave equation as applied to pile driving analysis. Bowles (1) has also outlined the method of analysis in some depth. Therefore, the intent herein will be to review the method briefly, avoiding repetition, within the framework of the particular wave equation program used in this study. For all analysis work, the wave equation program developed by T. C. Edwards (4) at Texas A & M University was used. The program is based upon the procedure developed by Smith.

The basis for the procedure is the classical one dimensional wave equation:

$$\frac{\partial^2 u}{\partial t^2} = c^2 \frac{\partial^2 u}{\partial x^2} \quad (3)$$

where

c = velocity of propagation of a longitudinal strain along a bar, equal to $\sqrt{E/\rho}$ (ft/sec)

x = direction of longitudinal axis

u = displacement of bar cross-sectional element in x direction from its original at rest position (ft)

t = time (sec)

E = modulus of elasticity of pile material (lb/in²)

ρ = mass per unit volume of the pile material (lb/in³)

For a pile, the external resistance to motion of a segment provided by the soil must be considered. Equation (3) would then become

$$\frac{\partial^2 u}{\partial t^2} = c^2 \frac{\partial^2 u}{\partial x^2} \pm R \quad (4)$$

where R is the soil resistance. Equation (4) describes the travel of a stress wave up and down the pile as the pile is being driven. As shown in Figure 3, as ram impact occurs a compressive stress wave is developed that travels toward the pile tip at constant velocity, c . As the stress wave propagates within the embedded

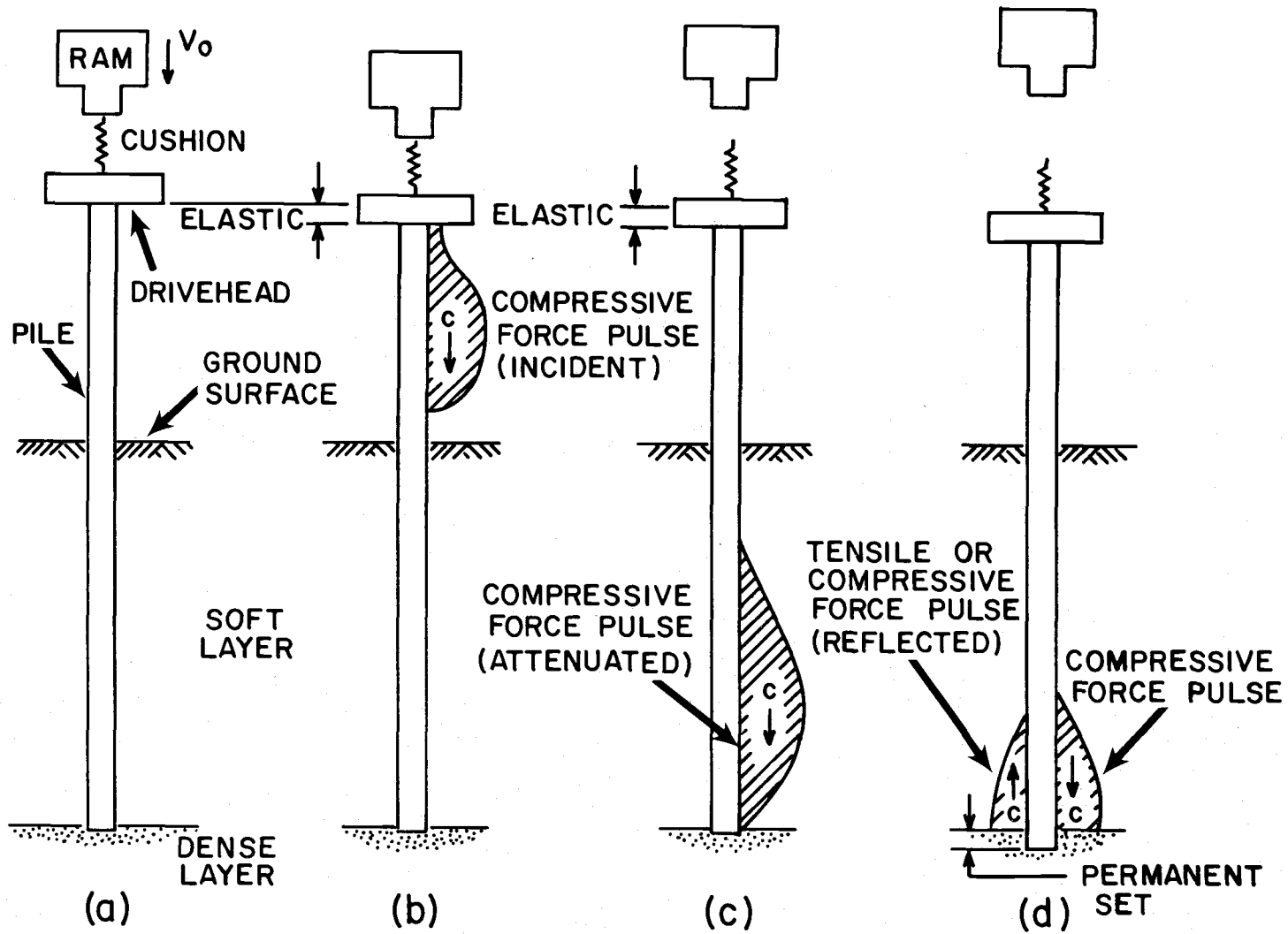


Figure 3. Stress wave propagation in a hammer-pile-soil system

portion of the pile, it is attenuated by soil resistance at the sides of the pile. When the compressive stress wave reaches the pile tip, either a compressive or tensile reflected stress wave, governed by the soil resistance at the tip, is generated. Pile penetration will occur when the peak pile force resultant of the stress wave exceeds the soil resistance.

An exact solution to Equation (4) is extremely complex. Attempts to arrive at an exact solution required the use of simplified boundary conditions including zero side soil resistance (10). Smith proposed a mathematical model of the hammer-pile-soil system and a corresponding numerical method of analysis which accounted for the same parameters which prevent a direct solution to Equation (4).

Smith's finite model simulates the soil, pile and driving equipment as a series of lumped masses connected by springs and dashpots. The hammer and pile are idealized by a system of discrete weights connected with massless springs. The springs represent the stiffness of the pile, cushion blocks and capblock, and sometimes the ram. As the weights of the cushion block and capblock are small relative to the weights of pile and ram, they are neglected and only their spring actions are considered. The soil resistance is simulated by a spring and dashpot acting on the side of each pile segment, and a spring and dashpot acting at the point. The soil is assumed massless; that is, the pile moves through the

soil and does not move the adjacent soil mass. The model is completely general. Elements can be deleted or added as necessary to model a given situation. For example, the pile cushion may be deleted or an anvil can be added between the ram and capblock.

In Figure 4, $W_{(1)}$ is the weight of the ram, $W_{(2)}$ is the weight of the pile cap, and $W_{(3)}$ through $W_{(8)}$ are the weights of each segment of pile. $K_{(1)}$ is the spring representing the stiffness of the cushion between the ram and pile cap. $K_{(2)}$ represents the combined stiffness of the cushion between the pile cap and the first pile segment, and the stiffnesses of this first element. $K_{(3)}$ through $K_{(7)}$ are the stiffnesses of the pile segments. $K'_{(5)}$ through $K'_{(8)}$ are the stiffnesses of the side soil springs, while $J'_{(5)}$ through $J'_{(8)}$ are the damping constants of the side soil spring. The slack values are indicative of the ability of a joint, or the interface between two segments, to transmit tension. Thus, the interfaces between ram and capblock, and capblock and first pile segment, which do not transmit tension, are given arbitrarily high values of 1000 inches. Interfaces between pile sections do transmit tension, and therefore have values of zero. The value of 1.25 inches for slack (5) indicates that amount of movement required before the joint is allowed to transmit tension, as may occur with some types of pile splices.

In general $W_{(m)}$ represents the weight of mass m , $K_{(m-1)}$ its spring stiffness. $K'_{(m)}$ and $J'_{(m)}$ are the side soil spring and the

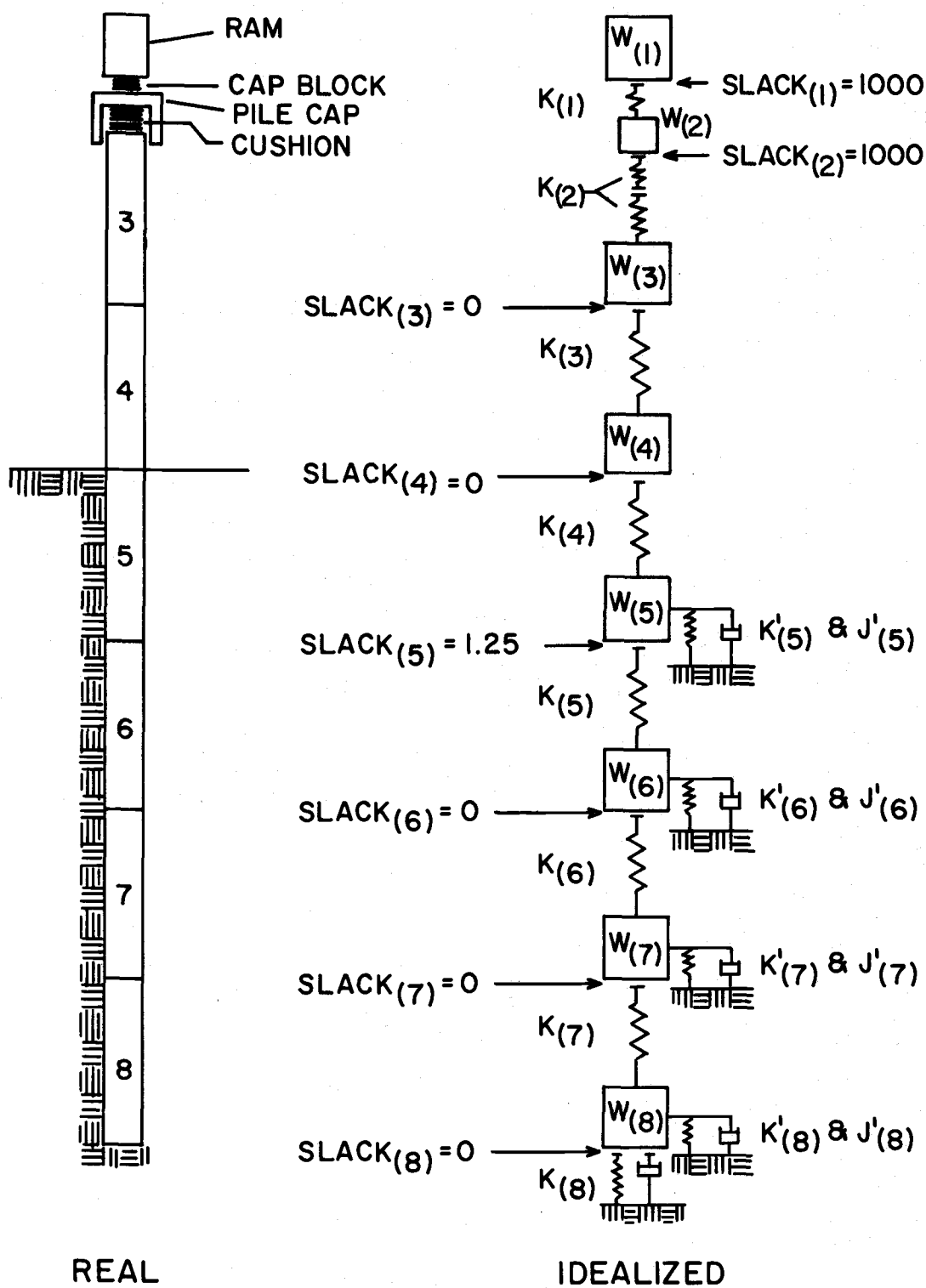


Figure 4. Mathematical model for pile driving analysis.

side damping constant acting on mass m . Slack (m) values are always associated with spring $K_{(m)}$. Idealizations for different combinations of driving equipment are given by Edwards (4).

Smith proposed a numerical solution for his model, based on a repetitive use of the following equations of motion and dynamic equilibrium that he derived for mass m :

$$D_{(m, t)} = D_{(m, t-1)} + 12 \Delta t V_{(m, t-1)} \quad (5)$$

$$C_{(m, t)} = D_{(m, t)} - D_{(m+1, t)} \quad (6)$$

$$F_{(m, t)} = C_{(m, t)} K_{(m)} \quad (7)$$

$$R_{(m, t)} = [D_{(m, t)} - D'_{(m, t)}] K'_{(m)} [1 + J_{(m)} V_{(m, t-1)}] \quad (8)$$

$$V_{(m, t)} = V_{(m, t-1)} + [F_{(m-1, t)} - F_{(m, t)} - R_{(m, t)}] \frac{g \Delta t}{W_{(m)}} \quad (9)$$

where:

m = mass number

t = time interval number in which a given value is considered

Δt = size interval (sec)

$D_{(m, t)}$ = total displacement of mass number m during time interval t (in)

- $V_{(m, t)}$ = velocity of mass m during time interval t (ft/sec)
 $C_{(m, t)}$ = compression of the spring m during time interval t
(in)
 $F_{(m, t)}$ = force exerted by spring number m between segment numbers (m) and $(m+1)$ during the interval t (lb)
 $R_{(m, t)}$ = total soil resistance acting on segment m (lb/in)
 $K_{(m)}$ = spring rate of mass m (lb/in)
 $K'_{(m)}$ = spring rate of the soil spring causing the external soil resistance force on mass m (lb/in)
 $D'_{(m, t)}$ = total inelastic soil displacement or yielding during the time t at segment m (in)
 $J_{(m)}$ = damping constant for the soil on segment number m (sec/ft)
 g = gravitational acceleration (ft/sec²)
 $W_{(m)}$ = weight of segment number m (lb)

Using equations (5), (6), (7) and (9), Bowles (1) has shown that the wave phenomena represented mathematically by equation (4) can be converted into a finite difference equation for solution by successive approximation. (The reader should note that Bowles equations 11-1, 11-2, 11-3, and 11-5 correspond to equations (5), (6), (7), and (9) herein, though the notation is changed.) This

difference equation is:

$$D_{(m,t)} = 2 D_{(m,t-1)} - D_{(m,t-2)} + \{ [D_{(m-1,t-1)} - D_{(m,t-1)}] K_{(m-1)} - [D_{(m,t-1)} - D_{(mt1,t-1)}] K_{(m)} - R_{(m,t)} \} \frac{12g \Delta t^2}{W_{(m)}} \quad (10)$$

The computations involved in the solution are outlined by Smith (15) and need not be presented here. The flowchart for the computer solution used in this study is presented with the Texas A & M program.

Simulation of Hammer-pile-soil System

The information required to simulate a given system, as modeled in Figure 4, can be categorized in three groups: the pile hammer and associated equipment, the pile, and the soil. For the pile hammer, the necessary information includes:

- 1) energy and efficiency of hammer
- 2) weight and dimensions of ram
- 3) weight and dimensions of anvil (if included)
- 4) dimensions and mechanical properties of capblocks and cushions
- 5) weight and dimensions of pile cap (or helmet)

The pile information needed includes its dimensions, weight and

mechanical properties. For the soil medium, the required information includes:

- 1) embedment of the pile
- 2) distribution of soil resistance over the embedded length of the pile expressed as a percentage of the total static soil resistance
- 3) point or pile tip soil resistance expressed as a percentage of the total static soil resistance
- 4) ultimate elastic displacement for the soil on the side and at the tip of the pile, termed Q' and Q respectively
- 5) the damping constant for the soil on the side and at the tip of the pile, termed J' and J respectively.

There are limitations and simplifications introduced in the model illustrated in Figure 4, as well as in the Texas A & M program. Further, until the wave equation is in general use, attempts to simulate specific systems will be hindered by certain of the above listed information not being recorded as part of the driving record. This will require assumptions by the analyst. Within the framework of the required input information, these factors are briefly considered in the following sections.

Critical Time Interval

Smith (15) noted that the accuracy of the numerical solution is related to the size of the time interval Δt . He expresses the critical time interval as

$$\Delta t_{cr} = \frac{1}{19.648} \sqrt{\frac{W_{(m)}}{K_{(m)}}} \quad (11)$$

where Δt_{cr} is in seconds, $W_{(m)}$ in lb, and $K_{(m)}$ in lb/in. If the time interval larger than that given by Equation (11) is used, the solution will diverge and no valid results can be obtained. This is because the numerical calculation of the finite difference stress wave does not progress as rapidly as the actual stress wave. If Δt is too small, it takes too many iterations to complete the computations.

The Texas A & M program calculates

$$\Delta t = 1/2 \Delta t_{cr} = \frac{1}{2(19.648)} \sqrt{\frac{W_{(m)}}{K_{(m)}}} \quad (12)$$

from the parameters of the system. A specific value may be input, but the program checks it against the calculated value. Bowles (1) recommends

$$\frac{\Delta t_{cr}}{2} < \Delta t < \Delta t_{cr} \quad (13)$$

as a compromise value, noting that the elements of the driving

equipment may have a different Δt than the pile segments. Smith recommends a value of $\Delta t = (1/4, 000)$ sec for steel and wood piles and $\Delta t = (1/3, 000)$ sec for concrete piles. The values calculated by the program were used in this study.

Hammer

Perhaps the most significant parameter involved in pile driving is the energy output of the hammer. Most manufacturers of pile driving equipment furnish maximum energy ratings for their hammers. These are usually modified by an efficiency factor when used by foundation engineers because of hammer condition during use, or because the energy output of many hammers can be controlled by regulating the steam pressure or quantity of diesel fuel supplied to the hammer. Based on analysis of a test pile study, Lowery, Hirsch and Samson (10) concluded that it is possible to determine reasonable values of hammer energy output simply by taking the product of the ram weight and its observed or equivalent stroke and applying an efficiency factor. For diesel hammers they suggested the equivalent stroke as being the total observed stroke minus the distance the ram moves after closing the exhaust ports and impacting the anvil. Their study indicated an efficiency of 100% as being appropriate for diesel hammers. For other hammers, they indicated values within the ranges suggested by Chellis (3).

It is generally known that diesel hammers and differential acting air-steam hammers are more efficient under hard driving conditions than during easy driving. Efficiency, then, might be expected to vary with the density or consistency of strata encountered, and would be indicated by observed stroke. Hammer strokes for each blow are not generally recorded on driving records, nor is the condition of the hammer reported. Therefore, for this study, the manufacturers' rated energy as modified by Chellis' recommended efficiency factor was used. The only exception is that an efficiency of 100% was used for diesel hammers. The Texas A & M program accounts for the work done on the pile by the diesel explosive force by using an explosive pressure. In this study, manufacturers' values for explosive force were used.

Capblocks and Cushions

Capblocks and cushions can significantly affect several aspects of pile driving. Their primary function is to limit impact stress in both the pile and hammer. In general, soft material such as wood is effective in reducing stresses, more so than a hard material such as Micarta or steel plate. However, there is a balance to be struck, as the softer material transmits a smaller percentage of the hammer's energy to the pile than a harder material.

The selection of a stiffness is important. Stiffness is given by

$$K = \frac{AE}{L}$$

where

A = crosssectional area (in²)

E = Young's Modulus (lb/in²)

L = pile length (in)

Edwards, Lowery and Hirsch (5) have reported that penetration will usually increase whenever the duration or magnitude of the impact force increases. Assuming driving energy is held constant, the duration of the force increases with either an increase in ram weight or a decrease in cushion stiffness, while the magnitude of the impact force decreases whenever the ram weight increases or the cushion stiffness decreases. While this is most important in selecting a capblock or cushion for use in a particular situation, it indicates the importance of accurately identifying the stiffness of a given capblock or cushion.

Smith (15) recommended values for material stiffness as listed below:

6" Hardwood - K = 20,000 A lb/in

4" Pine - K = 3,480 A lb/in

Micarta - K = 45,000 A lb/in

where A is the cross-sectional impact area, and the grain is vertical for the wood. Smith also proposed a linear stress-strain relationship be used, though he recommended investigation of a non-linear relationship for dynamic loading.

Edwards, Lowery and Hirsch (5) experimentally investigated the stress-strain relationship of several cushion materials under dynamic loading, and found a non-linear relationship. They found that the properties changed as the cushion was struck and that these properties stabilized at about the same number of blows required to stabilize the permanent deformation. Hirsch, Lowery, Coyle and Samson (8) found that a pile cushion possessing non-linear stress-strain behavior can be adequately represented by a simple linear relation for the loading and unloading phases so long as the loading portion was based on the secant modulus of elasticity for the material (as opposed to the initial, final, or average modulus of elasticity), and the unloading portion was based on the actual dynamic coefficient of restitution. Recommended values of secant modulus, E , and coefficient of restitution, e , reported by Hirsch, et. al. are listed in Table 1.

The Texas A & M program utilizes a linear stress-strain relationship, rather than a non-linear relationship, due to the difficulty of imputing the information required by the wave equation. The program manual (4) includes formulas for calculating combined

stiffness of spring elements in series, such as cushion and first pile segment in Figure 4. It also includes methods for determining the combined coefficient of restitution for spring elements in series.

Table 1. Typical secant moduli of elasticity, E , and coefficients of restitution, e , of various pile cushioning material.

Material	E , psi	e
Micarta plastic	450,000	0.80
Oak (green)	45,000	0.50
Asbestos disks	45,000	0.50
Fir plywood	35,000	0.40
Pine plywood	25,000	0.30
Gum	30,000	0.25

Soil Properties

True soil resistance to dynamic loading is not clearly understood. Several assumptions are made in the wave equation analysis. Equation (8) presented previously describes the spring-dashpot rheological model assumed. The soil spring behaves elastically until the deformation equals the quake Q , and then it yields plastically. The dashpot, with viscous damping constant J , develops a resisting force proportional to the velocity of loading V , accounting for the effects of dynamic loading. The general expression

for the spring constant is

$$K = \frac{R_u}{Q}$$

where R_u is the static soil resistance, lb, and Q is the quake, in.

At the pile tip only compressive loading is allowed, but at the sides the soil can be loaded in tension or compression.

The input values required by the numerical solution are Q (in) and J (sec/ft) for the soil at the pile tip and Q' (in) and J' (sec/ft) for the pile sides. The actual values of these constants are not known. The value of quake is assumed to be the same in both friction and point bearing, thus $Q=Q'$ is generally used. Smith (15) recommends a value of 0.10 for Q , citing a probably range of 0.05-0.15.

The damping constant in point bearing is assumed larger than in friction, as at the pile tip the soil is pushed aside, resulting in viscous action, while at the sides of the pile only relative movement is involved. Smith proposed in 1960 that $J' = 1/3J$. In the ensuing 15 years, this assumption has been neither proved nor disproved. The damping constant varies more with soil type than does the quake. Forehand and Reese (6) recommend values of 0.10 to 0.4 for sands, and 0.5 to 1.0 for cohesive soils. In correlating wave equation studies with load tests on clays, they arrived at possible combinations of Q and J to use:

$Q=0.1$ with $J=1.0$ and $Q=0.2$ with $J=0.15$ to 0.8 .

Lowery, Edwards and Hirsch (9), in a similar correlative study, found $J=0.1$ for sands and $J=0.3$ for clays resulted in the least deviation between actual and predicted soil resistance. However, for cohesive soils they accounted for freeze or set-up by increasing predicted soil resistances by a factor of 2.0.

Qualitatively, Forehand and Reese (5) found that increasing the ground quake increases the set in blows per inch for a given soil resistance. Lowery, Hirsch and Samson (10) in a wave equation parameteric study determined the same relationship, but found the percent increase is small for small soil resistances (200 kips or less) and large for large soil resistances. Parola (13) determined that the effect of quake in reducing driving capability is more pronounced at high pile impedances or areas ($6000 \frac{\text{lb-sec}}{\text{in}}$ or greater). Parola also found that a damping increase decreases driving ability for all pile impedances.

Lowery et. al (9) in a study comparing pile load test results with wave equation analysis verified a particularly useful method for inputting damping constants for sand-clay systems. Using values of $J=0.1$ for sand and $J=0.3$ for clay, they proportioned the input J relative to the type of soil surrounding the pile. The results varied from -32% error to +27% error when compared to load test resistance corrected for set. These values of J for sand and clay were used in the same manner for this study.

Soil Resistance

The Texas A & M program has two options available for inputting static soil resistance, R_u . The soil resistance can be entered for each segment as a percentage of the total soil resistance. The type of distribution for each segment (uniform or triangular) can also be entered. Thus, non-uniform subsurface profiles can somewhat be accounted for. The second option is to input only the percentage of total soil resistance acting at the pile tip. In either case, an estimate of the total static soil resistance is required.

The relative percentages of side and tip soil resistance are sensitive parameters in wave equation analysis. Forehand and Reese (6) found that increasing the percentage of total resistance at the side by 25% caused dramatic decreases in blows per inch for a given ultimate ground resistance for light (12 BP 53) piles. For heavier piles the effect was less pronounced and in some cases negligible. Bowles (1) similarly found that the pile set or penetration resistance depends heavily on the assumed point resistance, as well as the assumed ultimate pile resistance R_u . He found that varying the percent point load from 0 to 75 percent can vary the set 50 to 100 percent, and that increasing R_u by a factor of two will reduce the set as much as 95-100 percent. It is evident, then, that

reasonable care must be taken in estimating the total soil resistance R_u , as well as the relative resistance at the sides and point of the pile.

V. ANALYTICAL STUDIES

Project Selection

The work proposed for this study was preceded by an information gathering phase. Various consulting firms, construction companies and public agencies on the West Coast were contacted to assist with obtaining records for pile driving projects. The records required for this study were to be more comprehensive than those normally maintained on construction projects. They were to include a complete physical description of the piling and the driving equipment and a record of the penetration resistance for each foot of each pile driven. Soil conditions for each project were to be thoroughly documented in an engineering report.

A secondary criterion was to select projects representing a range of soil conditions, hammer types and energies, and pile types. Particular consideration was given to those sites where the energies of the hammers used differed significantly. Since it was felt impractical to analyze a large number of projects, a few projects representing the range of hammer-pile-soil systems encountered in practice were selected.

From the available data located, nine projects were selected for final consideration. Five were selected for the detailed

analyses presented in this study. An outline of these projects is presented in Table 2. Even with the selection process, not all criteria were met for each project. Site B was not analyzed completely as the criteria of similar subsurface conditions was not met. Both treated timber and steel pipe piles were driven at project B. Other less serious discrepancies are noted in the following detailed descriptions of the five projects. Each description is accompanied by mean driving records for each hammer, a site plan for the project, soil profile model, hammer and piling data table, and wave equation model of the hammer-pile-soil system. Predicted points are included on the driving records to avoid repetition of the plots in the appropriate section of this study.

Table 2. Projects selected for analysis.^a

Project Designation	Pile Hammers	Pile Types, (Number)	Soil Profile
A Portland, Oregon	Vulcan 50C Vulcan 65C	10" steel pipe, (25) 10" steel pipe, (167)	Silt
B Portland, Oregon	Vulcan 50C Vulcan 65C	Timber, (200) 10" steel pipe, (23)	Sand, silt, clayey silt
C Seattle, Washington	Vulcan 104C Vulcan 014	16-1/2" concrete, (28) 16-1/2" concrete, (27)	Silt, sand
D Richmond, California	Delmag D30 Delmag D36	14" concrete, (5) 14" concrete, (6)	Clay, sand
E South San Francisco California	Kobe K42 Delmag D44	12"/14" concrete, (24) 12"/14" concrete, (107)	Silt, clay, sand

^aProject identification by owner and specific location has been omitted by request.

Project A

Project A involved driving 10 inch nominal diameter steel pipe piling 15 to 30 feet through silt fill and in situ sandy silt to end bearing in decomposed or weathered bedrock. Differential acting steam hammers were used. Details of piling and hammer are listed in Table A1.

The 192 piles analyzed represent approximately 20 percent of the total number driven. As noted in Figure A3, those piles analyzed were located on the west side of the retail structure. The bedrock surface slopes from east to west as indicated by the mean driving records, Figures A1 and A2. A few of the piles driven by the Vulcan 65C began penetrating the weathered bedrock at a depth of 15 feet, as indicated by the significant increase in maximum blow count for that depth. Similar increases were not noted for the group of piles driven by the Vulcan 50C until a depth of 20 feet was penetrated. As this study is not concerned with end bearing, comparisons are made only where comparisons are relevant. Thus, comparisons of penetration resistance are made only to a depth of 20 feet, or until the effect of some piles in the group being driven in bedrock becomes significant. Similarly, to include piles located outside the area indicated in Figure A5 would impose the effect of driving in bedrock on the mean driving record for the Vulcan 65C, invalidating a comparison.

Soil static capacity analyses were made using parameters of $\phi = 34^{\circ}$ and $c = 0$. These soil indices were used by the project consultant in his analysis. The alternative of using a $\phi = 0$ analysis was considered. It was found that for the low soil resistances encountered, either approach could be employed. In the analysis, Terzaghi bearing capacity factors were used, and a triangular soil resistance distribution along the side of the pile was assumed. The on-site silts used as fill were assumed to have the same soil indices as the in situ sandy silts.

The driven length of piling varied from 25 to 60 feet, due to continuous cutoff and splicing procedures. Steel plates with welded H-pile sections were welded to the pile tips to afford penetration into the weathered bedrock. To conform, the analyses made assumed closed end piles, though the weight of the bearing attachments was neglected.

The spring stiffness of the combined capblock was determined assuming the steel plate and cable coils acted in series. The stiffness for the plate was calculated in a standard fashion, while that for the cable coil was assumed after contacting a local consulting firm to determine their experience with similar material.

The weight of the pile cap was assumed, based on descriptions provided by the construction contractor. Manufacturers equipment manuals were also consulted.

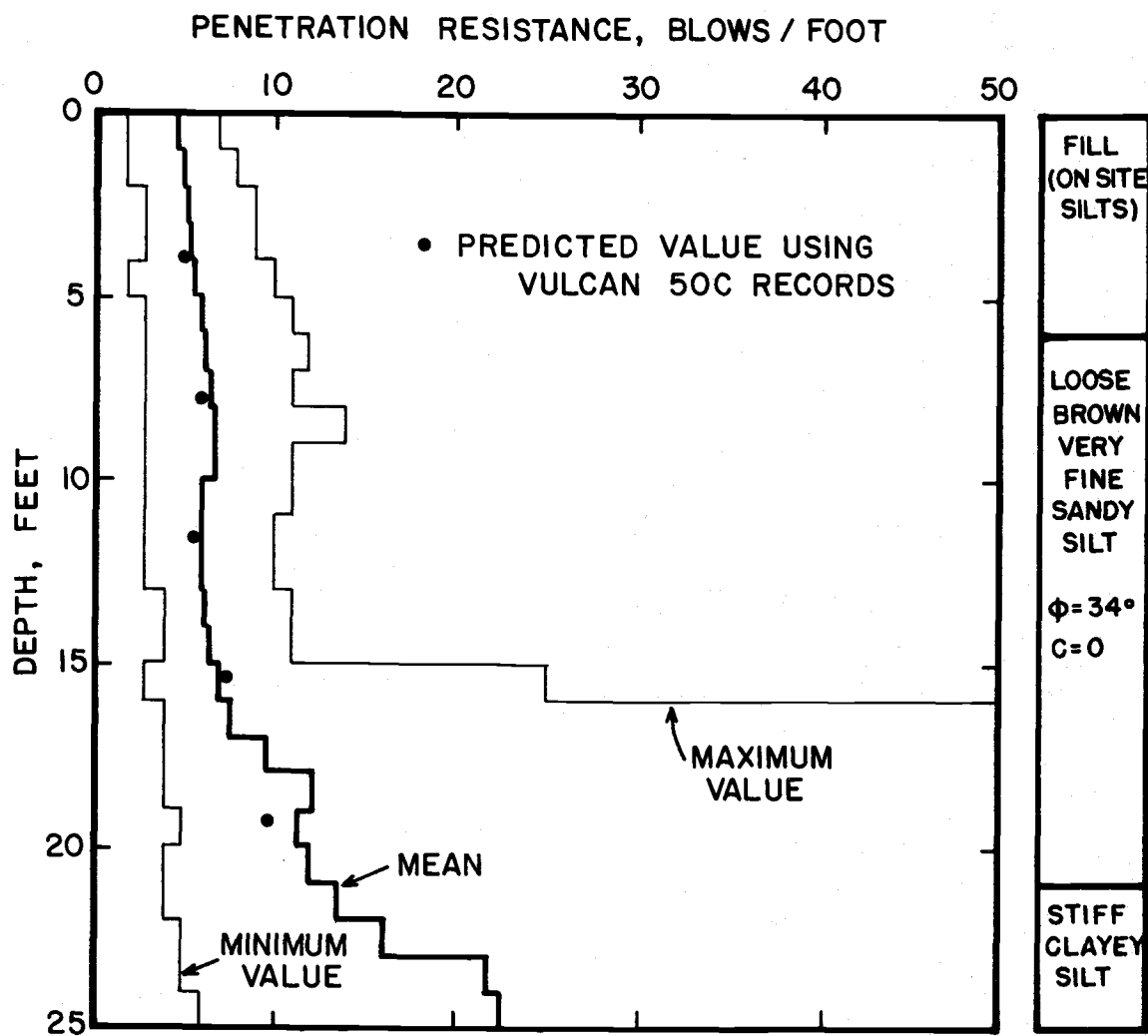


Figure A1. Penetration resistance vs. depth for Vulcan 65C, Project A.

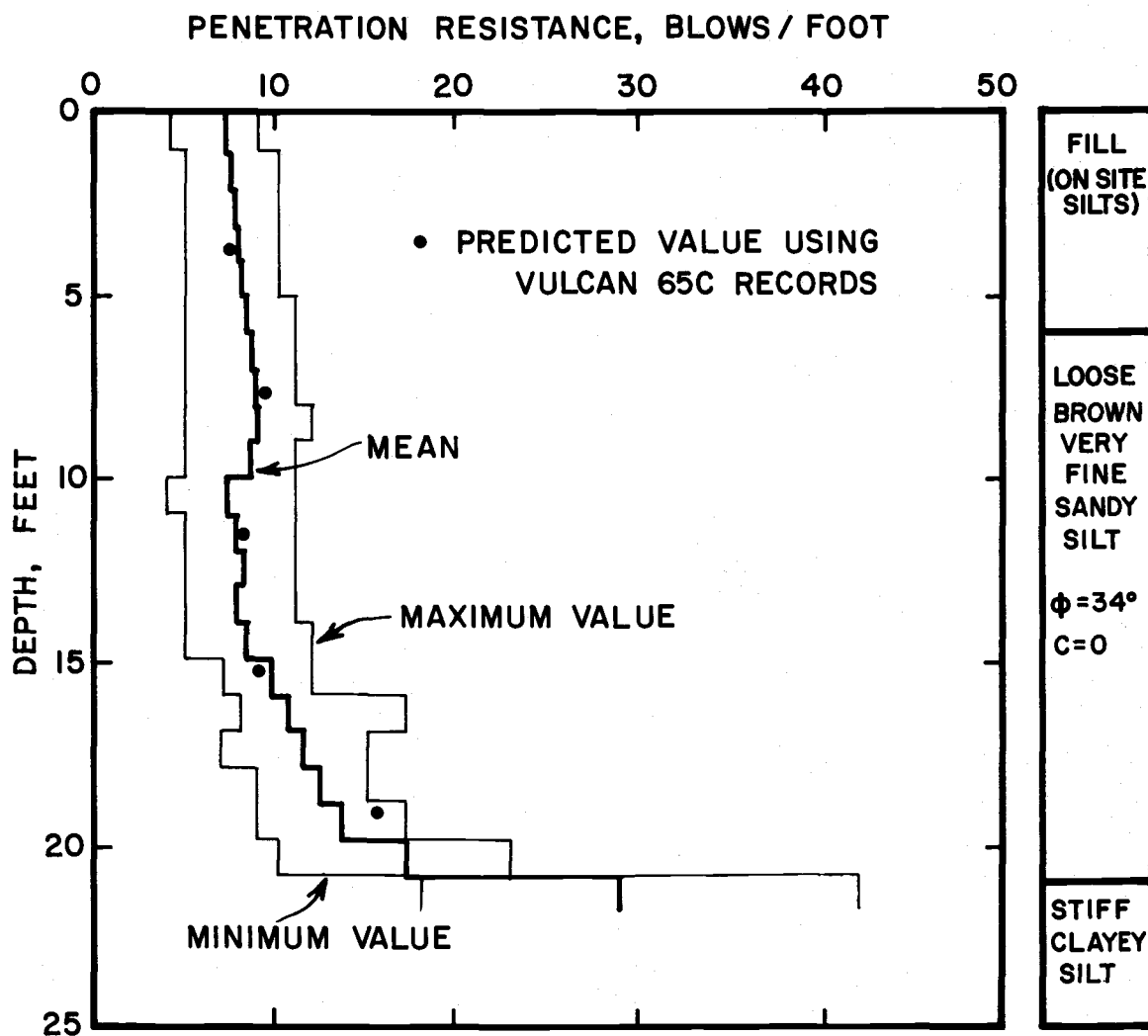


Figure A2. Penetration resistance vs. depth for Vulcan 50C, Project A.

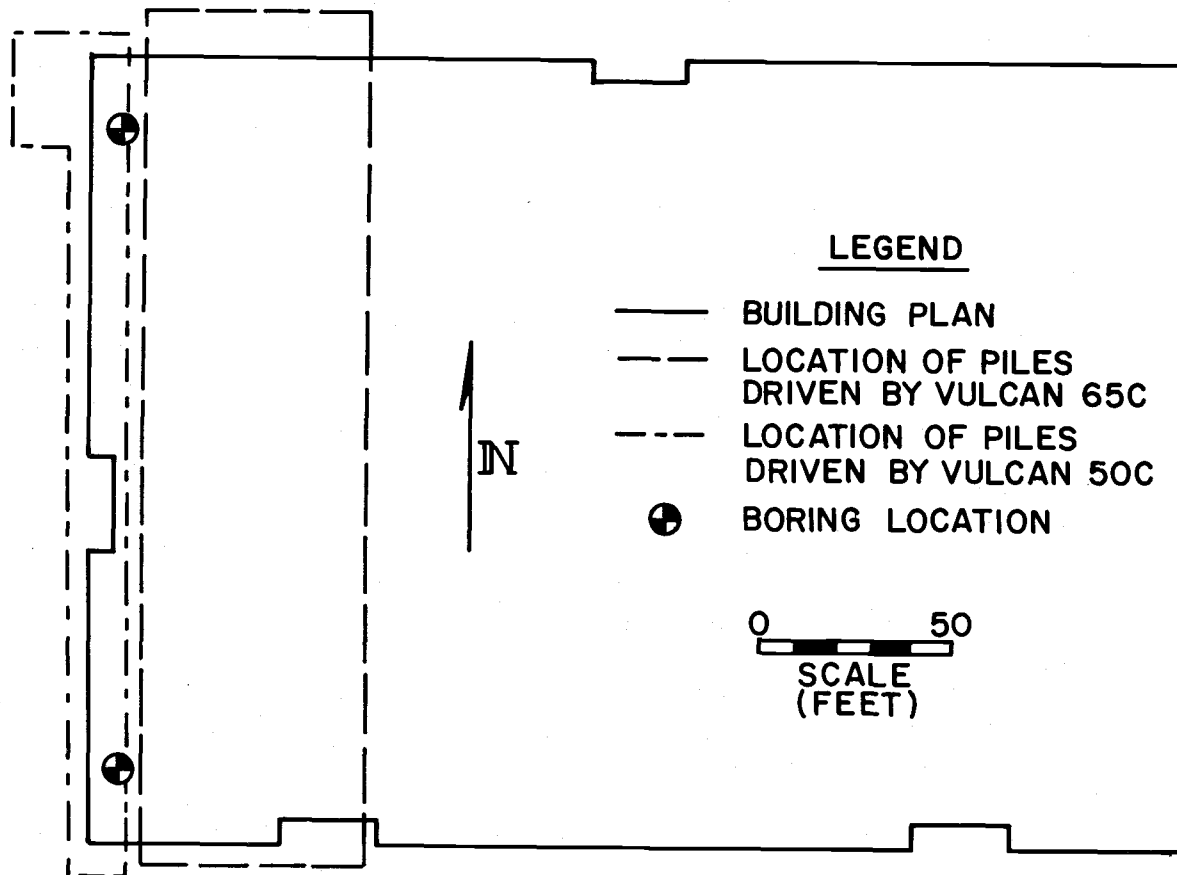


Figure A3. Pile and boring locations, Project A.

Table A1. Piling and hammer data, Project A.

HAMMER	VULCAN 65C	VULCAN 50C
Type	Diff. Air/Stream	Diff. Air/Stream
Rated Energy, Ft-Lb	19, 200	15, 100
Ram Weight, Lb	6, 500	5, 000
Capblock	3/4" Steel Plate over 3" of coiled 1" cable	3/4" Steel Plate over 3" of coiled 1" cable
Pile Cap	Shop built or standard tool	Shop built or standard tool
Pile Capweight, Lb	350	350
PILING: 10.75" outside diameter, 0.188" wall thickness, A-36 Steel Pipe, with welded end plates		
Length:		
Number of Records	167	25
Mean Length, Ft	38.1	53.6
Standard Deviation, Ft	8.5	6.2
Max. Length, Ft	60	60
Min. Length, Ft	25	37
Penetration:		
Number of Records	164	25
Mean Penetration, Ft	23.2	21.1
Standard Deviation, Ft	4.1	1.5
Max. Penetration, Ft	29.6	23.2
Min. Penetration, Ft	17.0	18.6

Table A2. Computer model of hammer, piling and soil, Project A.

HAMMER	VULCAN 65C	VULCAN 50C
W(1), Lb (Ram)	6,500	5,000
W(2), Lb (Pile Cap)	350	350
K(1), Lb/in (Capblock)	4.1×10^6	4.1×10^6
e(1) (Capblock)	0.50	0.50
e(2) (Pile Cap)	0.50	0.50
Energy, Ft-lb	19,200	15,100
Efficiency	1.00	1.00
PILING		
Length, Ft	38.3	53.7
Max. Penetration, Ft	23.0	23.0
For 46 in. Sections:		
W(3) - W(12), Lb	81.3	
W(3) - W(14), Lb		81.3
K(3) - K(11), Lb/in	4.07×10^6	
K(3) - K(13), Lb/in		4.07×10^6
e for Piling	0.50	0.50
SOIL CONSTANTS		
Q	0.10	0.10
Q'	0.10	0.10
J	0.15	0.15
J'	0.05	0.05

Project B

Project B includes two driving sites separated by a distance of approximately 1100 feet, as shown in Figure B3. The piling at both sites were driven through alluvial deposits of fine sands, silts and clayey silts to friction bearing in sands and sandy silts.

Blowcounts were not recorded for the upper strata, but were recorded continuously after a depth of 40 to 45 feet was reached. Mean driving records are shown in Figures B1 and B2.

Project B presented the most diverse soil-pile-hammer system of the five projects selected for analysis. At the south site, treated timber piles were driven using a differential acting steam hammer, while at the north site steel pipe piles were driven using a single acting steam hammer. As indicated by the mean driving records, dissimilar subsurface conditions existed at the two sites. Representative soil models were developed using particularly complete boring logs and extensive laboratory test results. Profiles were difficult to model, even with this input, as conditions varied extensively at each site. The range of blow counts recorded for any given depth, particularly at the South site (Vulcan 50C), is indicative of the varying nature of subsurface conditions.

Predictions were made, however, to illustrate the possible pitfalls of the proposed method of analysis. Comparing the mean

values of penetration resistance with predicted values stresses the importance of similar subsurface conditions to the proposed method of analysis. As it did not meet the criteria established for the study, Project B was not further analyzed.

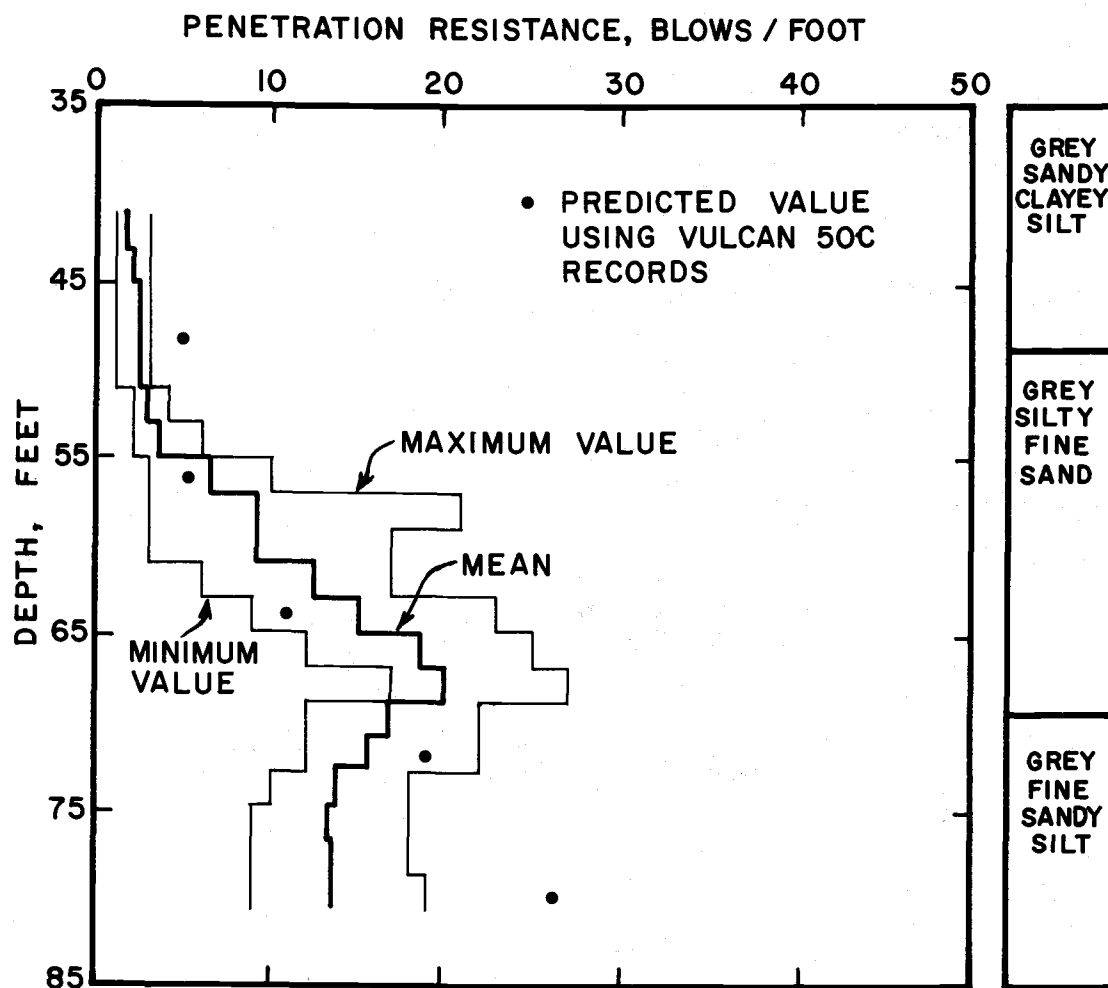


Figure B1. Penetration resistance vs. depth for Vulcan 06, Project B.

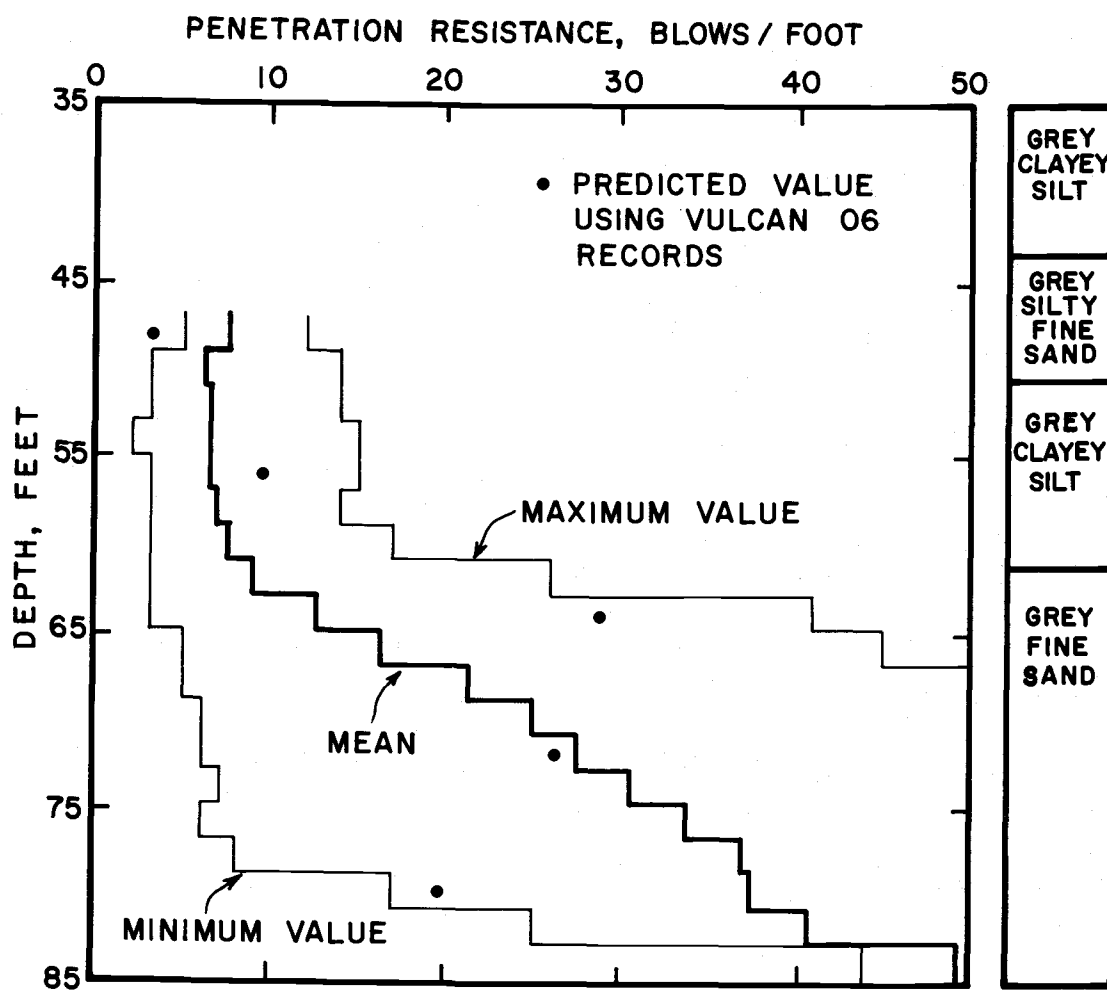


Figure B2. Penetration resistance vs. depth for Vulcan 50C, Project B.

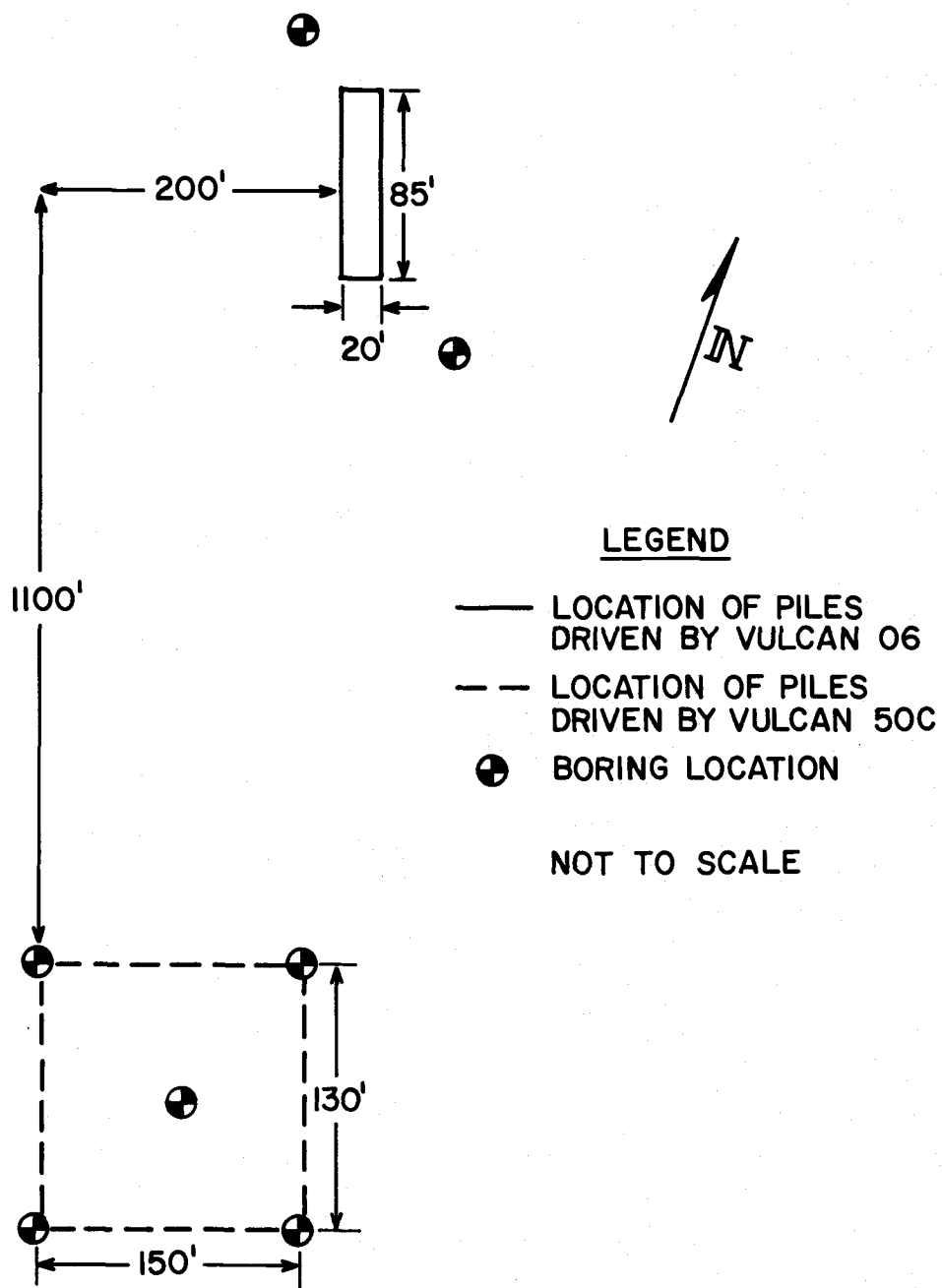


Figure B3. Pile and boring locations, Project B.

Table B1. Piling and hammer data, Project B.

HAMMER	VULCAN 06	VULCAN 50C
Type	Sngl. Air/Stream	Diff. Air/Stream
Rated Energy, Ft-Lb	19, 500	15, 100
Ram Weight, Lb	6, 500	5, 000
Capblock	Coiled Wire Rope	1-3/4" thick steel plate
Pile Cap	Vulcan Standard	None
Pile Cap Weight, Lb	1, 000	--
Cushion	None	None
PILING:	10.75" O.D. x 0.25" w.t. steel pipe with end plate	Treated timber
Length		
Number of records	23	200
Mean Length, Ft.	79.7	81.7
Standard Deviation Ft.	10.3	3.25
Min. Length, Ft.	67	75
Max. Length, Ft.	97	85
Tip Circumference		
Number of Records	-	181
Mean Circumference, in.	-	22.7
Standard Deviation, in.	-	3.5
Min. Circumference, in.	-	18
Max. Circumference, in.	-	36
Penetration		
Number of records		192
Mean Penetration, Ft.	Same	76.9
Standard Deviation, Ft.	as	5.4
Min. Penetration, Ft	Length	66
Max. Penetration, Ft.		83

Table B2. Computer model of hammer, piling and soil, Project B.

HAMMER	VULCAN 06	VULCAN 50C
W(1), Lb (Ram)	6, 500	5, 000
W(2), Lb (Pile Cap)	1, 000	--
K(1), Lb/in (Caplock)	2.38×10^6	2.62×10^6
K(2), Lb/in (Pile Cap-Pile)	2.6×10^6	--
e(1) Capblock	0.5	0.6
Energy, Ft-Lb	19, 500	15, 100
Efficiency	0.80	0.80
PILING		
Length, Ft	80	80
Max, Penetration, Ft	80	80
For 8-Ft Sections		
W(2) - W(11), Lb		270-90
W(3) - W(12), Lb	223	
K(2) - K(10), Lb/in		2.38×10^6 to 0.86×10^6
K(3) - K(11), Lb/in	2.6×10^6	
e for Piling	0.6	0.5
SOIL CONSTANTS		
Q	0.10	0.10
Q'	0.10	0.10
J	0.15	0.15
J'	0.05	0.05

Project C

At Project C, 16.5 inch octagonal prestressed concrete piles were driven on the outboard side of a dike constructed of black medium sand. The friction piles were to support a road and loading area extending over the slope of the dike. Hence, the piling at each bent varied from 65 to 120 feet in length. As this is too broad a range to realistically model, only the piling penetrating along the dike slope were included in the analysis. Their lengths varied from 120 feet at the outboard side of the areas shown in Figure C3 to 102 feet at the inboard side. Limiting the length variation further would have decreased the number of piling analyzed, as a limited number of driving records were available.

The dike was constructed after 10 to 30 feet of unsuitable grey soft silt was excavated. The dike was constructed of black sand underlying the silt, placed hydraulically. Boring logs of the in situ sand were available. However, data indicating the density of the sand as placed in the dike was not available. The driving logs, Figures C1 and C2, are plotted as a function of depth, rather than elevation, partially eliminating the effects of initial penetration occurring at different points on the outboard slope. The wide range of blow count values is probably resultant of the variable density and composition of the dike sand, as well as the variability of the

depth at which in situ sand is encountered.

Information concerning capblocks and helmets was not available, though a complete physical description of the cushion was obtained. A standard helmet for concrete piles, listed in the hammer manufacturer's catalog, was assumed. As noted in Table C1, a 3 inch thickness of fir was assumed for the capblock. To justify the assumption, a parametric study of cushion stiffnesses varying from 2,000,000 to 300,000,000 lb/in (equivalent thicknesses of 0.75 in to 113 in) was made. The study indicated that for total soil resistances equal to or less than 300 tons, cushion stiffness had no effect. The assumed stiffness listed in Table C2 is well within the range of the stiffnesses investigated, and the soil resistance for blow counts shown in Figures C1 and C2 is on the order of 50 tons.

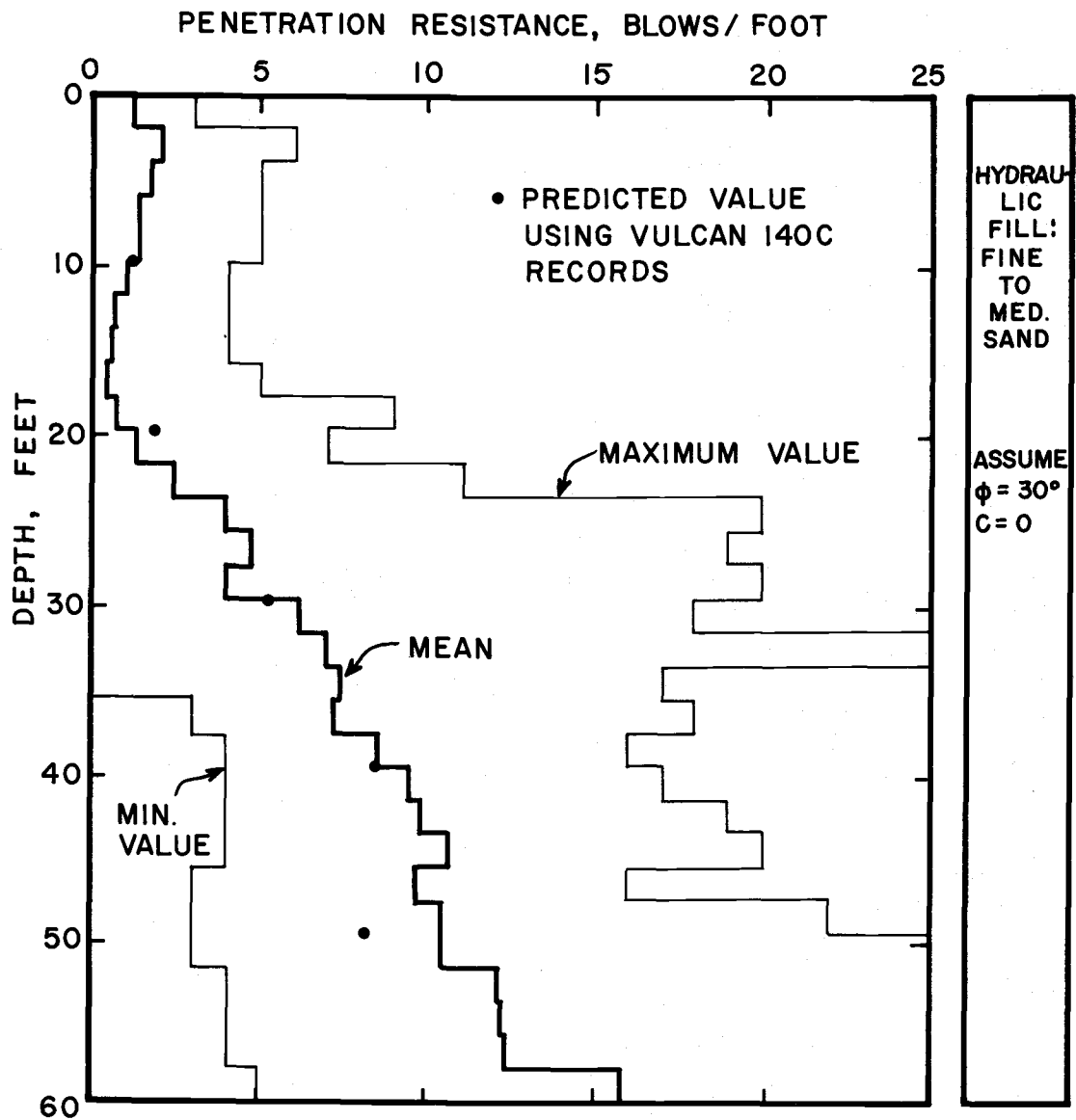


Figure C1. Penetration resistance vs. depth for Vulcan 014, Project C.

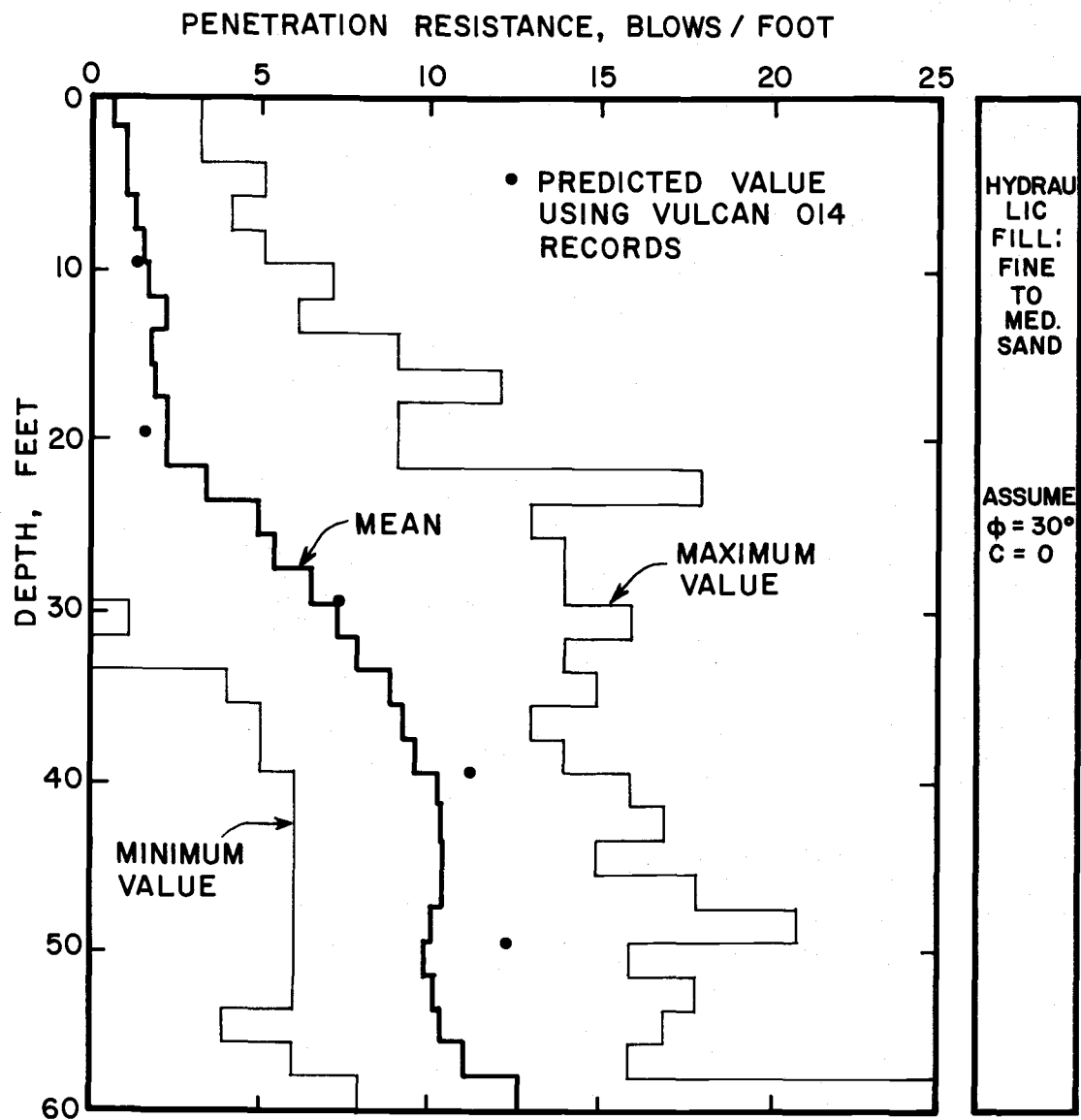


Figure C2. Penetration resistance vs. depth for Vulcan 140C, Project C.

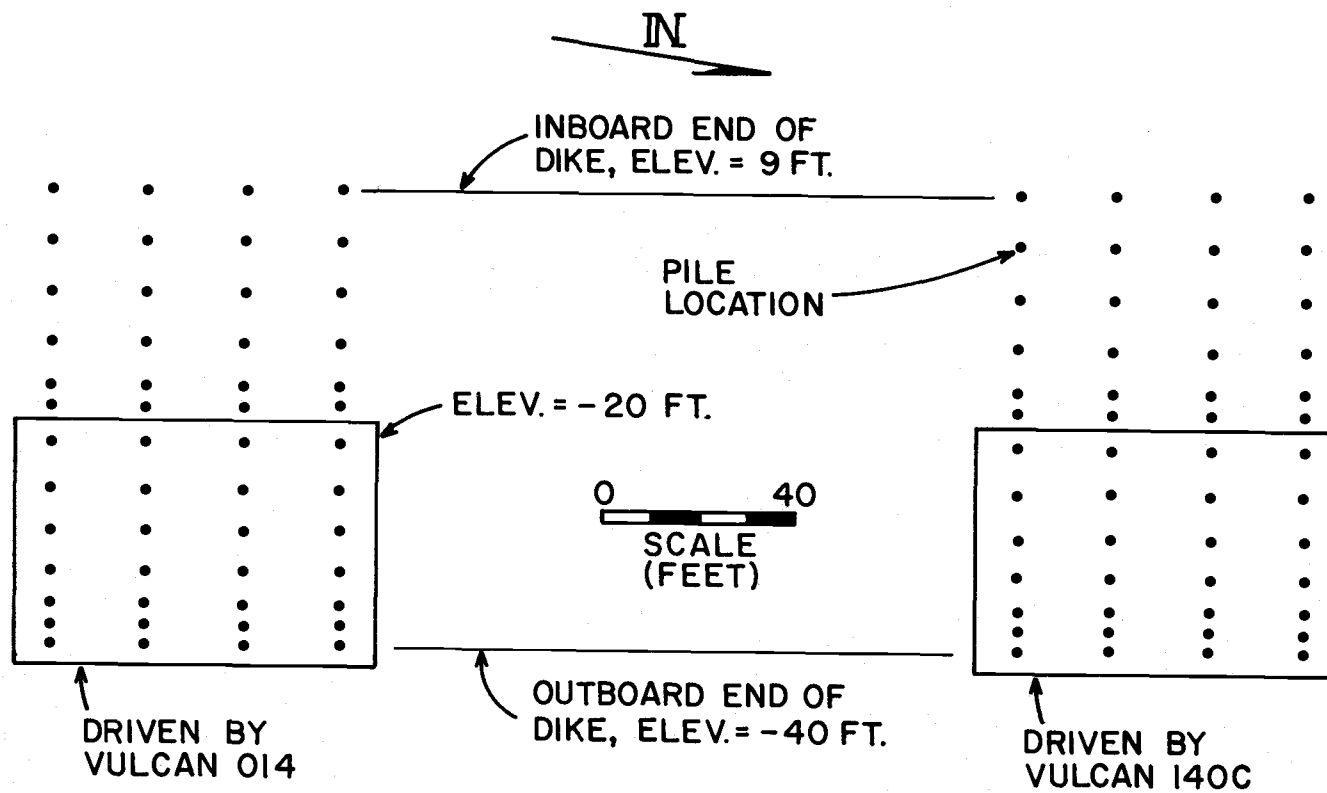


Figure C3. Pile locations, Site C.

Table C1. Piling and hammer data, Project C.

HAMMER	VULCAN 014	VULCAN 140C
Type	Sngl. Air/Stream	Diff. Air/Stream
Rated Energy, Ft-Lb	42,000	36,000
Ram Weight, Lb	14,000	14,000
Capblock	Assume 3" thickness of fir	Assume 3" thickness of fir
Helmet	Assume standard Vulcan Model	Assume standard Vulcan Model
Helmet Weight, Lb	1,710	1,710
Cushion Block	4-1/2" thickness of laminated green fir	4-1/2" thickness of laminated green fir
PILING: 16.5" Octagonal Prestressed Concrete		
Length		
Number of records	27	28
Mean Length, Ft	111.9	112.3
Standard Deviation, Ft	7.5	7.8
Max. Length, Ft	120	120
Min. Length, Ft	102	100
Penetration		
Number of records	27	28
Mean Length, Ft	71.3	71.8
Standard Deviation, Ft	6.2	4.7
Max. Length, Ft	81	80
Min. Length, Ft	63	65

Table C2. Computer model of hammer, piling and soil, Project C.

HAMMER	VULCAN 014	VULCAN 140C
W(1), Lb (Ram)	14,000	14,000
W(2), Lb (Helmet)	1,710	1,710
K(1), Lb/in (Capblock)	30×10^6	30×10^6
K(2), Lb/in (Cushion-Pile)	11.1×10^6	11.1×10^6
e(1) (Capblock)	0.35	0.35
e(2) (Cushion)	0.35	0.35
Energy, Ft-Lb	42,000	36,000
Efficiency	0.90	0.84
PILING		
Length, Ft	110	110
Max. Penetration, Ft	50	50
For 10 ft. Sections:		
W(3) - W(13), Ft	2,340	2,340
K(3) - K(12), Lb/in	14.3×10^6	$143. \times 10^6$
e for Piling	1.00	1.00
SOIL CONSTANTS		
Q	0.10	0.10
Q'	0.10	0.10
J	0.10	0.10
J'	0.03	0.03

Project D

Project D involved driving 12 inch square, approximately 66 foot long prestressed concrete piles through alternating strata of clay and sand. The piles were indicator piles, driven near locations of previous borings. Thus a boring log was available for each pile driving record. However, only 11 records were available for analysis. This limits the analysis, given the variability of the soils encountered.

The piles were driven at the excavated site for a multistory office building. Zero depth on the mean driving records, Figures D1 and D2, corresponds to the excavated depth of 20 foot at the site. As noted in Table D1, it was assumed the piles were driven to their full length. Information concerning order length was not available, though the purpose of the piling analyzed somewhat supports the assumption.

As illustrated by the model soil profile, several very different strata were encountered during driving. The location of the strata varied considerably from one pile location to another, as noted by the range of blow counts at any given depth. This is particularly noticeable when the sandy gravel and fine sand strata are encountered. The availability of very complete boring logs and laboratory test results lent confidence to the task of developing a representative

model. Water contents and densities were determined from samples taken at five foot intervals. Where cohesive soils were sampled, unconfined compressive strengths were determined.

Static capacity at any depth was calculated assuming ideal sands (ϕ' , $c=0$) or ideal clays ($\phi=0$, c). The side resistance distribution, then, was varied, which complicates the input data for the wave equation analysis. The side resistance was plotted as a function of depth, and it was decided to use a uniform distribution throughout. The alternative is to use non-uniform pile segments in the pile model, distributing an assumed total soil resistance to the segments proportionate to static capacity estimates, and repeating several times for each depth of penetration to develop the necessary penetration resistance versus capacity relationships. This procedure requires many more computer runs for little probable increase in accuracy.

Similarly, the soil constants J and J' were assigned values dependent on the strata encountered. A weighted value method was employed, based on values of $J=0.30$ for clays and 0.10 for sands ($J'=I/3J$). Referring to Figure D1 and D2, for a depth of embedment of 30 feet, 8 feet of sand and 22 feet of clay has been encountered. The damping constant, J , would then equal

$$(8/30)(0.10)+(22/30)(0.30)=0.25.$$

Of particular interest is the relative magnitudes of the rated

energies and explosive energies of the two hammers used. As can be calculated from data in Table D1, the energy ratios are approximately 1.6. This is unusually large, as contractors seldom need to make dramatic changes in driving equipment at a given site for driving the same piling.

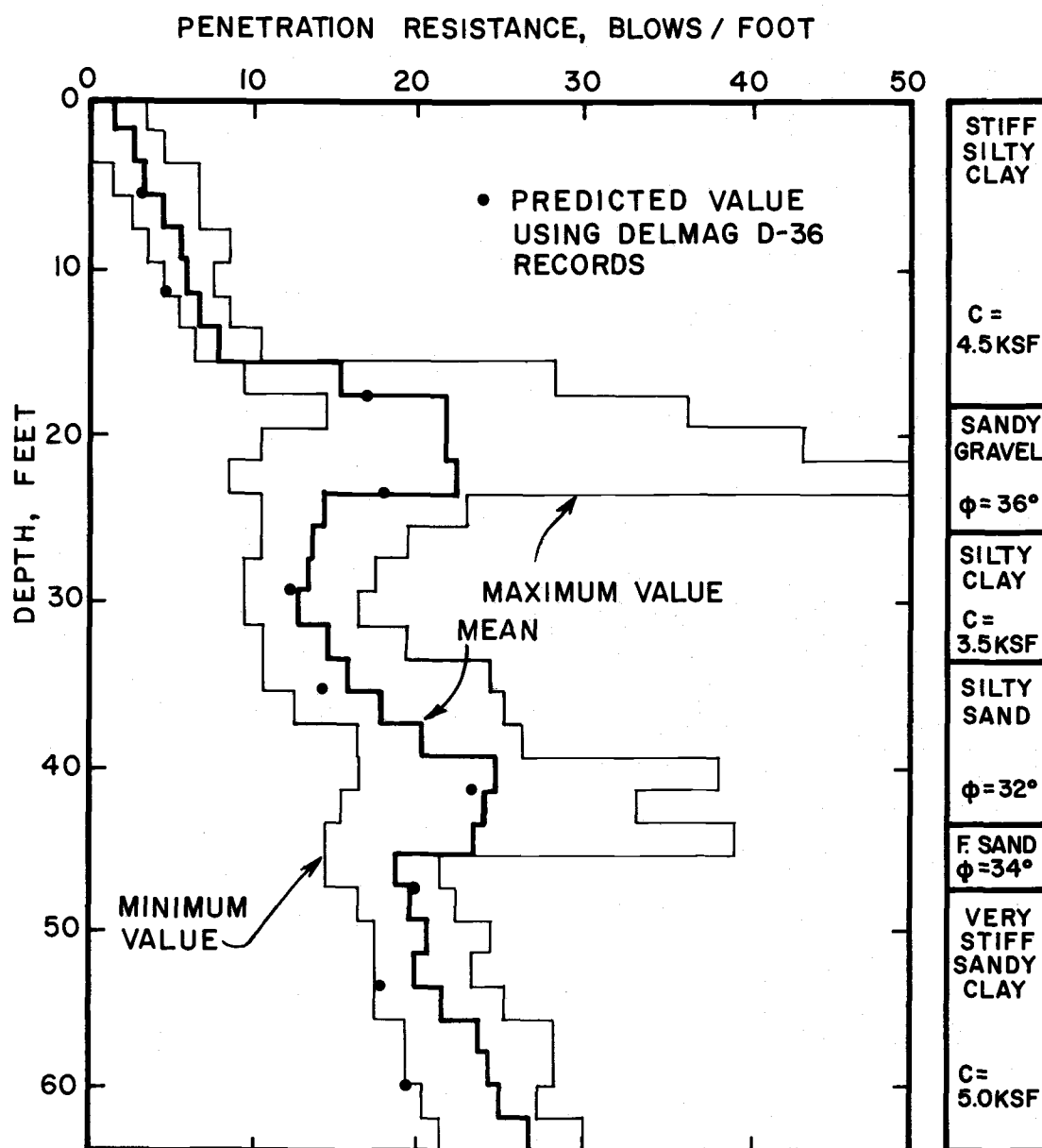


Figure D1. Penetration resistance vs. depth for Delmag D-30, Project D.

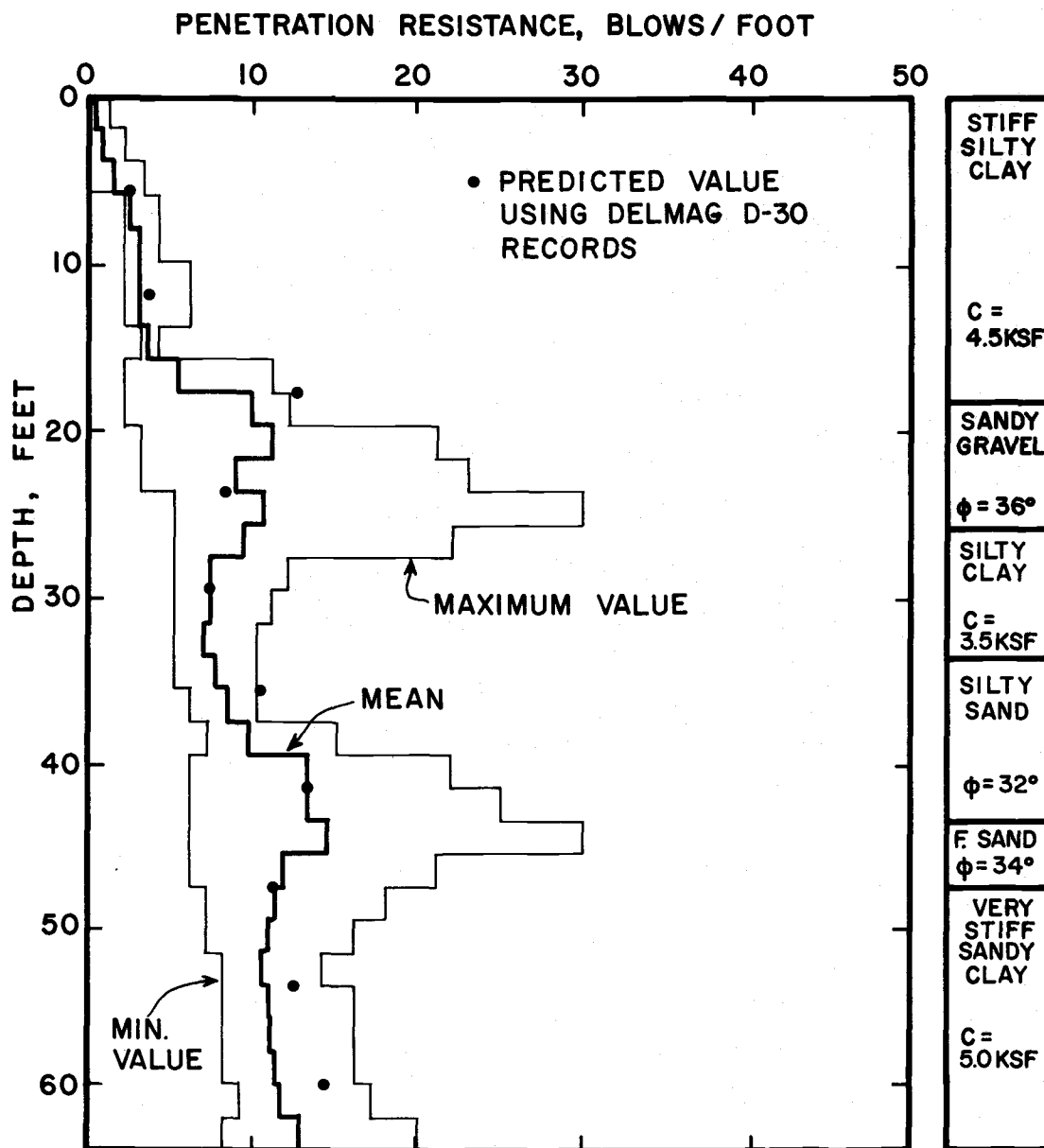


Figure D2. Penetration resistance vs. depth for Delmag D-36, Project D.

Table D1. Piling and hammer data, Project D.

HAMMER	DELMAG D-36	DELMAG D-30
Type	Diesel	Diesel
Rated Energy, Ft-lb	83, 200	54, 200
Explosive Force, Ft-lb	396, 000	242, 000
Ram Weight, Lb	7, 900	6, 600
Anvil Weight, Lb	2, 700	2, 200
Helmet Weight, Lb	1, 500	1, 500
Cushion Block	4-1/2" thickness of laminated plywood	4-1/2" thickness of laminated plywood
PILING: 12" square prestressed concrete		
Length:		
Number of records	6	5
Mean Length, Ft	66.8	66.6
Standard Deviation, Ft	0.7	0.9
Max. Length, Ft	66.0	65.5
Min. Length, Ft	67.7	68.0
Penetration: Assume same as length.		

Table D2. Computer model of hammer, piling and soil, Project D.

HAMMER	DELMAG D-36	DELMAG D-30
W(1), Lb (Ram)	7,900	6,600
W(2), Lb (Anvil)	2,700	2,200
W(3), Lb (Helmet)	1,500	1,500
K(1), Lb/in (Ram-Anvil)	87×10^6	75×10^6
K(2), Lb/in (Anvil-Helmet)	65×10^6	45×10^6
K(3), Lb/in (Cushion-Pile)	8.7×10^6	2.0×10^6
e(1) (Anvil)	0.35	0.35
e(2) (Helmet)	0.50	0.50
e(3) (Cushion)	0.50	0.50
Energy, Ft-lb	83,200	54,200
Explosive Force, Lb	396,000	242,000
Efficiency	1.00	1.00
PILING:		
Length, Ft	66	66
Max. Penetration, Ft	66	66
For 6 Ft. Sections:		
W(4) - W(14), Lb	900	900
K(4) - K(13), Lb/in	12×10^6	12×10^6
e for Piling	1.00	1.00
SOIL CONSTANTS		
Q	0.10	0.10
Q'	0.10	0.10
J	0.20-0.30	0.20-0.30
J'	0.07-0.10	0.07-0.10

Project E

Project E included both test and production piling. Diesel hammers were used to drive 12 and 14 inch square prestressed concrete piling through layers of fill, loose silty sand, and stiff organic clay to bearing in dense silty sand. Driving records are plotted in Figures E1 through E4. The piles were driven to support a large structure as outlined in Figure E5.

Though the possibilities of analysis are increased by the inclusion of a second size pile--i. e., use one size pile with one hammer to predict for a different size pile driven with a different hammer, or the use of one size pile with one hammer to predict for another size pile with the same hammer--the available data precluded making such analyses. The Kobe K-42 was used to drive test piles only, a total of eight, including four of each size. As noted in Figure E-5, the test piles were not all located within the boundary describing the location of production piles. The hammers used have very similar energies (ratio of approximately 1.1) and the piles are of the same type. Finally, the soil profile at the site varies considerably with depth and location, making it difficult to develop a representative model. The end result is that the four mean driving records are very similar.

It was decided to treat Project E as two separate projects for

the analyses. Analyses were made for the 12 inch piles and the 14 inch piles separately. This necessitated comparing the mean of 24 records and 107 records, respectively, with the mean of 4 records.

Approximately 15 piles were predrilled to a depth of 5 or 6 feet. An equal number required the use of a follower. The effects of these operations were not considered in the modeling of the hammer-pile-soil system. All test piles were cored to allow the placement of strain gauges for load testing. The reduction in cross-sectional area and weight was accounted for in the pile model

Soil data available were limited to boring log descriptions and N-values for Standard Penetration Tests. Friction angle and cohesion values were based on correlations with the N-values.

As for Project D, soil constants J and J' were determined using constant sand and clay values weighted for depth of pile penetration. As the strata encountered are mostly sands and silty sand, a triangular distribution for side soil resistance was assumed.

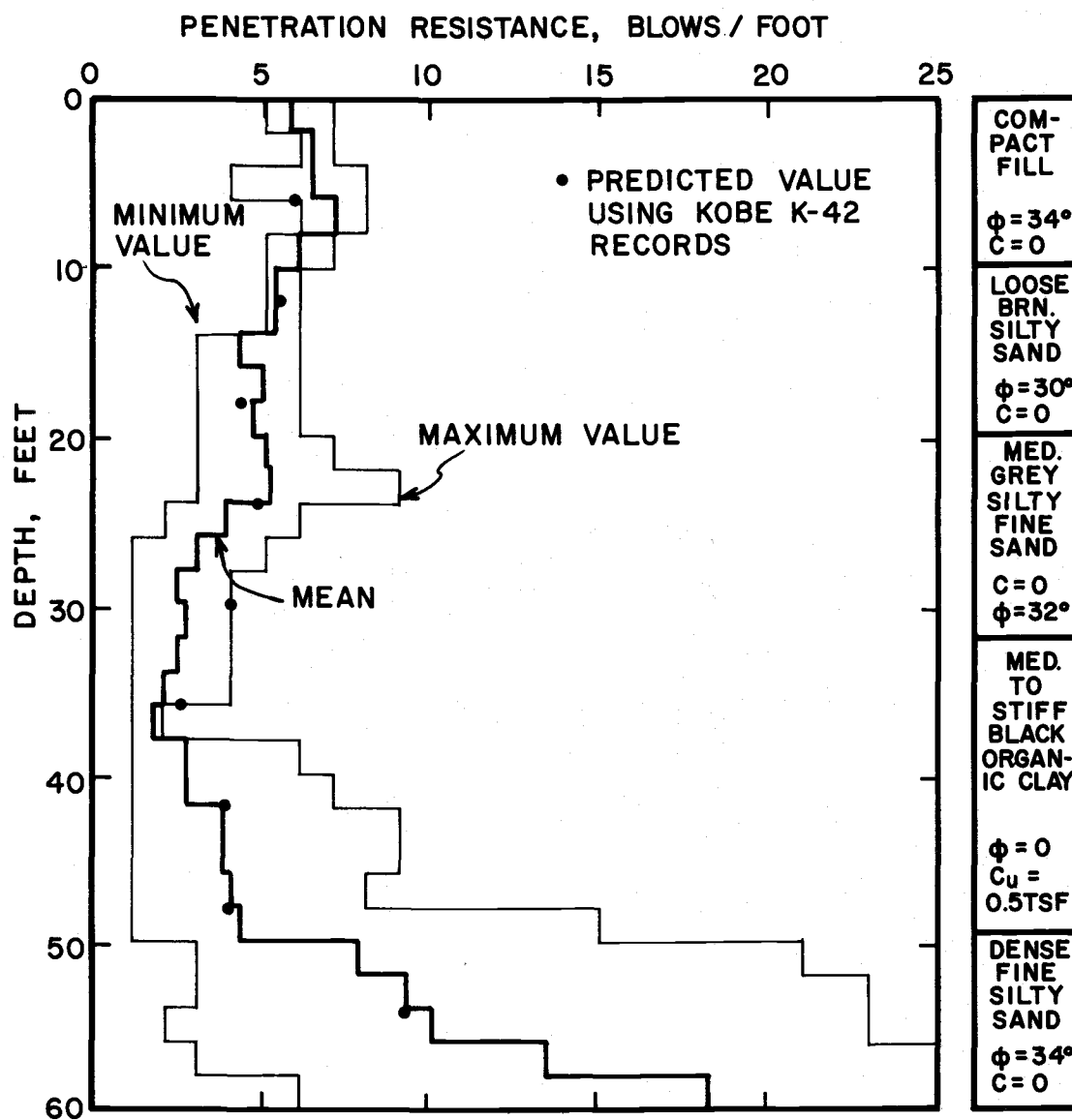


Figure E1. Penetration resistance vs. depth for Delmag D-44, 14" piles, Project E.

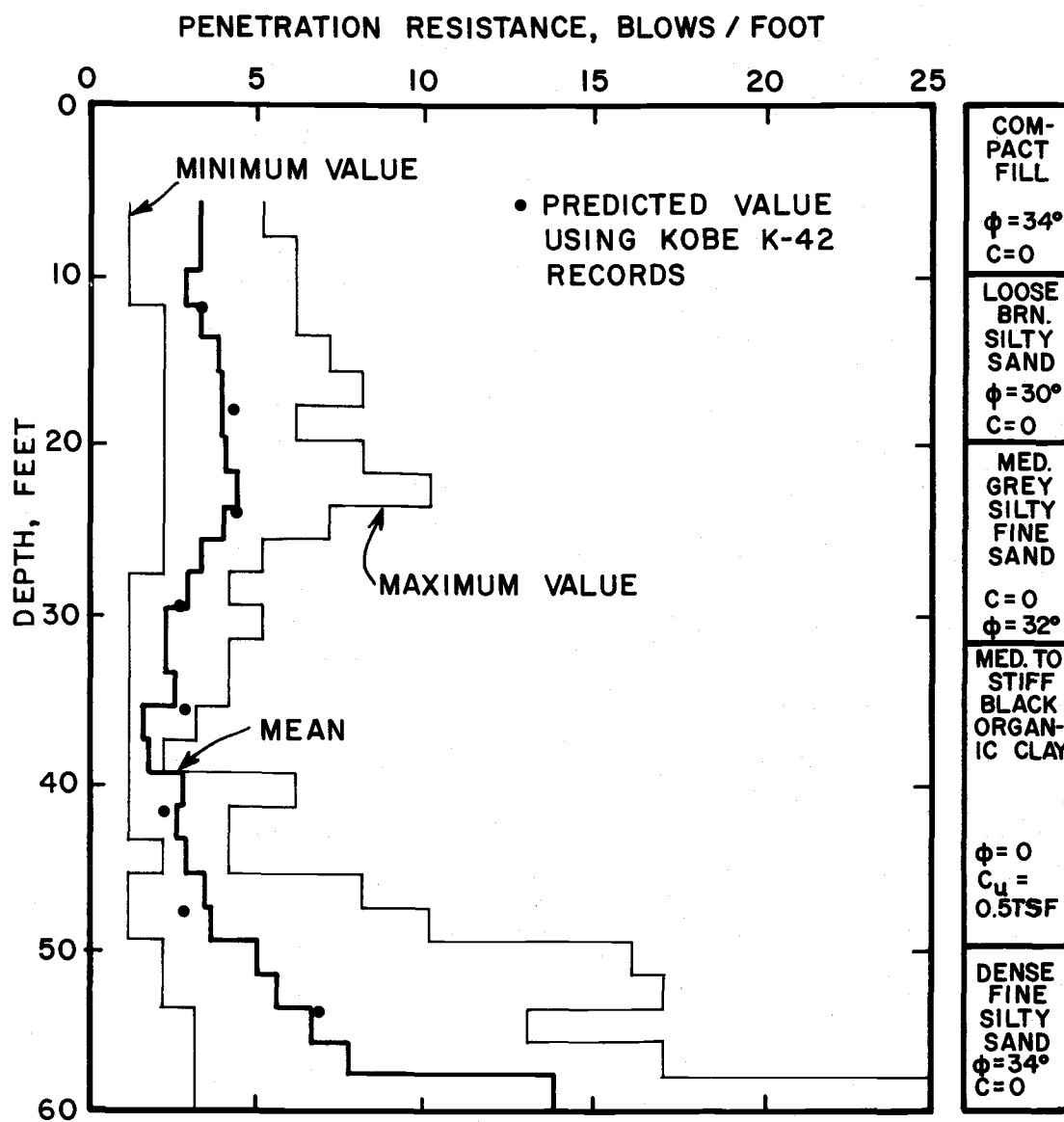


Figure E2. Penetration resistance vs. depth for Delmag D-44, 12" piles, Project E.

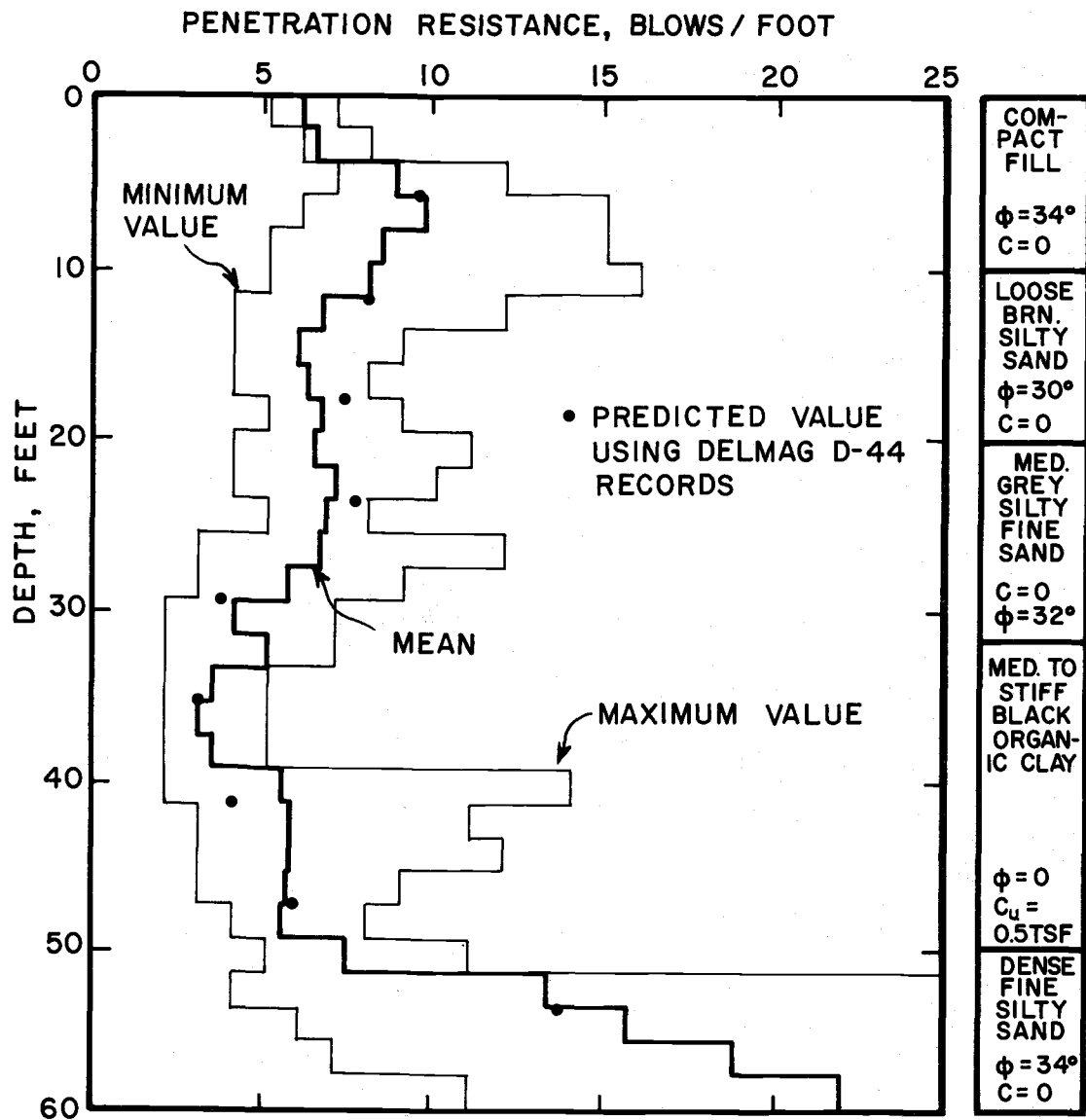


Figure E3. Penetration resistance vs. depth for Kobe K-42, 14" piles, Project E.

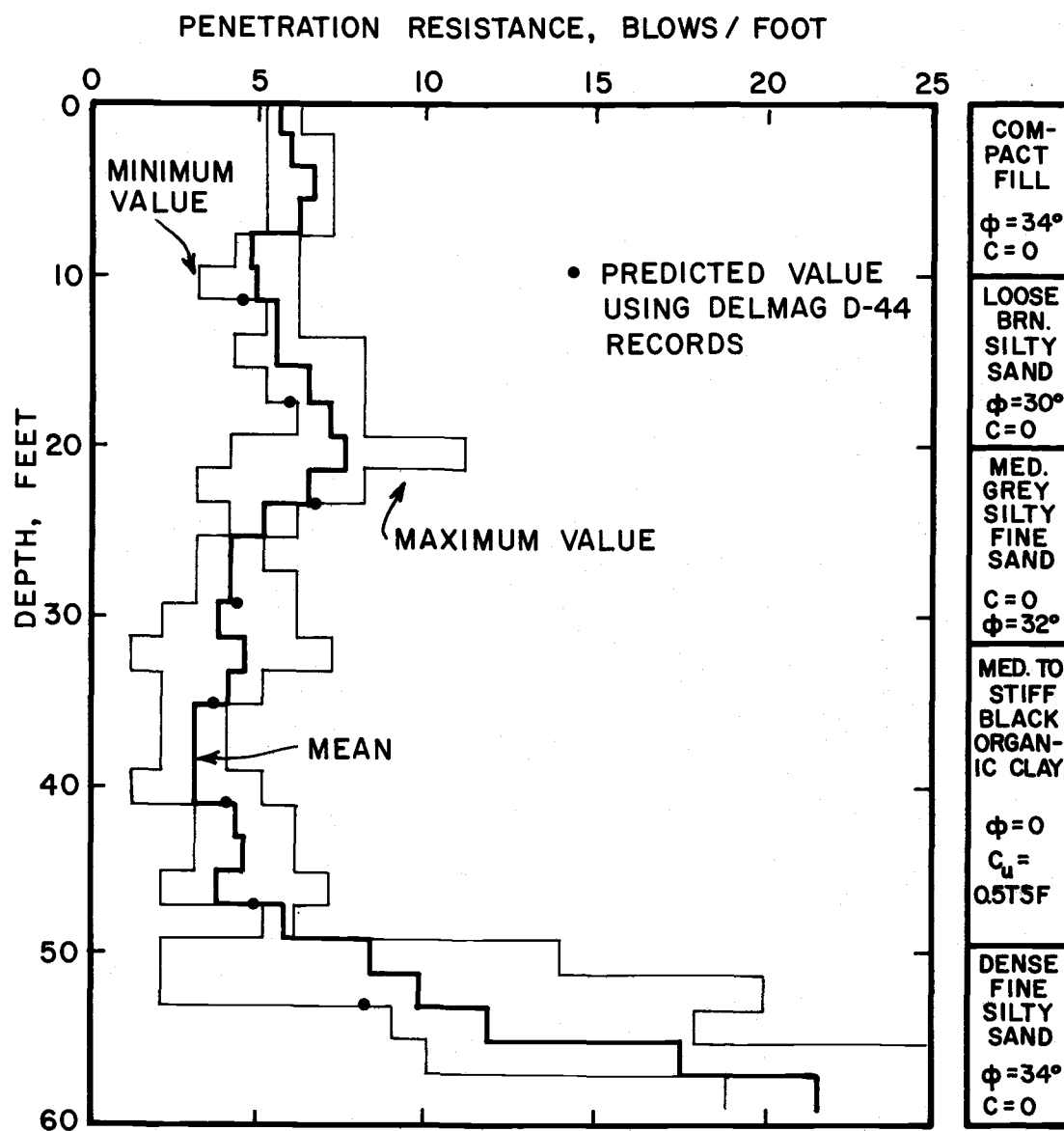
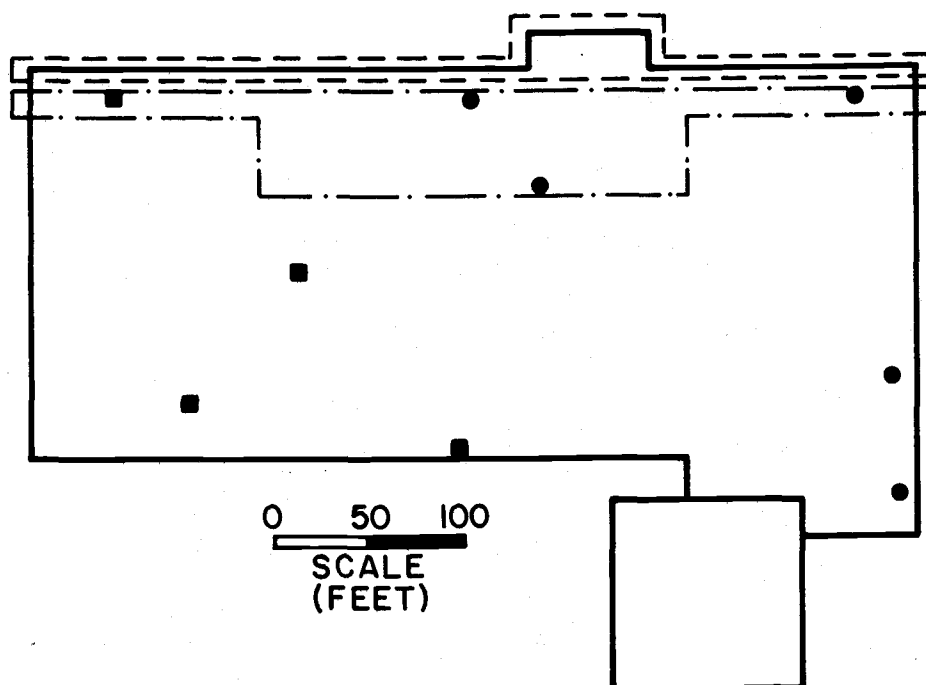


Figure E4. Penetration resistance vs. depth for Kobe K-42, 12" piles, Project E.



LEGEND

- — LOCATION OF 12" PILES DRIVEN BY DELMAG D-44
- · - · - LOCATION OF 14" PILES DRIVEN BY DELMAG D-44
- LOCATION OF 14" TEST PILE DRIVEN BY
KOBE K-42. ALSO BORING LOG.
- LOCATION OF 12" TEST PILE DRIVEN BY
KOBE K-42. ALSO BORING LOG.
- BUILDING PLAN

Figure E5. Pile and boring locations, Project E.

Table E1. Piling and hammer data, Project E.

HAMMER	DELMAG D-44	KOBE K-42
Type	Diesel	Diesel
Rated Energy, Ft-Lb	87,000	79,000
Explosive Force, Lb	440,000	280,000
Ram wt., Lb	9,500	9,260
Anvil wt., Lb	4,080	4,000
Helmet wt., Lb	1,390	1,300
Cushion Block	6" layered plywood	4" layered plywood
PILING: 12" Square Prestressed Concrete		
Length:		
Number of records	24	4
Mean Length, Ft	67.1	72.0
Standard Deviation, Ft	3.8	9.7
Min. Length, Ft	60	64
Max. Length, Ft	76	86
Penetration:		
Number of records	24	4
Mean Penetration, Ft	68.1	66.0
Standard Deviation, Ft	3.9	5.7
Min. Penetration, Ft	60	60
Max. Penetration, Ft	76	73
PILING: 14" Square Prestressed Concrete		
Length:		
Number of records	107	5
Mean Length, Ft	67.8	76.2
Standard Deviation, Ft	4.4	11.5
Min. Length, Ft	60	58
Max. Length, Ft.	84	84
Penetration:		
Number of records	107	5
Mean Length, Ft	64.5	65.4
Standard Deviation, Ft	3.0	7.2
Min. Length, Ft	59	56
Max. Length, Ft	72	76

Table E2. Computer model of hammer, piling and soil, Project E.

HAMMER	DELMAG D-44	KOBE K-42
W(1), Lb (Ram)	9,500	9,260
W(2), Lb (Anvil)	4,080	4,000
W(3), Lb (Helmet)	1,300	1,300
K(1), Lb/in (Ram-Anvil)	106×10^6	106×10^6
K(2), Lb/in (Anvil-Helmet)	60×10^6	60×10^6
K(3), Lb/in (Cushion-Pile)		
12" Piles	6.0×10^6	6.4×10^6
14" Piles	8.2×10^6	8.7×10^6
e(1) (Anvil)	0.5	0.5
e(2) (Helmet)	0.5	0.5
e(3) (Cushion)	0.35	0.35
Energy, Ft-Lb	87,000	79,000
Explosive Force, Lb	440,000	280,000
Efficiency	1.00	1.00
PILING (Both 12" and 14")		
Length, Ft	66	72
Max. Penetration, Ft	66	66
For 6-Ft. Sections:		
12" Piles:		
W(4) - W (15), Lb		869
W(4) - W(14), Lb	900	
K(4) - K(14), Lb/in		7.7×10^6
K(4) - K(13), Lb/in	8.0×10^6	
14" Piles:		
W(4) - W(14), Lb	1,225	1,194
K(4) - K(13), Lb/in	10.9×10^6	10.6×10^6
e for Piling	1.00	1.00
SOIL CONSTANTS		
Q	0.10	0.10
Q'	0.10	0.10
J	0.10-0.17	0.10-0.17
J'	0.03-0.06	0.03-0.06

VI. RESULTS AND DISCUSSION

To evaluate the suitability of the predictive method proposed, the driving records predicted are compared to the mean of those observed in each case. Comparisons for each case are shown in the driving records presented in the previous section. In each of the penetration versus depth plots, it is apparent that values obtained for a single pile on a typical job may range between considerably different values from minimum to maximum, even in reasonably homogeneous soils. For estimating purposes, therefore, the mean of a representative number of observations is required to obtain a valid prediction of the mean expected for a different project.

Comparisons are evaluated by two statistical methods. First, the predicted penetration resistance is plotted versus the mean observed penetration resistance for the same depth. A straight line relationship is fit to the data by the least squares method. The goodness of this best fit is expressed by a correlation coefficient, r . As the correlation coefficient is not as sensitive to the scatter of the data as desired, a second statistical method is employed. The ratio of predicted penetration resistance to mean field penetration resistance is calculated for each data point. The mean, \bar{X} , and standard deviation, S. D., for the set of data points is calculated. The standard deviation is more sensitive to the scatter of data

about the mean than is the correlation coefficient to a best fit line. The necessary equations for calculating a least squares fit correlation coefficient, and standard deviation are found in any standard textbook on statistical methods. They are not presented in this discussion. Similarly, for a more complete discussion of the relevance and limitations of the two methods, the reader is referred to a text on statistical methods or statistical inference (2).

Predictions Using the Wave Equation and a Field Driving Record

Predicted penetration resistance, determined using a mean observed driving record and wave equation analysis, is plotted versus mean field penetration resistance in Figure 5. For the 75 predictions made, representing all projects except Project B, the agreement between predicted and observed values is good. The least squares fit for best agreement would have the equation $(\text{PRED}) = (\text{FIELD})$, and a correlation coefficient of 1.00. The least squares fit of $(\text{PRED}) = 0.7 + 0.9 (\text{FIELD})$ with correlation of 0.97 indicates slight divergence from the best possible agreement.

Qualitatively, the agreement for each project is illustrated by including the predicted blow count value for each depth on the plots of the mean driving record determined for each hammer. These are presented in the previous section of this study.

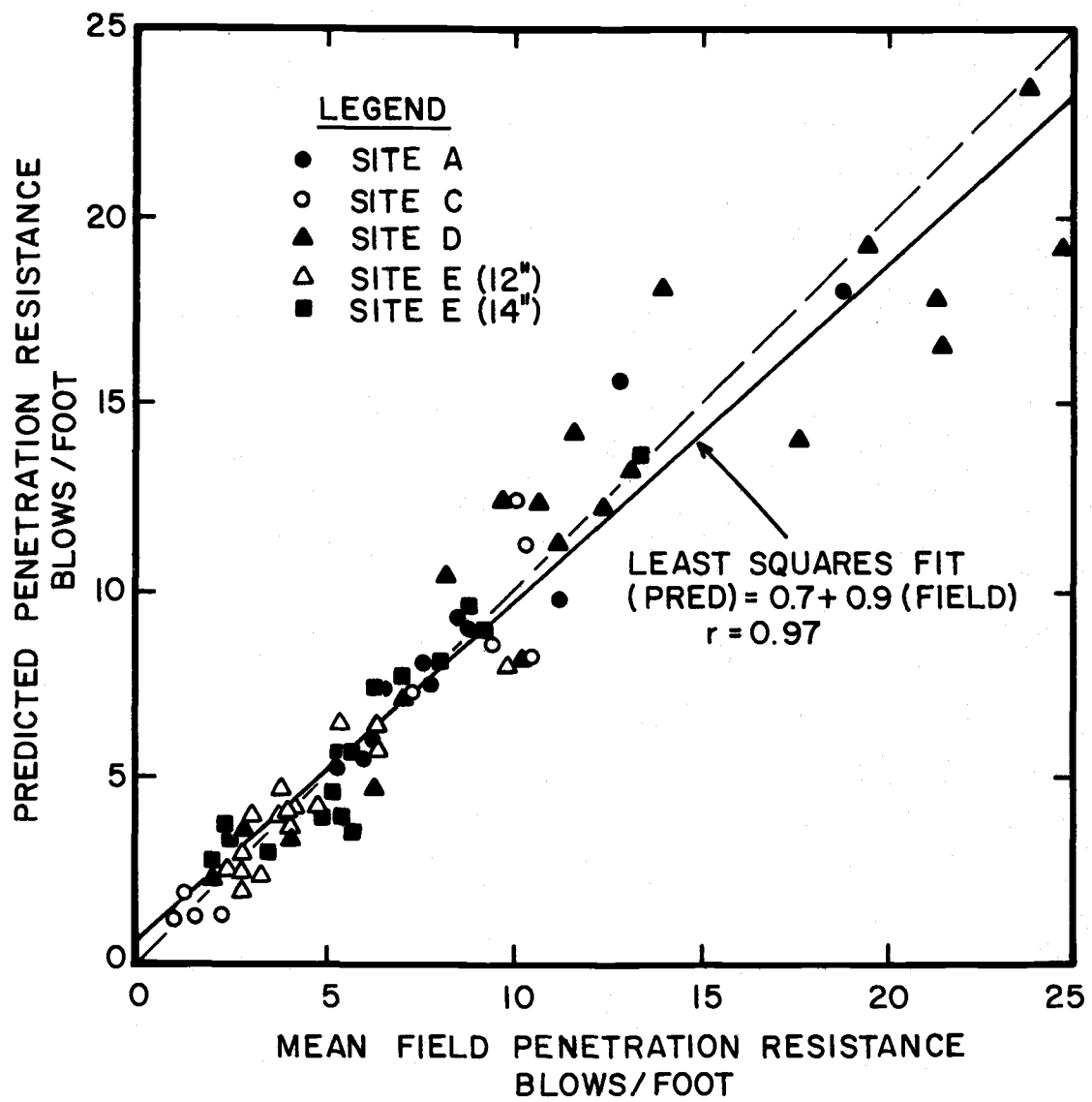


Figure 5. Predicted vs. mean field penetration resistance for Projects A, C, D, E, using field driving records and wave equation analysis.

Quantitatively, least squares fits were made for each hammer, and are appended to this study for reference.

In Figure 6, the computed ratios of predicted blows per foot to mean observed blows per foot are illustrated on a frequency plot. The mean ratio and the range of minus one standard deviation to plus one standard deviation are plotted on the diagram for reference. The mean ratio of 1.01 agrees quite well with a best possible agreement of 1.00, indicating that the proposed method will, on the average, predict a reliable value of penetration resistance. For normally distributed data approximately two-thirds of all data points fall within a range of plus or minus one standard deviation. By the method proposed, therefore, approximately two-thirds of the computed penetration resistances would be expected to fall within a range of 0.83 to 1.19 of the actual value. Or, approximately two-thirds of the computed values would agree within plus or minus 18% of the actual value.

Though methods of determining if a group of data is normally distributed are available, these were not used. The curve that could be fit to the bar graph shown in Figure 6 would be roughly bell shaped, equally distributed about the mean, as expected of a normal distribution. Other plots to be presented may not indicate normal distribution. Rather than represent these groups of data by other distributions, it was decided to assume normal

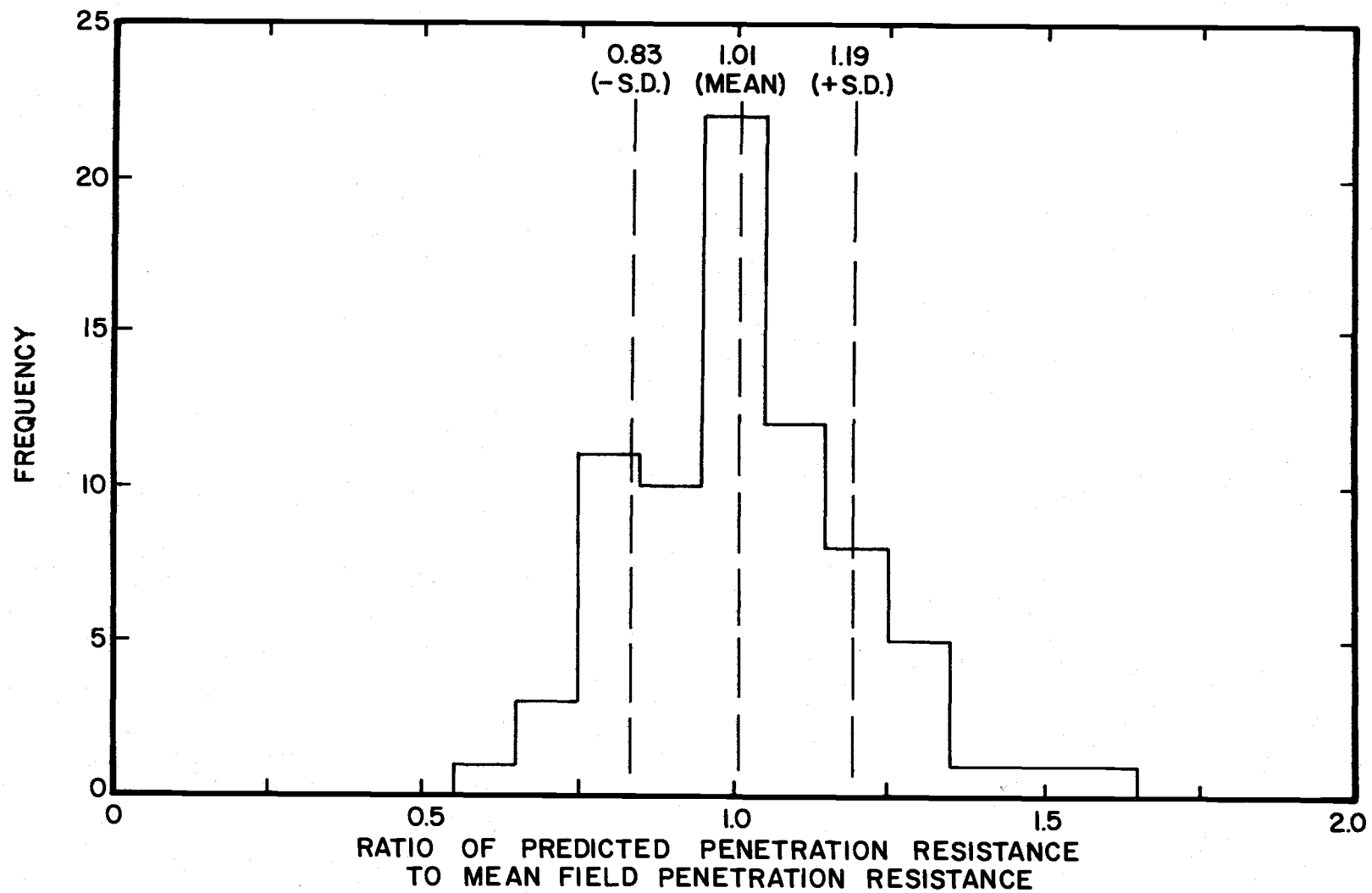


Figure 6. Statistical frequency plot for predictions made using field driving records and wave equation analysis.

distributions. The statistics of the normal distribution, mean and standard deviation, are well known to engineers, while those of other distributions are much less known.

Predictions Using the Hiley Formula and a Field Driving Record

To further evaluate the proposed method, and to develop a possible non-computer approach, predictions of penetration resistance were made using the Hiley pile driving formula. The same mean field penetration resistances selected for prediction by wave equation analysis were predicted by the Hiley formula. As shown in Figure 7, the predicted values are in good agreement with the mean field values. The least squares fit of $(\text{PRED}) = -0.1 + 1.1 (\text{FIELD})$ with correlation coefficient of 0.96 represents as good a fit as determined for wave equation predictions. As noted in Figure 8, the mean ratio of predicted blows per foot to mean field blows per foot is somewhat higher for the Hiley formula, 1.06, than the wave equation, 1.01. More indicative of the differences in ability to predict is that the standard deviation is 0.29 for the Hiley formula, while it is only 0.18 for the wave equation. Predictions made by the Hiley formula, therefore, are expected to be higher, with two-thirds expected to fall between 0.77 and 1.35 of the actual field value.

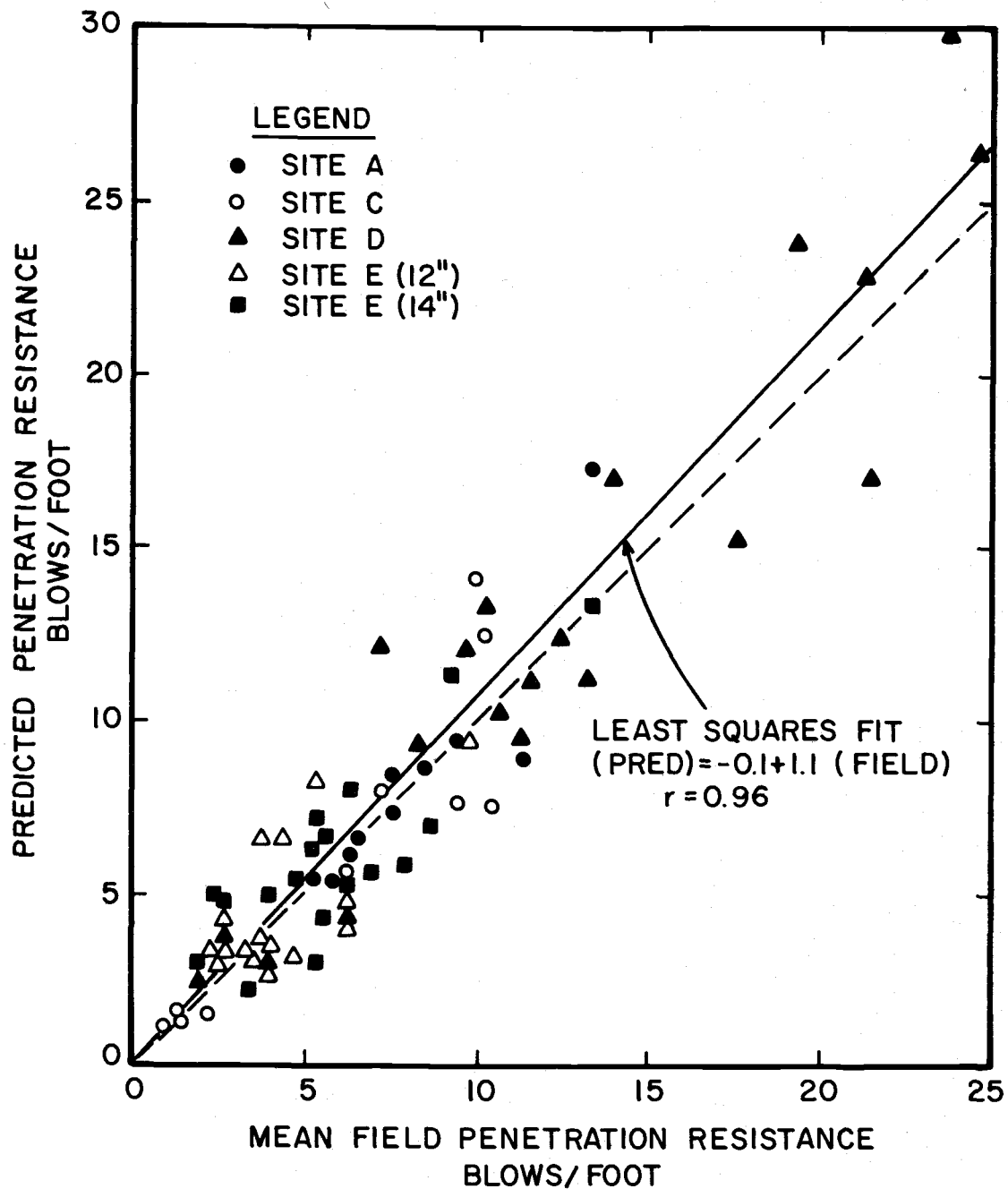


Figure 7. Predicted vs. mean field penetration resistance for Projects A, C, D, E, using field driving records and the Hiley formula

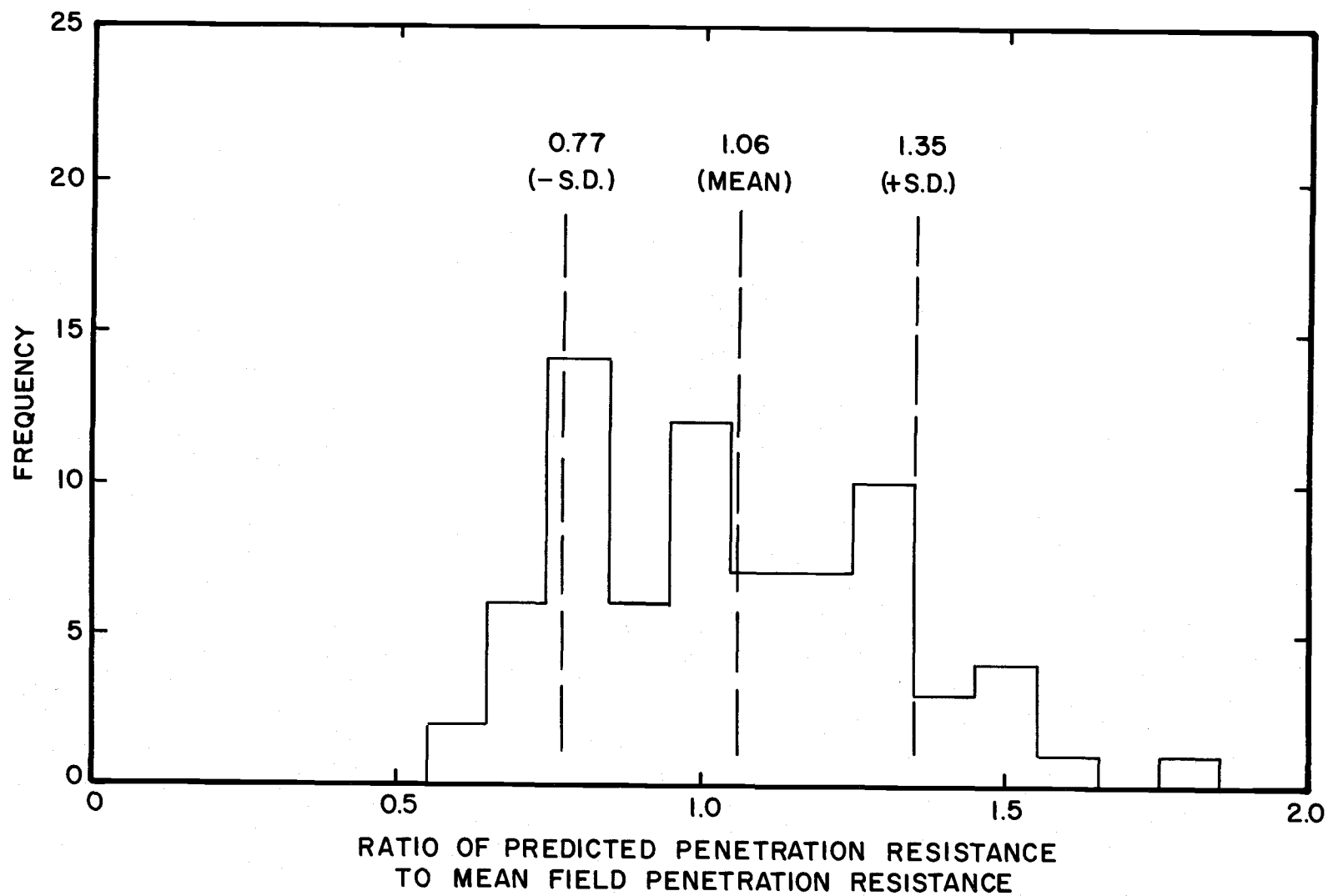


Figure 8. Statistical frequency plot for predictions made using field driving records and the Hiley formula.

Comparison of Wave Equation and Hiley Formula Predictions

While the distribution of predicted to actual ratios is normal for the wave equation analysis, as shown in Figure 6, it has spikes near ratios representing the mean and plus or minus one standard deviation for the Hiley formula analysis, as shown in Figure 8. It was thought this might be indicative of a given hammer-pile-soil system predicting significantly higher or lower than the overall mean. The mean and standard deviation, therefore, were calculated for each of the five hammer-pile-soil pairs. The results are listed in Table 3. For the wave equation, the mean ratio varied from 1.00 to 1.02, while for the Hiley formula, the mean ratio varied from 1.01 to 1.13. Similarly, the standard deviation varied from 0.09 to 0.24 for the wave equation, and 0.13 to 0.41 for the Hiley formula. It does not appear that either predictive method does a significantly better job for any one of the hammer-pile-soil systems analyzed than another.

The proposed method of analysis, using the numerical solution to the wave equation, is a better predictive method than a similar method using the Hiley pile driving formula, when pile driving records are available. It is not a significantly better method, however, as was expected. The Hiley formula is empirical, even

Table 3. Statistics, by project, for ratio of predicted to mean field penetration resistance (driving record available).

Project	Wave Equation				Hiley Formula			
	N	\bar{X}	S. D.	Range	N	\bar{X}	S. D.	Range
A	11	1.00	0.09	0.87-1.16	10	1.01	0.13	0.79-1.29
C	10	1.02	0.24	0.67-1/46	10	1.03	0.25	0.72-1.14
D	20	1.01	0.19	0.77-1.29	20	1.02	0.20	0.71-1.39
E(12")	16	1.00	0.15	0.74-1.26	16	1.08	0.34	0.64-1.55
E(14")	18	1.02	0.22	0.64-1.58	18	1.13	0.41	0.55-2.10
Combined	75	1.01	0.18	0.64-1.58	74	1.06	0.29	0.55-2.10

if it attempts to account for such factors as elastic compression of the pile, restitution and elastic compression of capblocks and cushions, and elastic compression of the soil. The numerical solution to the wave equation is a rational description of the behavior of the pile-hammer-soil system during pile driving. It would be expected to be a better predictive tool. In another study, where static capacity predicted by the wave equation and the Hiley formula are compared with load test determined capacities, the wave equation predicted the load test value more accurately. Forehand and Reese (6) compared the ultimate resistance for 15 piles, and found that the percentage error for the wave equation varied from -38.3 to 3.0, with an average of 6.6 percent (absolute value). For eight piles, the wave equation prediction agreed exactly with the load test value. For the Hiley formula, the percentage error varies from -58.4 to 25.0, with an average of 25.8 percent (absolute value).

By way of explanation, in the present study a known driving record is used to predict another driving record. A driving record is a measureable parameter indicative of the behavior of the hammer-pile-soil system during driving. By using a known driving record, the effects of the differences in the wave equation and Hiley formulations are lessened. The relationship between the dynamic system and a static capability is bridged, in a sense, by eliminating

an unknown, the dynamic behavior of the system. The remaining differences are due to our inability to model the elements of the system exactly: the soil profile is variable, the energy delivered to the pile varies from blow to blow, and the reaction of the pile varies with each blow. In predicting ultimate resistance for comparison with a load test result, the prediction does not have the benefit of this indicator of dynamic behavior. It would be expected, then, that the wave equation, which models the hammer-pile-soil system in a more exact manner than the Hiley formula, would better predict the ultimate resistance.

Predictions Using the Wave Equation and Soil Data Only

If driving records from an adjacent project are unavailable, soil boring data represent the sole basis for predicting penetration resistance. The situation more nearly resembles that of estimating the static capacity or ultimate resistance of a pile at a given depth. Rather than having the penetration resistance, or set in blows per foot, and using it to estimate capacity, the estimated capacity from soil data is used to calculate the penetration resistance.

Figure 9 is a comparison using least squares fitting, of predicted penetration resistance from the wave equation and static analysis of capacity to that observed during driving for the four projects. The agreement is not as good as that found using the

known driving record with either the wave equation or the Hiley formula. The least squares fit is $(\text{PRED}) = 1.3 + 0.8 (\text{FIELD})$, with correlation coefficient equal to 0.86. The scatter is extensive, for both high and low ranges of blow count.

The scatter is more evident in Figure 10, a frequency plot of computed ratios of predicted penetration resistances to mean field penetration resistances. The mean of these ratios is 0.96, indicating that overall one can make reasonable predictions of penetration resistance using soil data alone. However, as indicated by the standard deviation of 0.46, two-thirds of the time the predicted value will fall between 0.50 and 1.42 of the actual value. While this may not be critical at low blow counts, say 2, it can be critical at high blow counts. In the field, in counting the blows per foot, if two thirds of the values fall between 1 and 3, more often than not, a value of 2 would be written down. However, for an actual value of 20, the distinction between 10 and 30 is more clearly drawn, and the probability of error much greater.

The curve that could be fit to the points indicated by the bars in Figure 10 would not describe a normal distribution. There are significant numbers of ratios near values of 0.25 and 1.75. This further lessens the impact of the mean value being near a best value of 1.00.

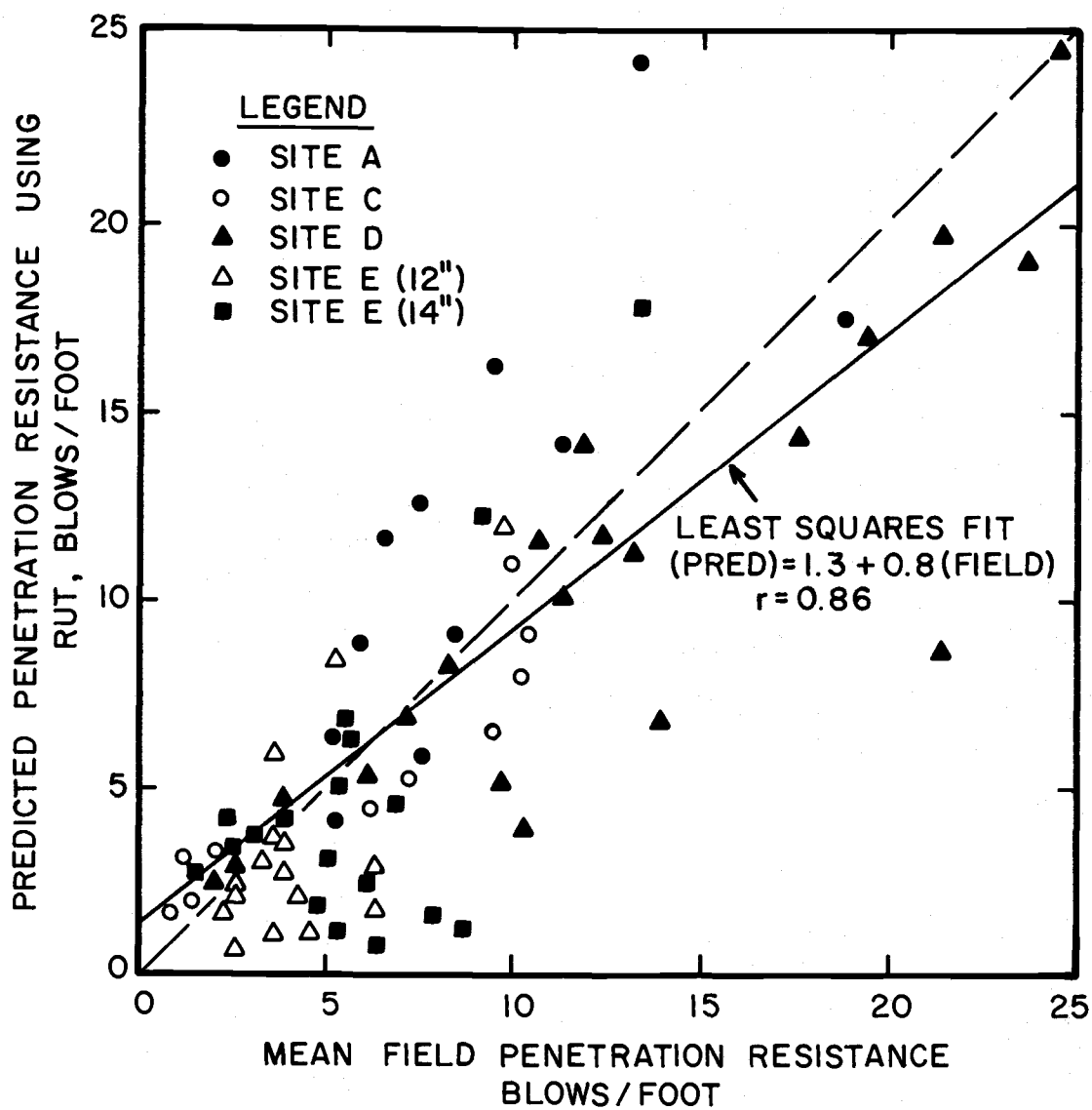


Figure 9. Predicted vs. mean field penetration resistance for Projects A, C, D, E, using wave equation analysis and soil data only.

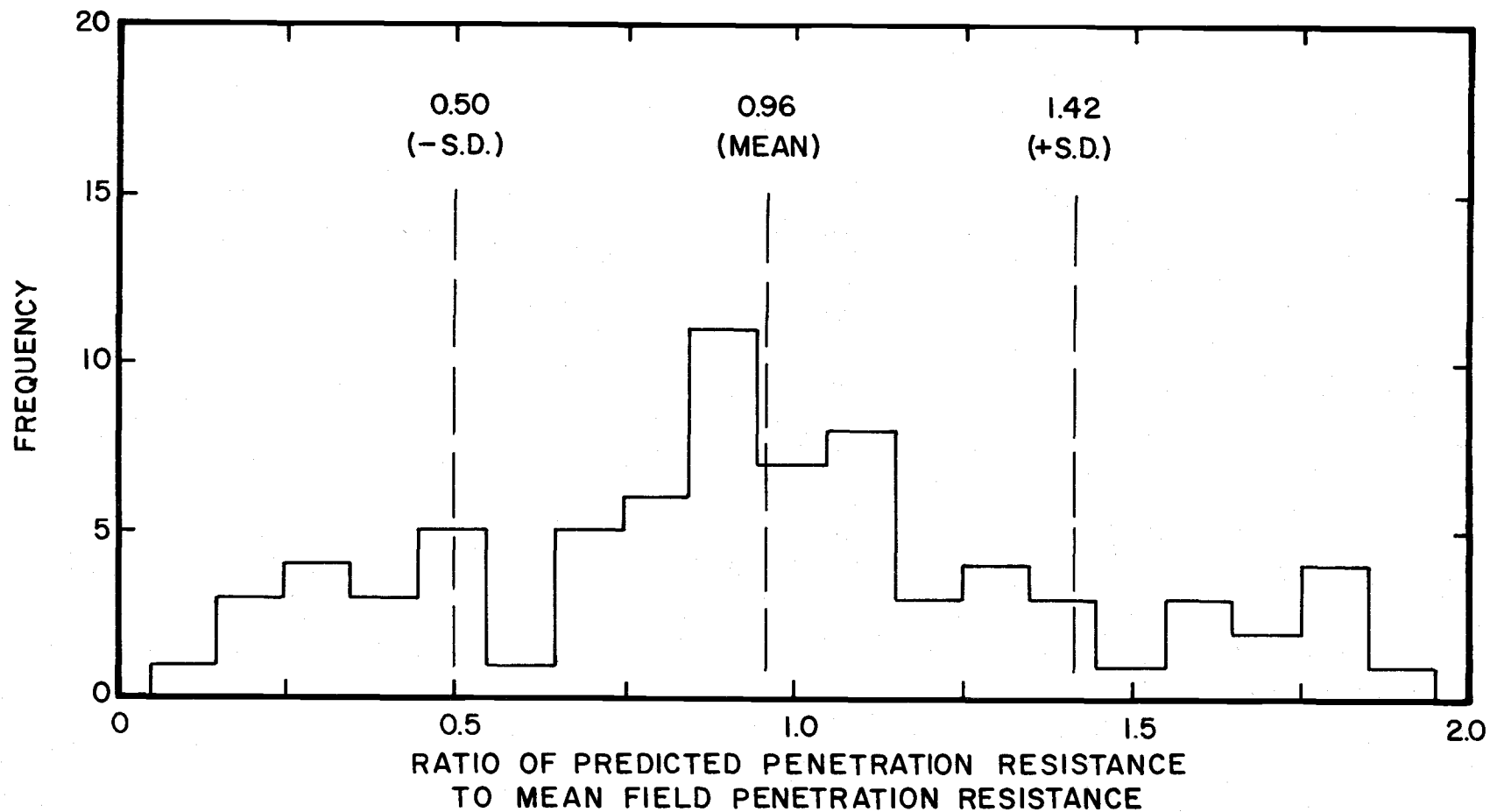


Figure 10. Statistical frequency plot for predictions made using wave equation analysis and soil data only.

Predictions Using the Hiley Formula and Soil Data Only

Predictions of penetration resistance using the Hiley pile driving formula and static analysis of capacity are plotted versus mean field values in Figure 11. The least squares fit is $(\text{PRED}) = -1.0 + 0.8 (\text{FIELD})$ with a correlation coefficient of 0.75. The fit relationship has approximately the same slope as that for the wave equation, but the difference in correlation coefficient indicates significantly more scatter.

As shown in Figure 12, the mean ratio of the predicted to field penetration resistance ratios calculated is 0.68, significantly below the best fit of 1.0. With the Hiley formula, predicted penetration resistances would be expected to be much lower than the actual values. Also, though the standard deviation is 0.58, it is felt less scatter would be expected than if the wave equation were used. The standard deviation is sensitive to data points that deviate greatly from the mean. As shown in Figure 12, there were several calculated ratios that varied by approximately 1.00 or more from the mean. (It should be noted that three ratios having values greater than 2.00 were excluded from the diagram, in order that a continuity of form and size of class interval be maintained.) If we neglect these, a more accurate mean would be 0.50. Also, the scatter of the data is less if we neglect the few high ratios. The Hiley formula

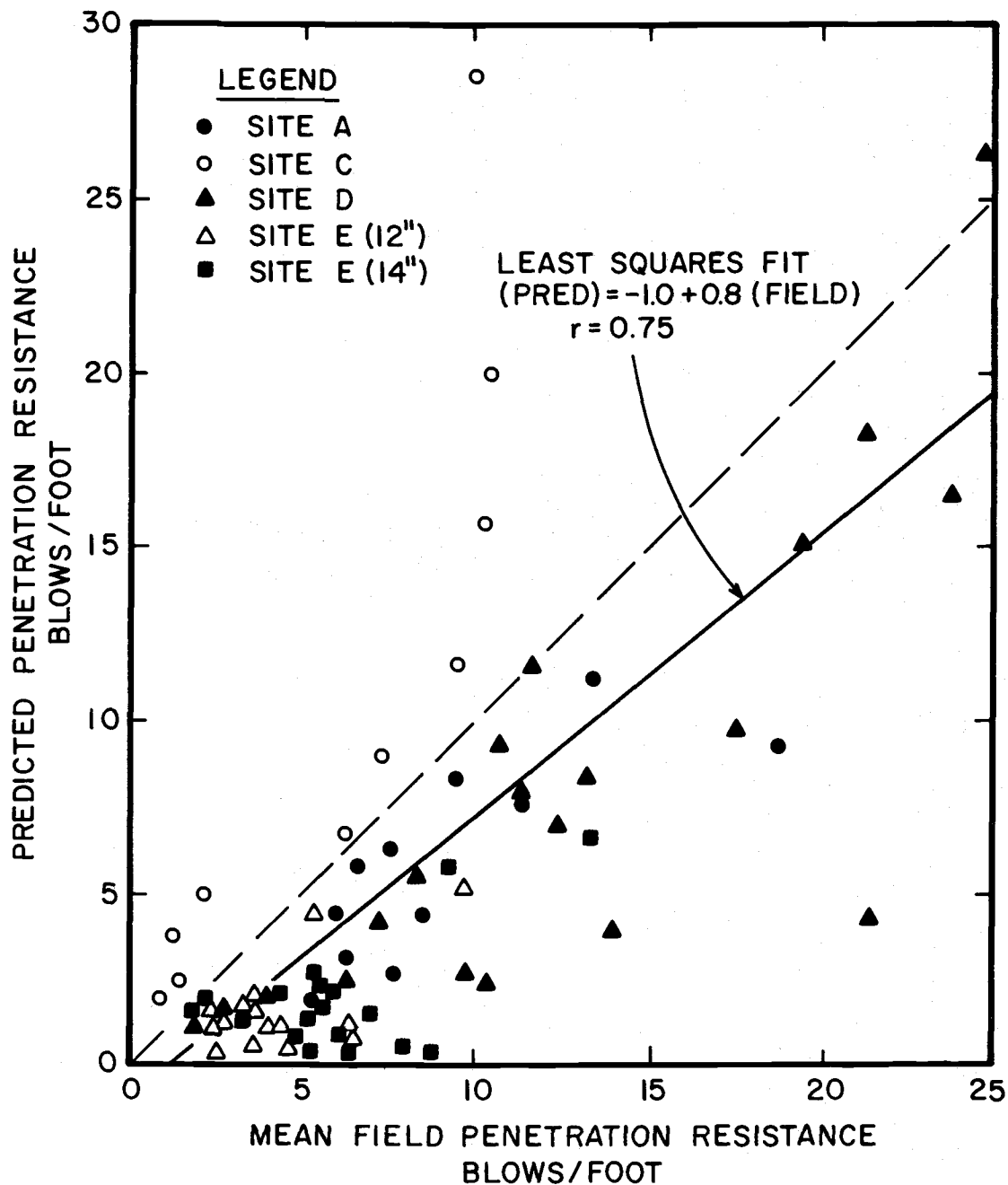


Figure 11. Predicted vs. mean field penetration resistance for Projects A, C, D, E, using the Hiley formula and soil data alone.

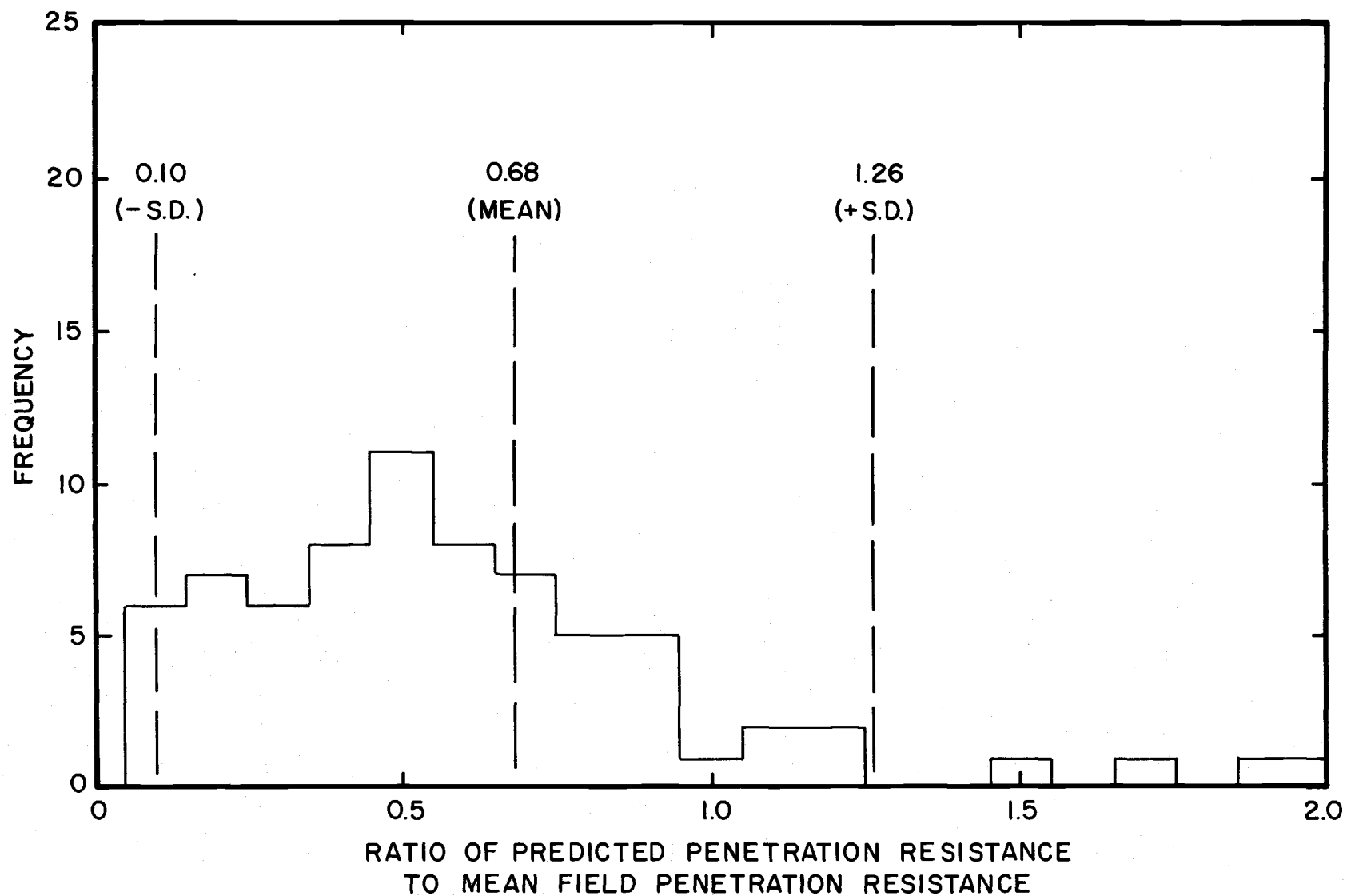


Figure 12. Statistical frequency plot for predictions made using the Hiley formula and soil data alone.

then, predicts a value about half of the actual value, with two-thirds of the predictions being between approximately 0.10 and 0.90 of the actual value.

Comparison of Wave Equation and Hiley Formula Predictions

The mean and standard deviation were calculated for the ratios of predicted penetration resistance to mean field penetration resistance calculated for each project, and for each method of analysis used. These are listed in Table 4. It should be reiterated that for each comparison, the same estimate of static capacity was used for both the wave equation and Hiley formula analyses. Several observations can be made after comparing the statistics listed in Table 4. The wave equation, in one sense, is less sensitive to the estimate of static capacity than the Hiley formula. Overall the mean ratios predicted are less variable by project (0.80 to 1.29) for the wave equation than they are for the Hiley formula (0.37 to 1.90). Within each project, however, the range of ratios is smaller for the wave equation for Project C only.

The wave equation analysis uses the estimate of static capacity twice. First, the percent point resistance is input, based on the relative estimates of point bearing capacity and side friction resistance. An ultimate resistance, or static capacity, versus

Table 4. Statistics, by project, for ratio of predicted to mean field penetration resistance (driving record unavailable).

Project	Wave Equation				Hiley Formula			
	N	\bar{X}	S. D.	Range	N	\bar{X}	S. D.	Range
A	11	1.29	0.40	0.77-1.81	11	0.65	0.21	0.37-0.89
C	10	1.20	0.57	0.71-2.38	10	1.90	0.67	1.12-3.00
D	20	0.89	0.26	0.39-1.35	20	0.61	0.24	0.21-1.06
E(12")	16	0.80	0.43	0.25-1.58	16	0.39	0.21	0.10-0.83
E(14")	18	0.85	0.50	0.14-1.75	18	0.37	0.25	0.05-0.87
Combined	75	0.96	0.46	0.14-2.38	75	0.68	0.58	0.05-3.00

penetration resistance relationship is computed. The estimated static capacity is then used directly to determine the penetration resistance. It has been found (1) that the wave equation is particularly sensitive to the percent point resistance input. Thus an inaccurate estimate could be amplified when used a second time.

The Hiley formula also uses the estimate of static capacity twice, but in the same operation. The values of constants C_2 and C_3 , elastic compression of pile and cushioning material, are determined using pressures calculated from the ultimate resistance. The penetration resistance is then calculated directly from the formula. For the present case, Equation (2) can be simplified and rearranged to

$$S = \frac{(\text{ENERGY})}{R_u} - \frac{1}{2}(C_1 + C_2 + C_3)$$

The set calculated is more sensitive to the estimated static capacity, R_u , than the value of $\frac{1}{2}(C_1 + C_2 + C_3)$. For a given project, then, or given soil profile, the static capacity estimate would be more or less uniformly incorrect with depth, dependent on the uniformity of the profile and the soil parameters assumed. Similarly, the penetration resistance calculated would be more or less uniformly incorrect with depth. For a given project, the ratio of predicted to field penetration resistance would be expected to have less

scatter about a mean value than ratios calculated using the wave equation.

Summary

The statistics used to evaluate the proposed method of predicting penetration resistance, as well as the three methods investigated for comparison, are summarized in Table 5. The proposed method of using a mean driving record from an adjacent site in conjunction with wave equation analysis more reliably predicts penetration resistance for a variety of hammer-pile-soil systems than the other methods used. The use of a known driving record for the same type piling in similar soil conditions is of particular importance, as indicated by the difference between estimates made using an available driving record and estimates made with a static capacity estimate alone. Predictions made using the proposed method varied from 0.83 to 1.19 of the actual mean field penetration resistances, with the mean prediction being 1.01 of the actual value.

Table 5. Summary of statistics by method.

	Least Squares Fitting			Frequency Distribution		
	Slope b	Intercept a	Correlation Coefficient	Mean Ratio \bar{X}	Standard Deviation S. D.	Number of Observations
Wave Equation w/Driving Record	0.9	0.7	0.97	1.01	0.18	75
Wave Equation w/Static Capacity Estimate	0.8	1.3	0.86	0.96	0.46	75
Hiley Formula w/Driving Record	1.1	-0.1	0.96	1.06	0.29	74
Hiley Formula w/Static Capacity Estimate	0.8	-1.0	0.75	0.68	0.58	75

VII. CONCLUSIONS AND RECOMMENDATIONS

On the basis of the case studies made, it is shown that where soil conditions are reasonably uniform and adequate numbers of driving records for driving the same type piling are available, the mean penetration resistance versus depth relationship under any soil conditions may be reliably estimated by the proposed method. The criteria of similarity of soil conditions is to be stressed, as evidenced by an examination of the partial analysis of Project B. That a proposed project is close to a completed project with available driving records is not sufficient. Engineering judgment must be utilized in determining if two projects can be represented by the same model soil profile, and in determining that model.

It is also shown that the Hiley pile driving formula is nearly as reliable a predictive tool as the wave equation, if the same criteria pertaining to the proposed method are met. For the projects studied, the choice of either the wave equation or Hiley formula is secondary to the use of a known mean driving record.

When a driving record is not available, and penetration resistance must be estimated on the basis of soil boring data alone, the wave equation is a significantly better tool than the Hiley pile driving formula. However, the difference between actual and predicted values may vary considerably with depth and the estimate

of static capacity that is required for that depth. It is recommended that in the absence of a known mean driving record, predictions be made at several depths of penetration. This will tend to reduce the effects of scatter in the predictions made for each depth. The same result would not be expected when the Hiley formula is used with knowledge of soil conditions alone.

The intent in evaluating the predictive method proposed was to determine the overall feasibility it might have as a working method. Hence, a range of soil conditions, hammer types and energies, and pile types were considered. But for each project studied only the hammer and associated driving equipment was varied. In most cases, based on the ratio of hammer energies involved, this factor was still only slightly varied. This is resultant primarily of selecting completed projects for analysis. The cases studied, therefore, can be used only to evaluate overall feasibility.

While the criteria of similar soil conditions at proposed and completed sites is essential, further studies should be made to evaluate the method with respect to pile type and hammer. Though it is doubtful that projects can be found where divergent hammer types were used, more projects could be analyzed to determine the predictability of a given hammer type in a given soil type. Or the predictability of driving a given pile type with a given

hammer type could be analyzed. No attempt has been made in this study to evaluate the predictive method on such a basis: the body of data was too limited. Now that overall feasibility has been demonstrated, a study evaluating the predictability with respect to each element of the hammer-pile-soil system is recommended. Such a study should include selection of projects prior to the construction phase, so that the driving records can be more completely recorded.

BIBLIOGRAPHY

1. Bowles, T. E., Analytical and Computer Methods in Foundation Engineering, New York, McGraw-Hill, 1974, pp. 349-386.
2. Chapman, D. G. and R. A. Schawtele, Elementary Probability Models and Statistical Inference, Xerox College Publishing Company, Waltham, Massachusetts, 1970.
3. Chellis, Robert, Pile Foundations, New York, McGraw-Hill, 1951, pp. 27-33, 449-450, 525-538.
4. Edwards, T. C., "Piling Analysis Wave Equation Computer Program Utilization Manual," Research Report 33-11 of the Texas Transportation Institute, Texas A & M University, College Station, Texas, August, 1967.
5. Edwards, T. C., L. L. Lowery, Jr. and T. J. Hirsch, "Properties of Pile Cushioning Materials," Journal of the Soil Mechanics and Foundations Division, ASCE, Vol. 95, No. ST7, Proc. Paper 6663, July, 1969, pp. 1431-1441.
6. Forehand, P. W. and J. L. Reese, "Prediction of Pile Capacity by the Wave Equation," Journal of the Soil Mechanics and Foundation Division, ASCE, Vol. 90, No. SM2, Proc. Paper 3820, March, 1964, pp. 1-26.
7. Hill, W. C., "A Study of Friction Pile Resistance," Oregon State Highway Department, Bridge Division, Foundation Section, January, 1969.
8. Hirsch, T. J., L. L. Lowery, H. M. Coyle and C. H. Samson, Jr., "Pile Driving Analysis by One-Dimensional Wave Theory: State of the Art," Highway Research Record 333, Highway Research Board, Washington, pp. 33-54.
9. Lowery, L. L., Jr., T. C. Edwards and T. J. Hirsch, "Use of the Wave Equation to Predict Soil Resistance on a Pile During Driving," Research Report 33-10 of the Texas Transportation Institute, Texas A & M University, College Station, Texas, August, 1968.

10. Lowery, L. L., Jr. T. J. Hirsch and C. H. Samson, Jr., "Pile Driving Analysis--Simulation of Hammers, Cushions, Piles and Soil, " Research Report 33-9 of the Texas Transportation Institute, Texas A & M University, College Station, Texas, August, 1967.
11. Mosley, E. T., "Wave Equation Analysis, " Foundation Facts, Raymond Concrete Pile Division, New York, Vol. 3, No. 2, 1967, pp. 15-17.
12. Mosley, E. T. and T. Raamot, "Pile Driving Formulas, " Highway Research Record 333, Highway Research Board, Washington, pp. 23-32.
13. Parola, J. F., "Pile Driving Behavior, " preprint of paper presented to Pile Talk Seminar, Associated Pile and Fitting Corp., Marriott Hotel, St. Louis, Missouri, September 26-27, 1974.
14. Peck, R. B., W. E. Hanson and T. H. Thornburn, Foundation Engineering, New York, John Wiley & Sons, Inc., 1974, pp. 216-225.
15. Smith, E. A. L., "Pile-Driving Analysis by the Wave Equation, " Journal of the Soil Mechanics and Foundation Division, ASCE, Vol. 86, No. SM4, Proc. Paper 2574, August, 1960, pp. 35-61.
16. Terzaghi, K. and R. B. Peck, Soil Mechanics in Engineering Practice, New York, John Wiley and Sons, Inc., 1967.

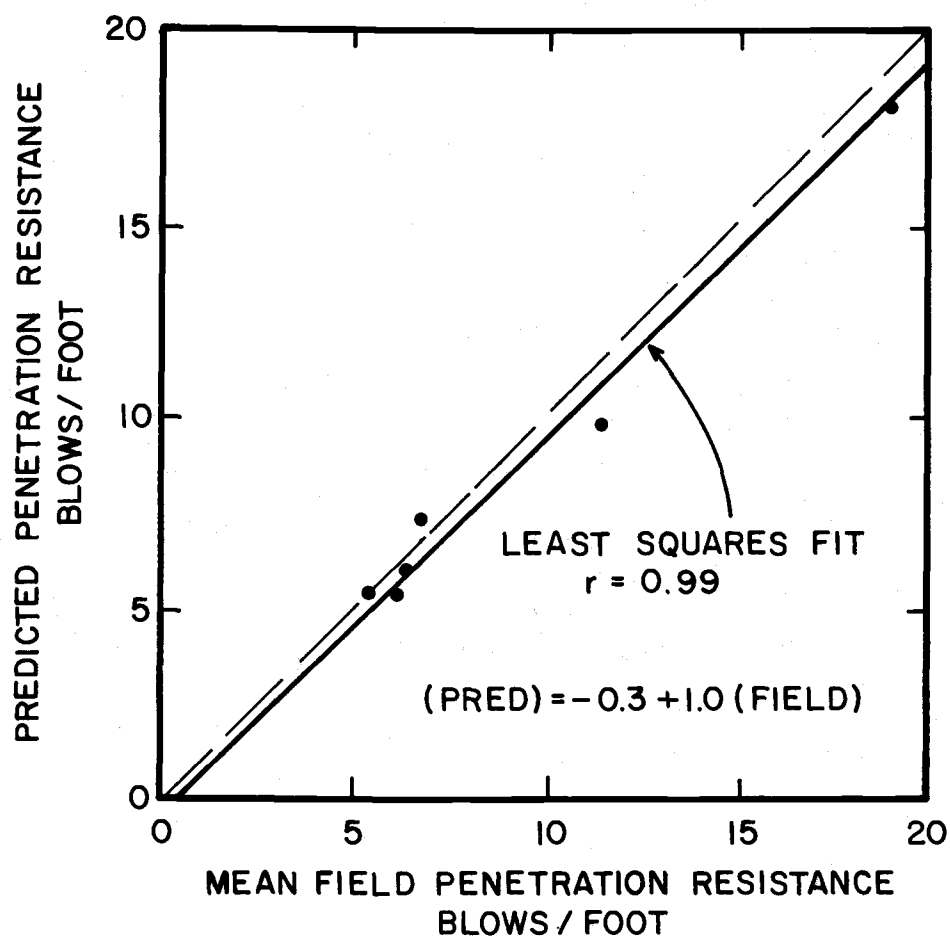


Figure 13. Predicted vs. field penetration resistance for Vulcan 65C, Project A.

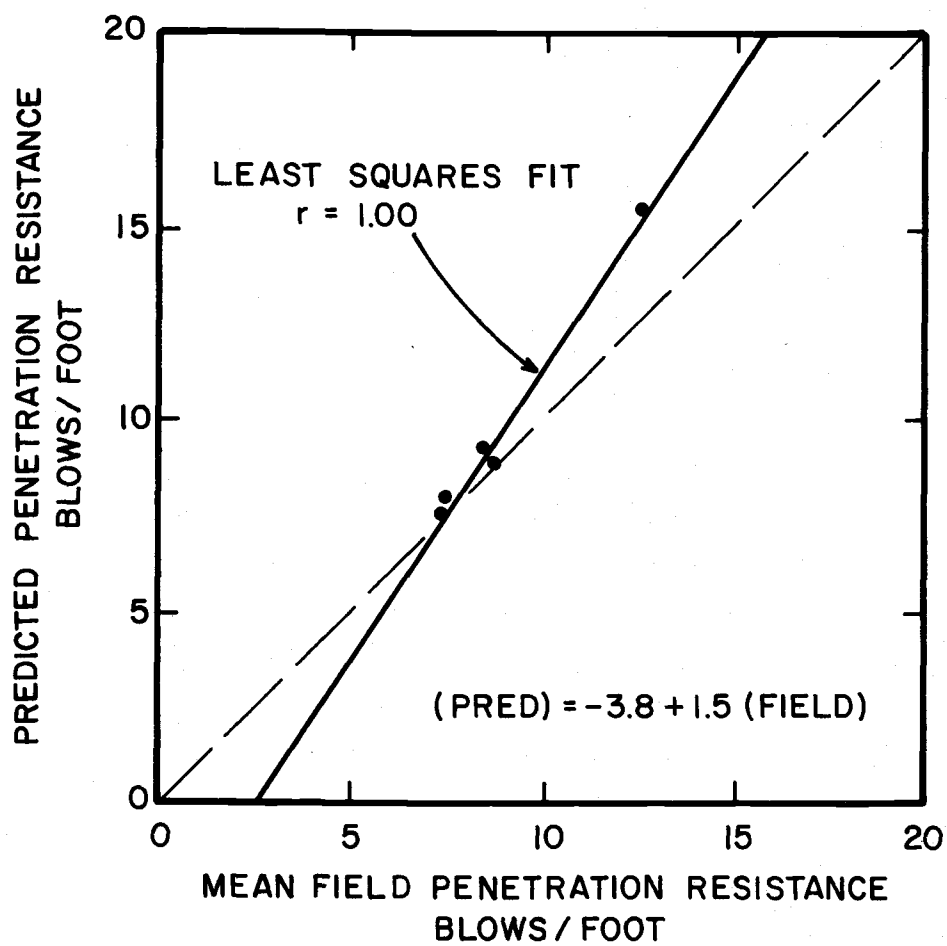


Figure 14. Predicted vs. field penetration resistance for Vulcan 50C, Project A.

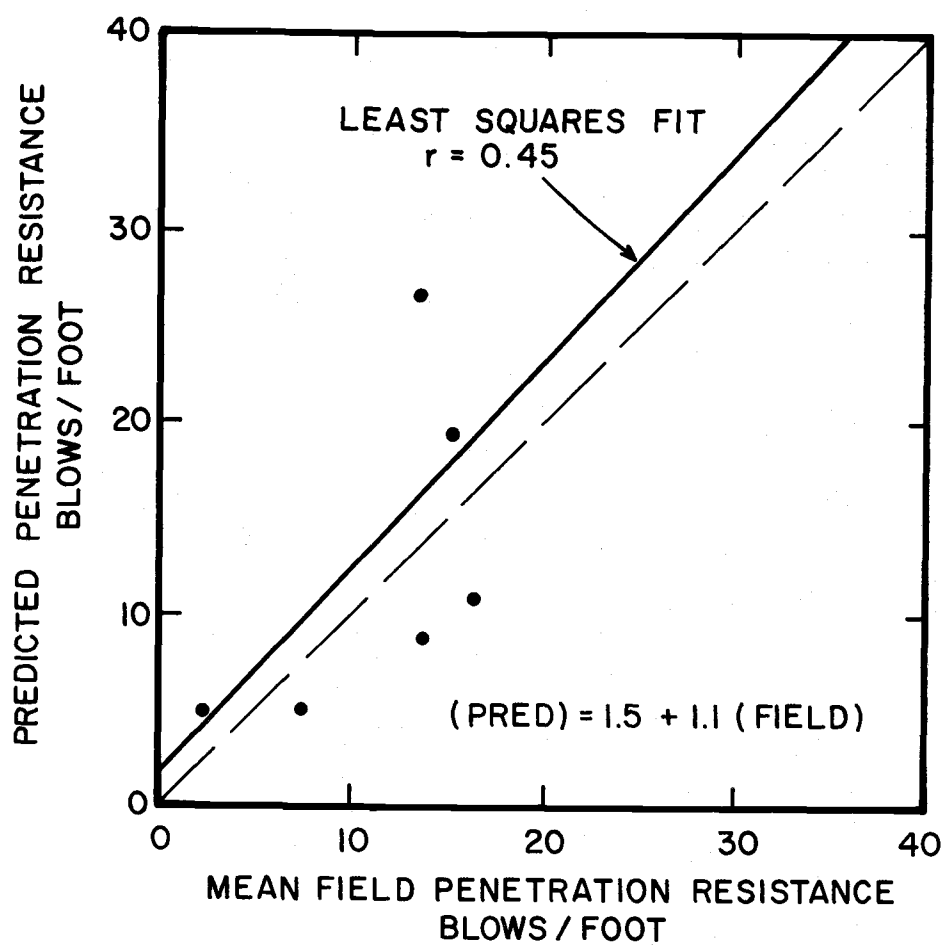


Figure 15. Predicted vs. field penetration resistance for Vulcan 06, Project B.

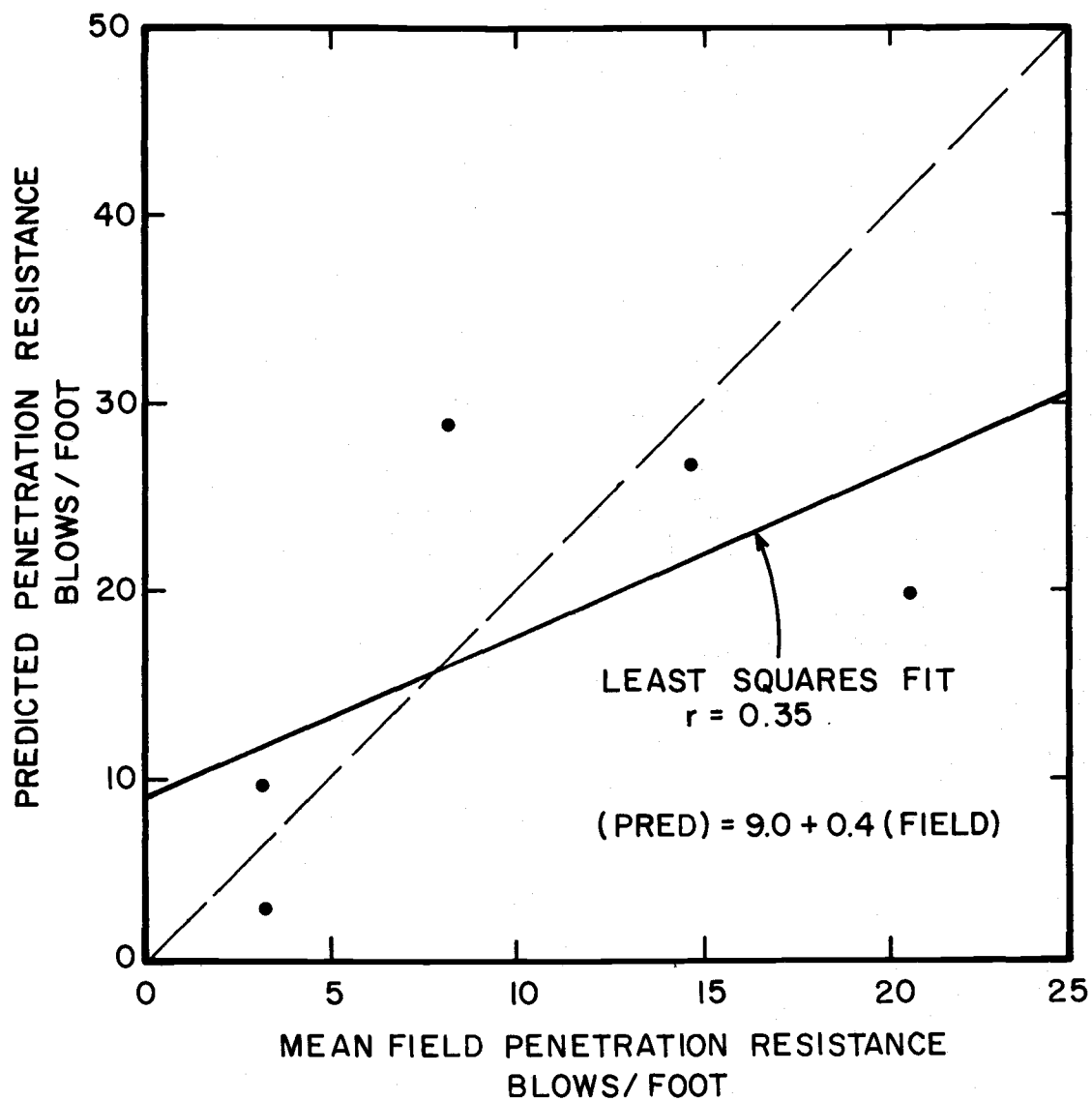


Figure 16. Predicted vs. field penetration resistance for Vulcan 50C, Project B.

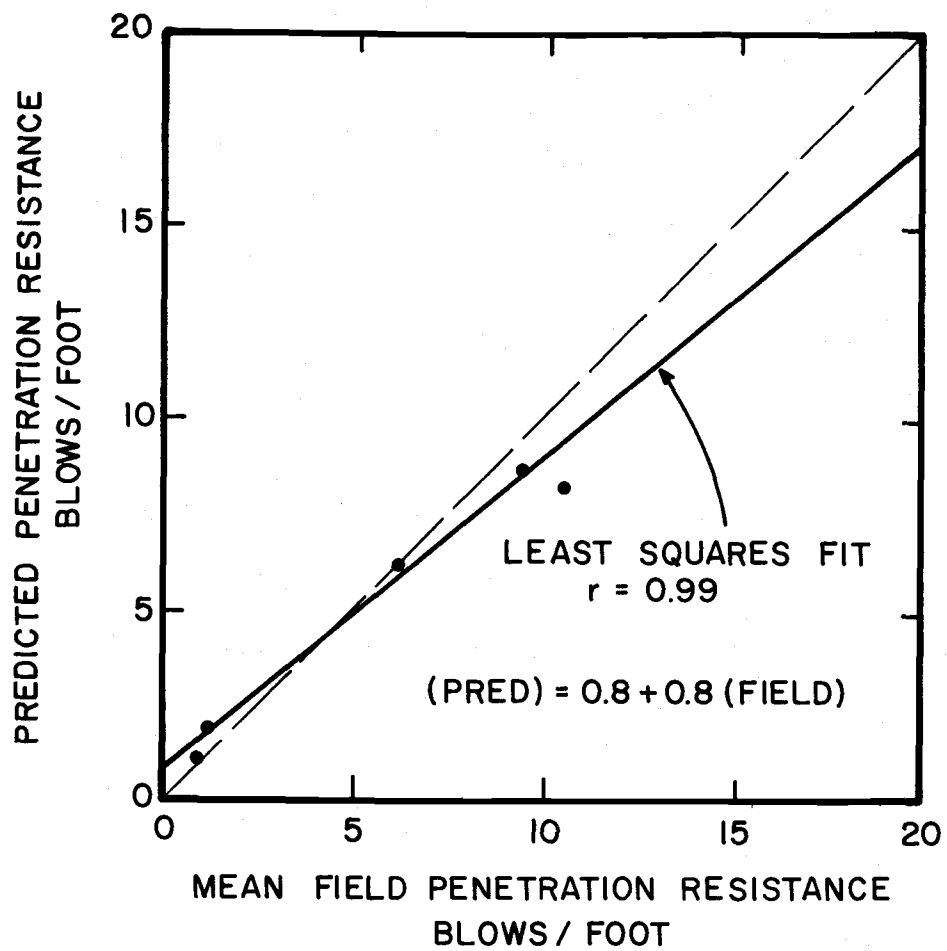


Figure 17. Predicted vs. field penetration resistance for Vulcan 014, Project C.

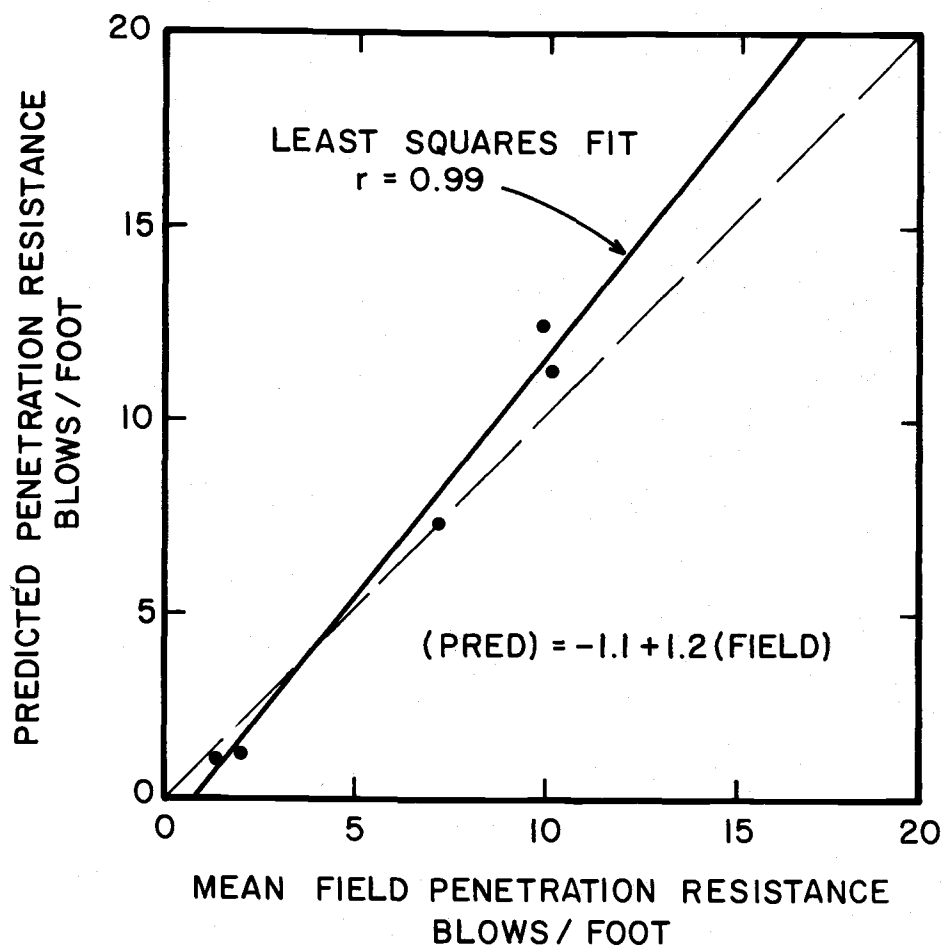


Figure 18. Predicted vs. field penetration resistance for Vulcan 140C, Project C.

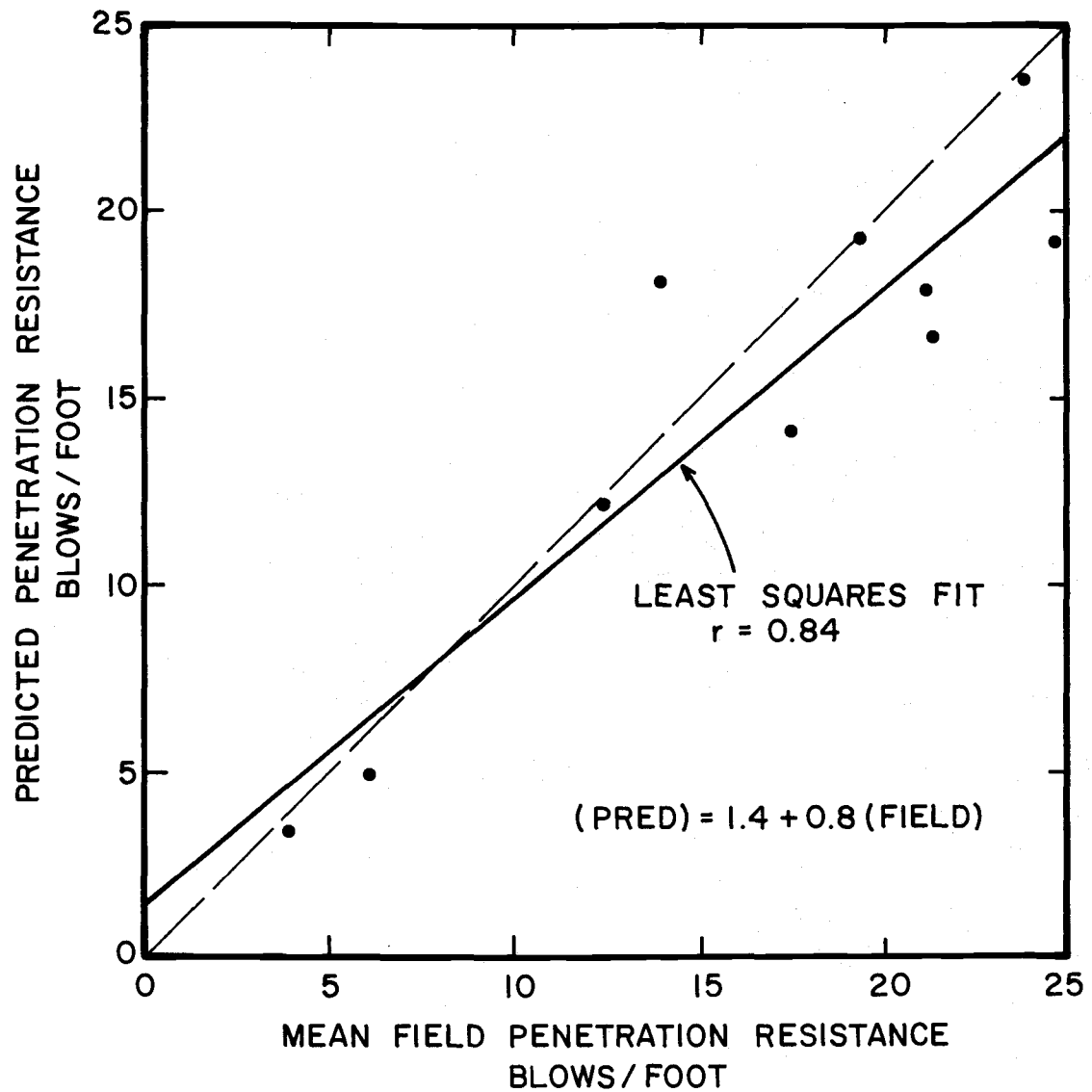


Figure 19. Predicted vs. field penetration resistance for Delmag D-30, Project D.

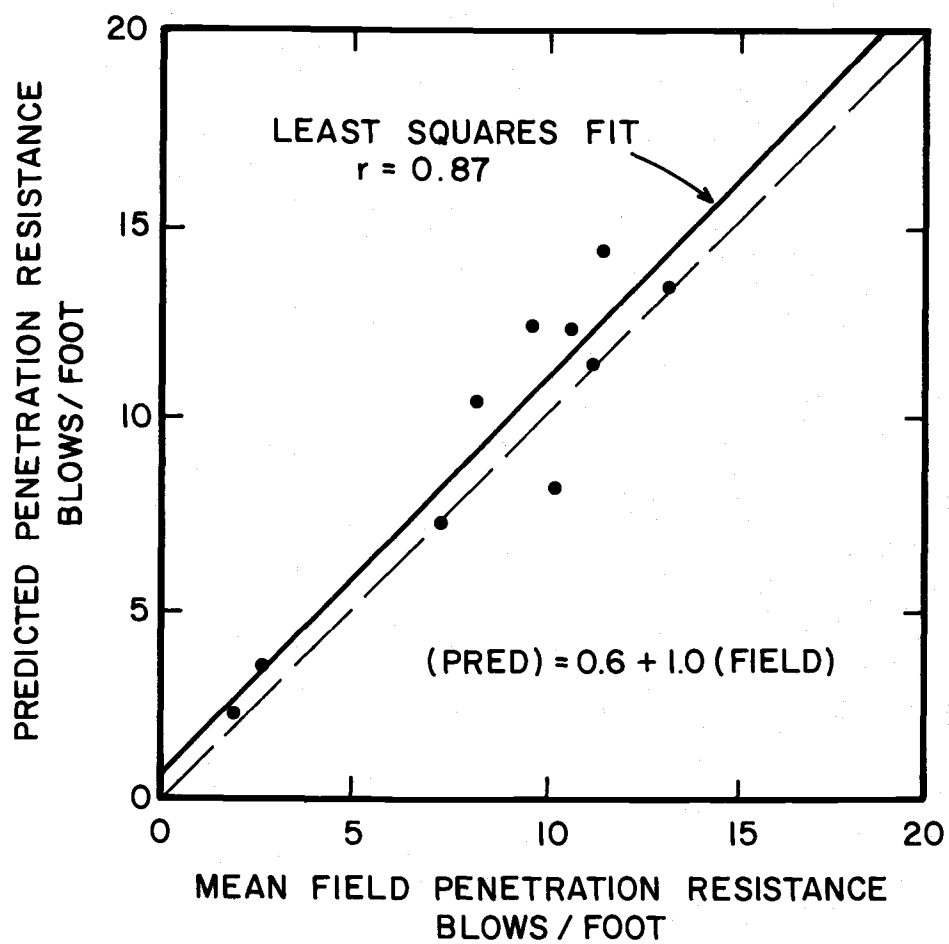


Figure 20. Predicted vs. field penetration resistance for Delmag D-36, Project D.

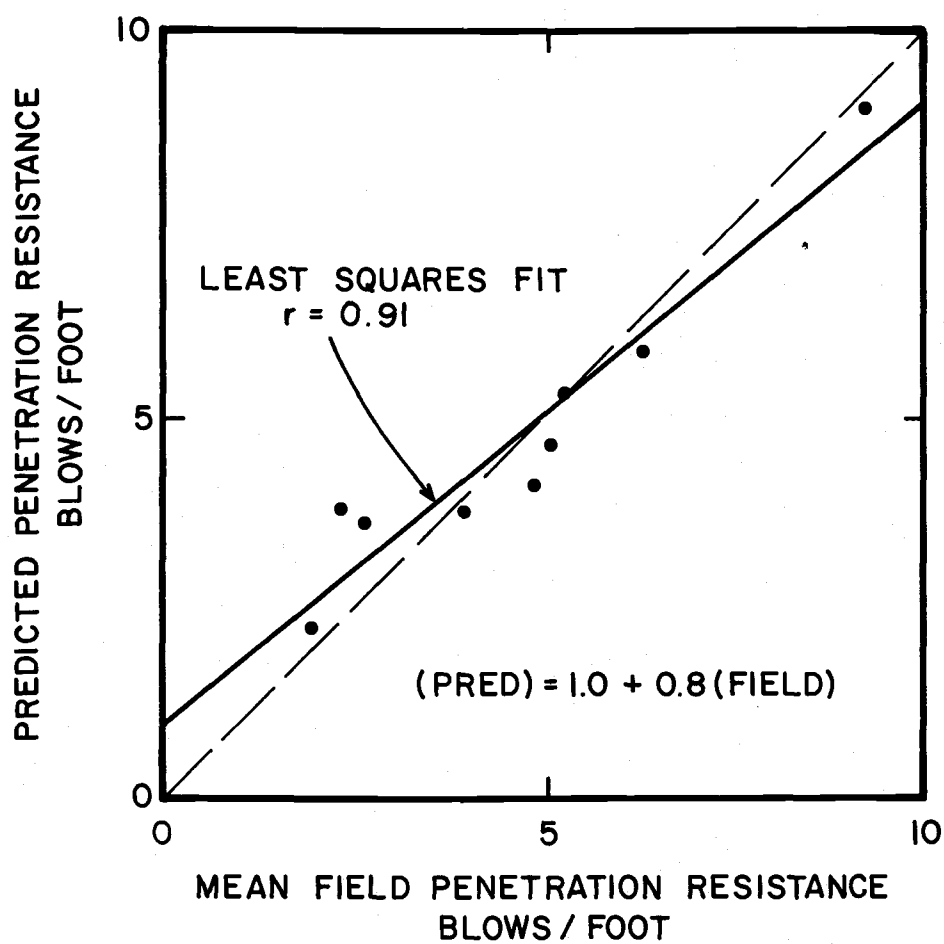


Figure 21. Predicted vs. field penetration resistance for Kobe K-42, 14" piles, Project E.

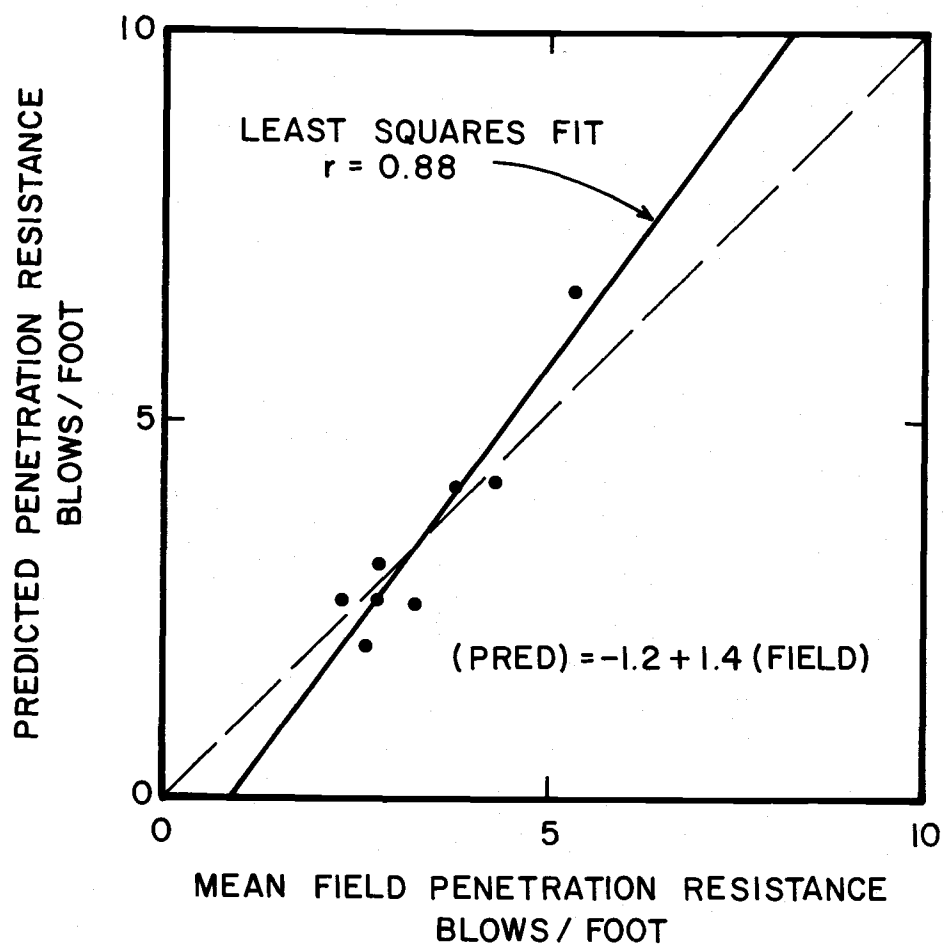


Figure 22. Predicted vs. field penetration resistance for Delmag D-44, 12" piles, Project E.

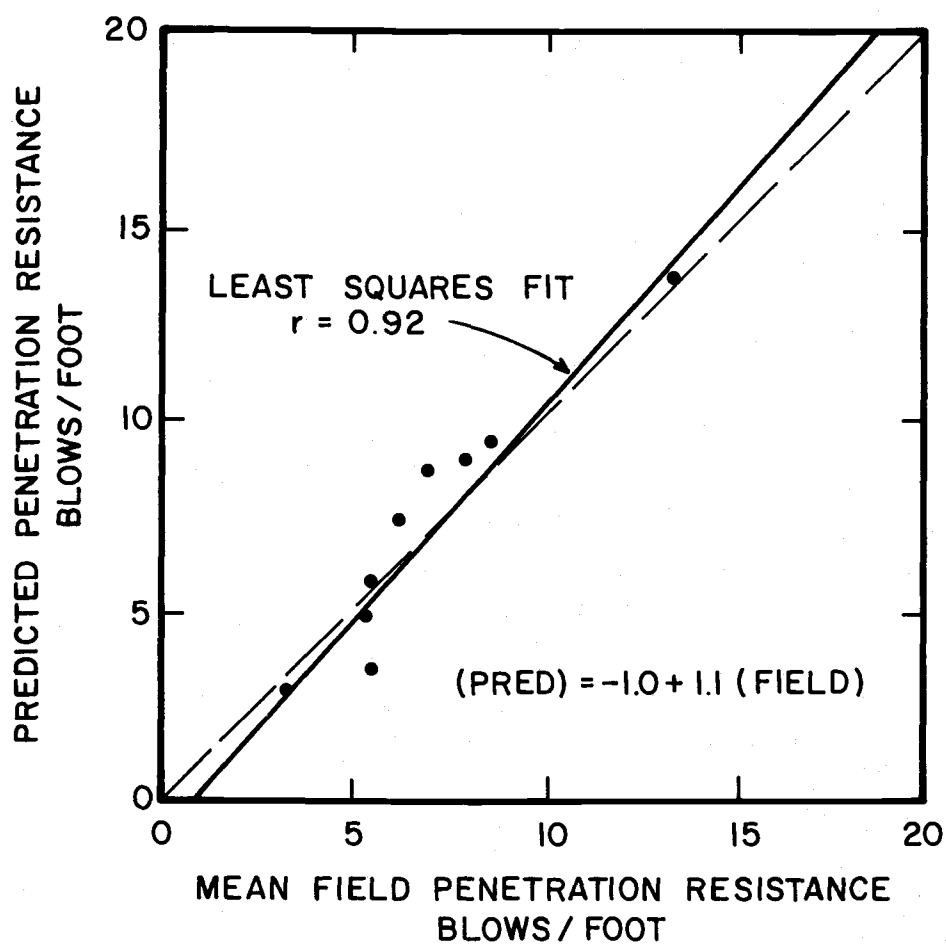


Figure 23. Predicted vs. field penetration resistance for Delmag D-44, 14" piles, Project E.

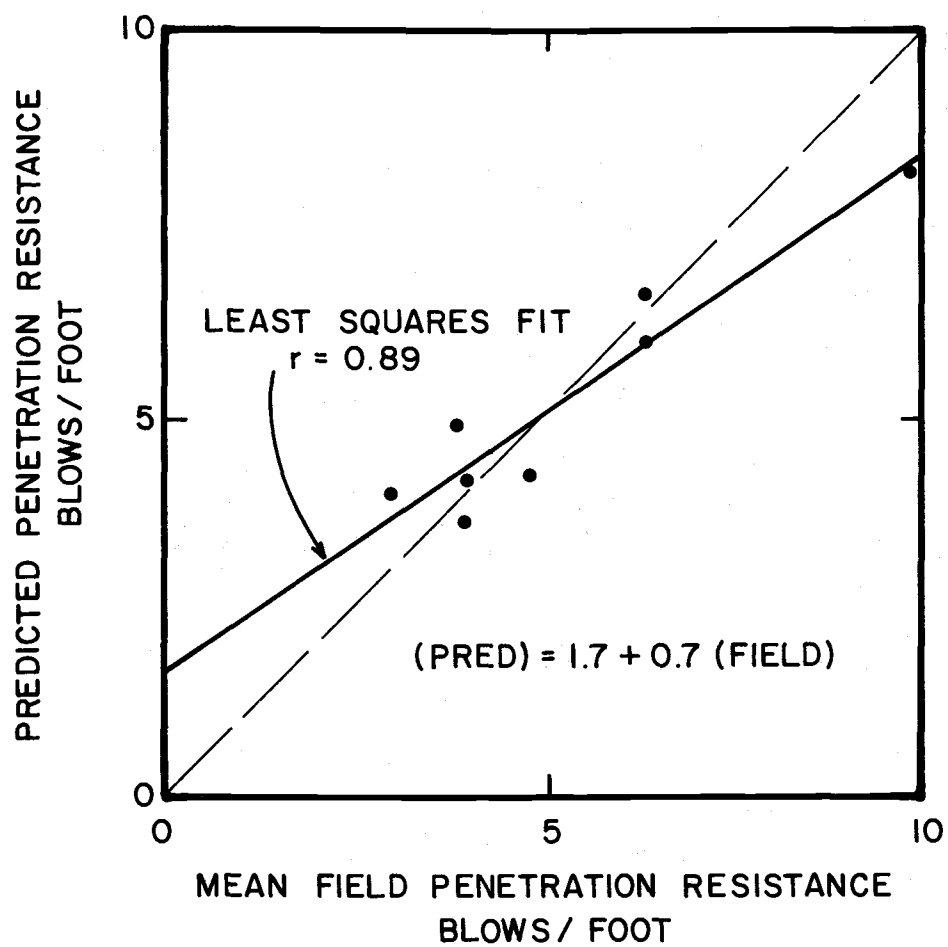


Figure 24. Predicted vs. field penetration resistance for Kobe K-42, 12" piles, Project E.